NASA Tech Briefs

THE DIGEST OF NEW TECHNOLOGY

Official Publication of the
National Aeronautics and
Space Administration
July 1994 Vol. 18 No. 7

Transferring Engineering
Technology to Over 200,000
Qualified Readers Throughout
Industry and Government

Special Focus:
New Graphics And Simulation Tools

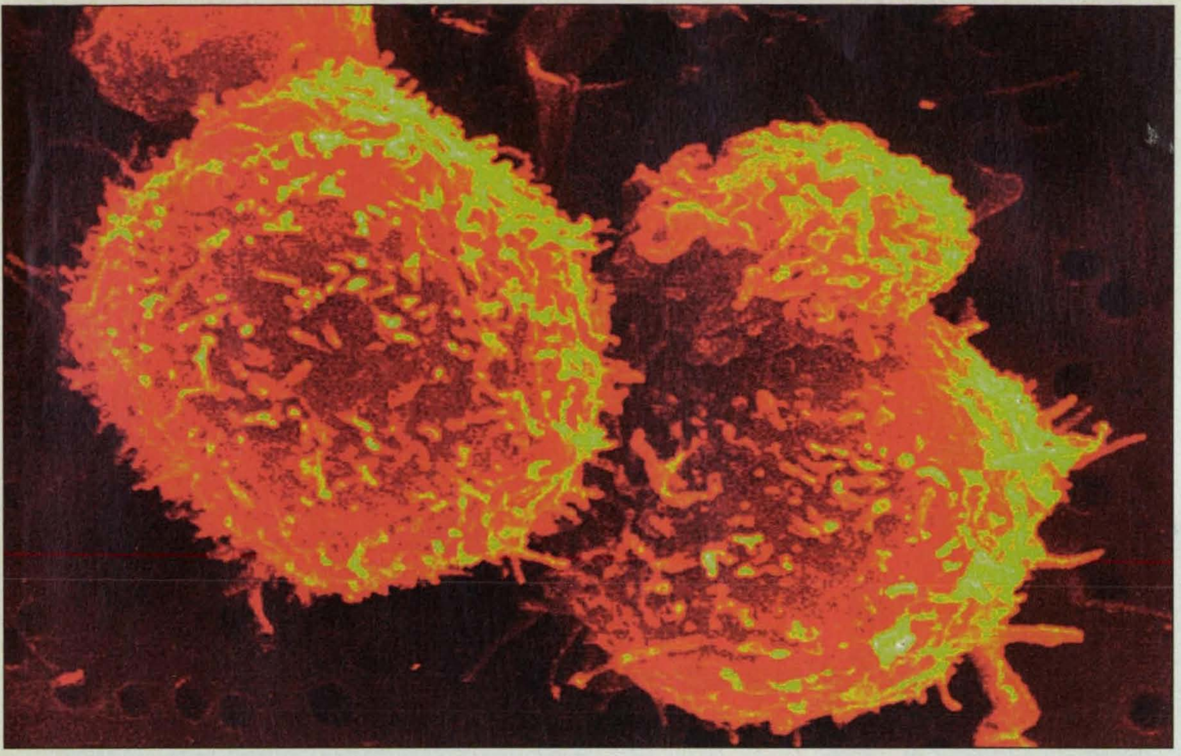

Image from a scanning electron microscope, rendered and enhanced with MATLAB. Nonlinear contrast adjustment emphasizes object details.

See beyond the limits of ordinary image processing–with MATLAB®

The Image Processing Toolbox is the latest addition to the MATLAB Technical Computing Environment. In the world's most powerful system for numeric matrix computation, an image is simply a matrix. That's why you can take image processing further with MATLAB.

Open doors to advanced image processing

The MATLAB Image Processing Toolbox gives you an unrivaled ability to visualize, manipulate, and analyze images and two-dimensional signals. It's easy to explore, apply, and create the innovative image processing methods that let you keep up with—and advance—the leading edge.

Break through the barriers

Until now, all image processing packages have fallen short when it comes to crunching the numbers behind the images.

The Image Processing Toolbox is different. It gives you all the tools you need, in the interactive MATLAB environment. You can easily treat image data visually or numerically. And since you never have to scale data or juggle multiple packages, you get accurate results immediately.

Build on a solid foundation

In MATLAB, you can easily modify any function or add custom tools without writing a single line of Fortran or C code.

You can also create portable GUI applications that look and feel like pre-packaged software, but address specific end-user problems.

Free your imagination

Image processing technology has become essential to scientific and engineering work. And now, within the MATLAB environment, you can easily integrate image processing with powerful computational techniques such as statistics, optimization, and neural networks. Move beyond the limits of ordinary image processing packages — with MATLAB.

Image Processing Toolbox

- *Image and feature enhancement*
- *Image restoration and filtering*
- *Linear and nonlinear filter design*
- *Image analysis and 2-D transforms*
- *Color, geometric, and morphological operations*
- *Color, gray scale, and binary images and sequences*
- *Imports/exports standard image formats*
- *Runs on PCs, Macs, and workstations*

To order or for more information, call

508-653-1415

The MATH WORKS Inc.

24 Prime Park Way
Natick, MA 01760-1500
Fax: 508/653-6284
Email: info@mathworks.com
Mosaic: http://www.mathworks.com

The MathWorks is represented in the following countries: Australia: +61-2-922-6311 • Brazil: +55-11-816-3144 • France: +33-1-45-34-23-91 • Germany: +49-89-995-9010 • India: +91-80-2-260-260 • Israel: +972-3-561-5151 • Italy: +39-11-24-85-332 • Japan: +81-3-5978-5410 • Portugal: +34-3-415-49-04 • Scandinavia: +46-8-15-30-22 • Spain: +34-3-415-49-04 • South Korea: +82-2-517-1257 • Switzerland: +41-31-998-44-11 • Taiwan: +886-2-501-8787 • For Belgium, Luxembourg, The Netherlands, United Kingdom and Republic of Ireland call Cambridge Control, Ltd: +44-223-423-200 **or** Rapid Data, Ltd: +44-903-821-266

July 1994
Volume 18 Number 7

Contents

NASA Tech Briefs
Transferring Engineering Technology
to Over 200,000 Qualified Readers
Throughout Industry and Government

FEATURES

TECHNICAL SECTION

(continued on page 8)

Photo courtesy Mine Safety Appliances Company

Valve components in the self-contained breathing apparatus worn by these firefighters have been coated with Krytox® lubricants from the Du Pont Company, Wilmington, DE. Used by NASA since the 1960s, the nonflammable and chemically inert lubricants can withstand the harsh environments and high temperatures of a wide variety of aerospace, safety, industrial, and automotive applications. See Mission Accomplished on page 12.

At 200 MB Per Minute, We're Setting The Pace.

TRUE COMPATIBILITY WITH	
Alliant	Macintosh
Alpha Micro	McDonnell Douglas
Altos	Motorola
Apollo	NCR
Arix	NeXT
AT&T	Novell
Basic-4	OS/2
Concurrent	PS/2
Convergent	Parallel Port
Data General	PC 386/ix
DEC SCSI	PC MS-DOS
DEC BI-Bus	PC Xenix/Unix
DEC DSSI	Pertec
DEC HSC	PICK
DEC Q-Bus	Plexus
DEC TU/TA81	Prime
DEC Unibus	Pyramid
Gould/Encore	Sequent
HP	Silicon Graphics
IBM AS/400	STC
IBM Mainframe	Stratus
IBM RISC/6000	Sun
IBM RT	Texas Instruments
IBM S/38	Unisys
ICL	Ultimate
Intergraph	Wang
	— and more

The CY-ASP is the fastest digital data storage solution on the market, able to store up to 70 GB at speeds of up to 200 MB per minute, unattended.

But there's more.

The fastest subsystem is also the most flexible, giving you a choice of four recording modes plus offline copy and verify functions.

In ***Single Mode*** the drives operate independently.

In ***Cascade Mode*** data automatically writes to the next tape once the previous tape is full.

In ***Mirroring Mode*** the same data writes to multiple tapes simultaneously.

In ***Striping Mode*** data writes to two or more tapes at once, maximizing throughput.

Consider it a data storage management tool, a solution that will help you solve the problems you encounter every day: the need for higher capacity and speed, the need to make duplicate tapes for off-site storage and data exchange, the need for real-time status information, and the need to save resources and boost productivity on every level.

Of course, we also know that a storage solution is only as good as the data you get back. With a bit error rate of less than 1 in 10^{17} bits read, the CY-ASP gives you the *highest* data integrity.

Based on proven 8mm helical scan technology, each drive supports our switch-selectable *data compression* option. And each drive features a 2-line, 40-column backlit display that gives complete status information.

Backed by a two year warranty that includes expert service and support from our in-house engineering group, the CY-ASP is setting the pace in performance, flexibility and value.

Other configurations are available, ranging from a 2.5 GB subsystem to an intelligent, automated 3 TB tape library. And they're all compatible with the widest range of computer systems and networks.

When you're ready for a data storage solution that means business, call for complete information.

(804) 873-9000

CONTEMPORARY
CYBERNETICS

Rock Landing Corporate Center • 11846 Rock Landing • Newport News, VA 23606 • Fax: (804) 873-8836

For More Information Write In No. 658

Contents *(continued)*

On the cover:

Computational fluid dynamics software developed by Fluent Inc., Lebanon, NH, in conjunction with NASA Lewis Research Center is used to compute air flow around complex shapes such as aircraft contours. RAMPANT™ does not impose a fixed order on computational flow cell layouts, utilizing tetrahedral cells to divide the flow field into discrete pieces instead of traditional six-sided cells. The image depicts RAMPANT's computation of the aerodynamic forces encountered by a ski jumper. For more on NASA's work with computer graphics and simulation, see the tech briefs on pages 22, 24, 26, and 28.

NASA Tech Briefs, ISSN 0145-319X, USPS 750-070, copyright © 1994 in U.S. is published monthly by Associated Business Publications Co., Ltd., 41 E. 42nd St., New York, NY 10017-5391. The copyright information does not include the (U.S. rights to) individual tech briefs that are supplied by NASA. Editorial, sales, production, and circulation offices at 41 East 42nd Street, New York, NY 10017-5391. Subscription for non-qualified subscribers in the U.S., Panama Canal Zone, and Puerto Rico, $75.00 for 1 year; $125 for 2 years; $200.00 for 3 years. Single copies $10.00. Foreign subscriptions one-year U.S. Funds $150.00. Remit by check, draft, postal, express orders or VISA, MasterCard, and American Express. Other remittances at sender's risk. Address all communications for subscriptions or circulation to NASA Tech Briefs, 41 East 42nd St., New York, NY 10017-5391. Second-class postage paid at New York, NY and additional mailing offices.

POSTMASTER: Please send address changes to NASA Tech Briefs, 41 E. 42nd Street, Suite 921, New York, NY 10017-5391.

NASA Tech Briefs

Official Publication of the National Aeronautics and Space Administration

ABP BPA

NASA Tech Briefs

Published by .... **Associated Business Publications**
President/Chief Executive Officer .... **Bill Schnirring**
Publisher/Editor .... **Joseph T. Pramberger**
Executive Editor .... **Sarah L. Gall**
Contributing Editor .... **Robert Clark**
Assistant Editor .... **Gregg McQueen**
Director of Manufacturing .... **Gregg Weatherby**
Traffic Manager .... **Margery Koen**
Art Director .... **Pierre Granier**
Marketing Director .... **Wayne Pierce**
Telemarketing Specialist .... **Evelyn Mars**
Reader Service Manager .... **Scott Floman**
Assistant to Reader Service Manager .... **Damiana Garcia**
Circulation Director .... **Martin J. Horan**

BRIEFS & SUPPORTING LITERATURE: Written and produced for NASA by **Advanced Testing Technologies, Inc.**, Commack, NY 11725
Technical/Managing Editor .... **Ted Selinsky**
Sr. Technical Analyst .... **Dr. Larry Grunberger**
Art Manager .... **Eric Starstrom**
Administrator/Chief Copy Editor .... **Greg Galitzine**
Staff Writers/Editors .... **Dr. Theron Cole, Dr. Claude Swanson, George Watson, Howard Falk**
Graphics .... **Robert Simons**
Editorial & Production .... **Deborah Satinsky, Brian Bochicchio, Teresa Johnson**

NASA:
NASA Tech Briefs are provided by the National Aeronautics and Space Administration, Technology Transfer Division, Washington, DC:
Administrator .... **Daniel S. Goldin**
Deputy Assistant Administrator(Programs) .... **Frank E. Penaranda**
Deputy Director Technology Transfer Division (Publications Manager) .... **Leonard A. Ault**
Manager, Technology Transfer Office, NASA Center For AeroSpace Information .... **Walter M. Heiland**

ASSOCIATED BUSINESS PUBLICATIONS
41 East 42nd Street, Suite 921, New York, NY 10017-5391
(212) 490-3999 FAX (212) 986-7864
President/Chief Executive Officer .... **Bill Schnirring**
Executive Vice President/Chief Operating Officer .... **Domenic A. Mucchetti**
Treasurer .... **Joseph T. Pramberger**
Controller .... **Athena Thomas**
Credit/Collection .... **Felecia Lahey**
Staff Accountant .... **Larry Duze**
Trade Show Director .... **Wendy S. Janiel**
Trade Show Coordinator .... **Danielle Krasny**
Human Resources Manager .... **Lourdes Del Valle**
MIS Manager .... **Ted Morawski**
Assistant MIS Manager .... **Pak Tong**
Office Manager .... **Sylvia Valentin**
Mailroom Operations .... **Thomas C. Snyder, Rose D'Addozio**
Receptionist .... **Tracy A. Wenz**

ADVERTISING: New York Office: (212) 490-3999 FAX (212) 986-7864

Manager, Direct Response Products .... **Paul Lesher, CBC** at (312) 296-2040

***NASA TECH BRIEFS* ACCOUNT EXECUTIVES**
NY, NJ .... **Brian Clerkin** at (201) 366-2751
PA, DE, NJ (Area Code 609), VA, DC, MD, WV, NC .... **Tara Morie** at (215) 640-3118
Eastern MA, NH, ME, RI .... **Paul Gillespie** at (508) 429-8907; **Bill Doucette** at (508) 429-9861
Western MA, CT, VT .... **George Watts** at (802) 875-3310
Southeast, South Central .... **Douglas Shaller** at (212) 490-3999
OH, MI, IN, KY .... **Scott Burrows** at (216) 928-1888
IL, WI, MO, IA, MN, ND, SD, NE, KS .... **Melinda Mead** at (312) 296-2040
Northwest—WA, OR, ID, MT, WY, CO .... **Bill Hague** at (206) 858-7575
West Coast—CA, AZ, NV, NM, UT .... **Stillman Group** at (310) 372-2744
for Area Codes 310/213/818/805/801: **Tom Stillman** at (619) 940-0141
for 505/602/619/702/714: **Stan Roach**
for 408/415/510/707/916: **Robert Hubbard** at (510) 846-6816
Japan .... **Akio Saijo** at 03 (3555) 0106

For More Information Write In No. 404

Mission Accomplished

Through the technology transfer process, many of the systems, methods, and products pioneered by NASA are reapplied in the private sector, obviating duplicate research and making a broad range of new products and services available to the public.

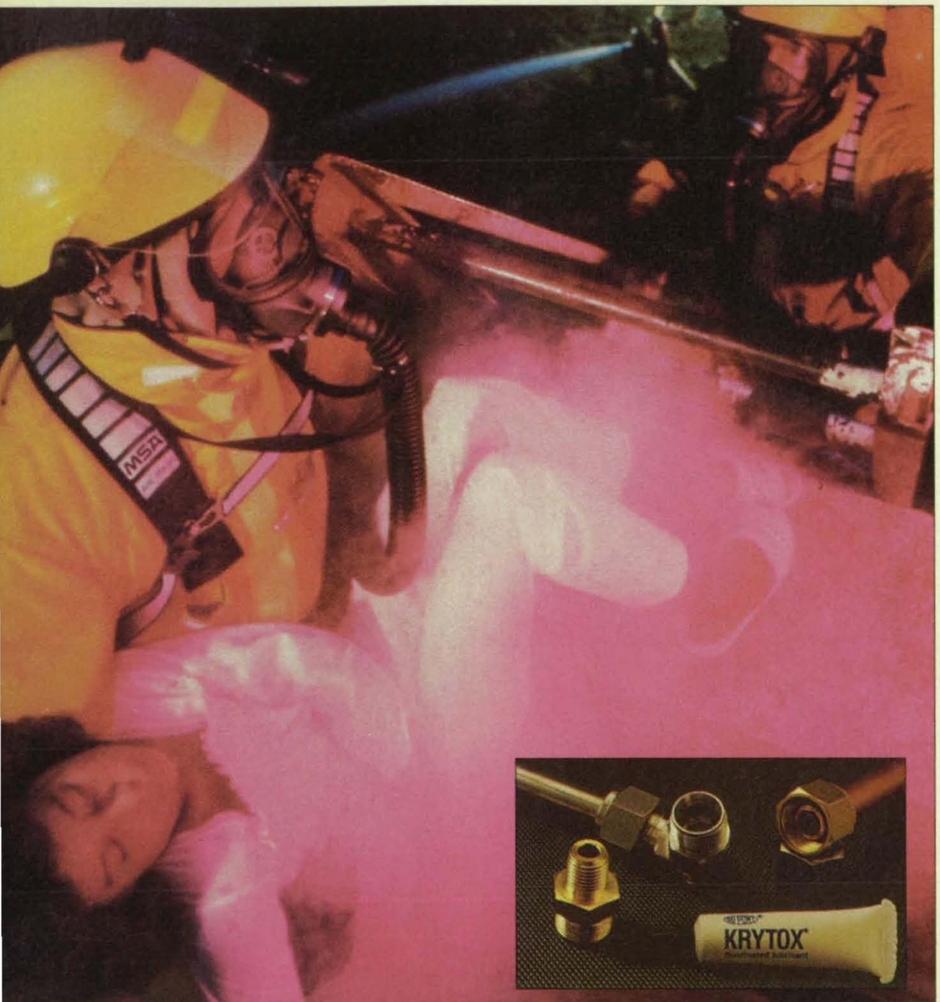

Originally used by NASA to protect aerospace materials, highly temperature resistant Krytox® lubricants perform well in critical applications such as life support systems for firefighters. (Inset) Krytox lubricants can be applied easily to metallic, plastic, and rubber surfaces to decrease maintenance and extend service life.

Firefighters routinely brave extreme danger to enter burning buildings, save lives, and preserve property. In these critical situations, a firefighter's own survival depends upon the flawless operation of his breathing apparatus. Many manufacturers of firefighting equipment ensure the smooth functioning of life support systems with Krytox® performance lubricants from the Du Pont Company, Wilmington, DE.

Used by NASA since the 1960s as aerospace lubricants, Krytox fluorinated oils, greases, and vacuum pump fluids are suited for applications where component failure cannot be tolerated, such as valves on life support devices or in hydraulic systems on aircraft. All Krytox products are nonflammable and demonstrate an exceptionally high chemical inertness. They are nonreactant to gaseous and liquid oxygen, making them preferable for oxygen systems.

Krytox lubricants are perfluoroalkylpolyether (PFPE) fluids, composed entirely of carbon, fluorine, and oxygen. Colorless and odorless, the fluids are compatible with most materials and liquids over a wide temperature range. They have high-temperature resistance, exhibiting no ignition points up to 649 °C and maintaining lubricity for extended periods in temperatures ranging from -57 °C to 343 °C.

Unlike conventional hydrocarbon and synthetic lubricants, the Krytox products do not decompose or form solid deposits after use. "The biggest problem with hydrocarbon lubricants is that they form degradation products, and a lubricating agent turns into an adhesive after a while," said Du Pont chemist Tom Del Pesco. "Krytox just doesn't do that. It doesn't change."

The extreme nontoxicity and nonreactivity of the Krytox products makes them environmentally friendly. "It's used in environmental testing equipment because it doesn't dissolve things," stated Del Pesco. "It's a hydrocarbon world out there, and we're making a fluorochemical that's not compatible with the hydrocarbon world. In that sense, it's safe."

Krytox dates back to 1958, when Du Pont was producing fluorinated polymers in an attempt to create a new synthetic lubricant. After much experimentation, Krytox oil was born. "It was the most stable thing I had ever subjected a sample to—I got it all the way up to 800 °F [427 °C], and nothing happened to it," remarked Earl Sommers, a former Du Pont research associate.

The product that later would find commercial success as a thread sealant, chlorine compressor fluid, heat transfer fluid, and lubricant for paper corrugating machines needed a proving ground, and found an ideal one in the harsh environment of space. Following the January 1967 Apollo disaster in which three astronauts died when their command capsule was engulfed by fire, finding nonflammable materials for aerospace use became paramount. The search led NASA to

Merlin™ Mesh Enhancement Technology gives you the highest quality finite element mesh available

Typical unconditioned meshes from "competitive" products

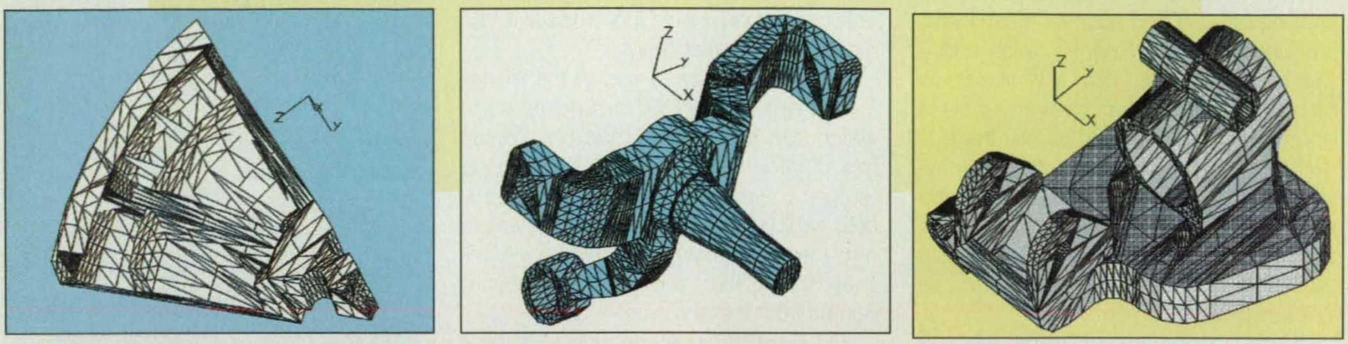

After Merlin™ one-step mesh enhancement technology

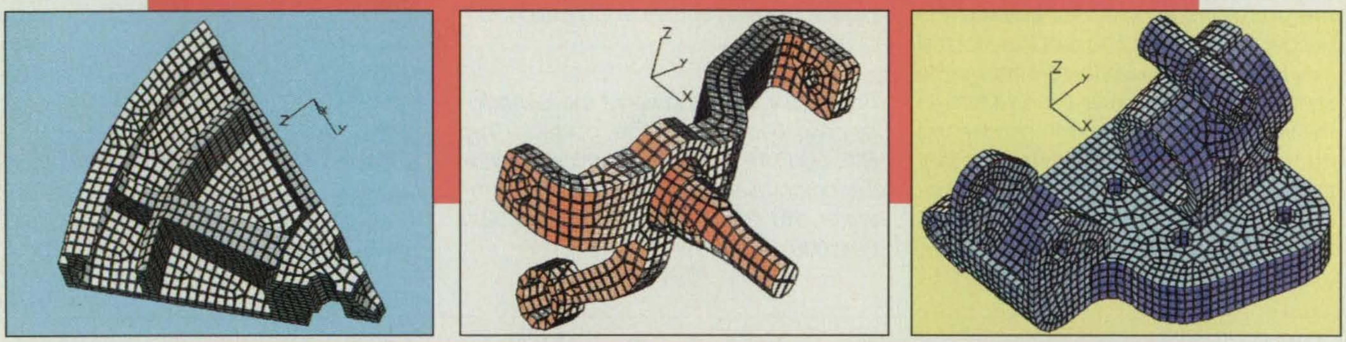

(Algor brick element models above shown with an 85% shrink-element factor.)

Merlin produces engineering-quality, quadrilateral surface meshes for high-accuracy plate/shell FEA or 8-node "brick" element generation using Hexagen (fully automatic). Merlin enhances the mesh quality of Algor's modeling and design software. In addition, Merlin is included in Houdini™ which is unique software that takes existing or new CAD solid models and automatically creates high-accuracy, 8-node "brick" finite element models.

Additional "After Merlin" Examples

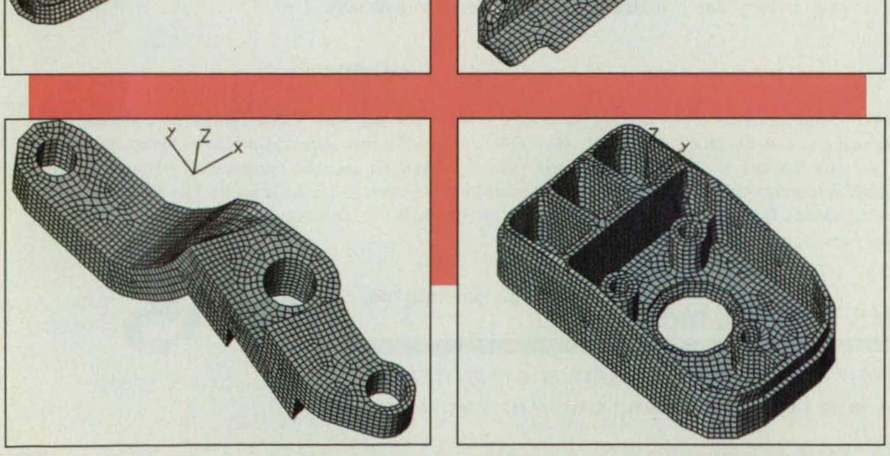

Merlin technology turns a 3- or 4-node surface mesh or CAD solid model into a high quality 4-node mesh in an easy, one-step process.

ALGOR®

When the Engineering Has to be Right ™

Algor backs its software products with a Satisfaction Guarantee. Call or write for details.

For DOS, UNIX and Windows NT

150 Beta Drive
Pittsburgh, PA 15238-2932 USA
Phone: (412) 967-2700
Fax: (412) 967-2781
California: (714) 564-2541
Europe (UK): +44 (784) 442 246
Tokyo: +81 03-3589-6148

For More Information Write In No. 518

Krytox, which quickly found a home in many space projects, such as the Lunar Rover's traction motors.

Lewis Research Center recently used Krytox to protect components in its Geostationary Operational Environmental Satellite (GOES), which provides satellite weather pictures for meteorology. GOES' imaging devices and sounder instruments are lubricated with Krytox grease and a filter wheel is coated with a Krytox liquid lubricant. "Krytox has proven to be a good boundary lubricant where there is metal-on-metal contact between slow speed parts, such as scan bearings, and parts moving at a higher speed rotation, such as filter wheels," said Bill Jones, a research engineer in Lewis' Surface Science Branch.

Earth observation systems such as GOES feature sensors to measure different spectral ranges in space. Although the components are well-sealed, the danger remains that some of the material may leak out. Because there is no wind in space, the leaked material would stay in the vicinity of the spacecraft, condensing on the coolest surface nearby—usually the windows of the detectors. This condensation would block the radiation that the sensors are trying to detect. Krytox, unlike conventional hydrocarbons, absorbs in only a small region of the infrared spectrum and would not interfere with sensor performance.

Engineers at Stennis Space Center employ Krytox in testing space shuttle main engines. It is used to lubricate the bearing housings of liquid oxygen pumps that transfer cryogenic fuel oxidizer to the run tank during test firings.

Krytox also plays a role in the manufacturing of an AT&T computer chip, which can store more than one million bits of information. The chips are made using a metal oxide semiconductor process, which involves etching silicon wafers with gases in a vacuum chamber. AT&T uses Krytox fluid to protect the vacuum pumps from these corrosive gases.

Du Pont is experimenting with new formulations of Krytox, in hopes of expanding its consumer applications, especially in the area of bicycle lubrication. ❑

For more information about the technology described in this article, contact: Greg Bell, Du Pont Specialty Chemicals, Krytox Technical Service Department, Deepwater, NJ 08023. Tel: 800-424-7502; Fax: 609-540-4489.

Du Pont is expanding the Krytox line into commercial applications such as competitive cycling.

Multiple Pages Intentionally Left Blank

New Product Ideas

New Product Ideas are just a few of the many innovations described in this issue of *NASA Tech Briefs* and having promising commercial applications. Each is discussed further on the referenced page in the appropriate section in this issue. If you are interested in developing a product from these or other NASA innovations, you can receive further technical information by requesting the TSP referenced at the end of the full-length article or by writing the Technology Utilization Office of the sponsoring NASA center (see page 20). NASA's patent-licensing program to encourage commercial development is described on page 20.

System Would Generate Virtual Heads-Up Display

A proposed helmet-mounted display would superimpose full-color alphanumeric or graphical information onto an observer's field of vision. Pilots, surgeons, security officers, and possibly stock-exchange personnel may benefit by viewing two sources of information simultaneously.
(See page 22.)

Fully Three-Dimensional Virtual-Reality System

A proposed system would simulate free flight in three-dimensional space. The virtual traveler would see interstellar, aerial, or underwater scenes and use a joystick to navigate through space. Pilot training and many other computerized simulations, including entertainment, may benefit from this development.
(See page 24.)

Three-Dimensional Vertical-Bloch-Line Memory System

The advantages of this proposed magnetic memory system include high storage density, high speed, nonvolatility, and insensitivity to ionizing radiation. Memory modules would be arranged in a linear array of parallel stripe domains called "minor loops." Hall-effect sensors would read out data from all minor loops simultaneously.
(See page 40.)

Composite Solid Electrolyte for Lithium Cells

This electrolyte promises to further the development of Li/TiS_2 or other batteries to overall power densities greater than 100 W/kg and specific energy of 100 W•h/kg.
(See page 49.)

Improved Dielectric Films for Capacitors

Blends of cyanoresins and cellulose triacetate have high breakdown strengths plus high dielectric constants. The dielectric constants can be as high as 16.2.
(See page 54.)

Cooled-Spool Piston Compressor

This proposed compressor would limit the temperature rise of the compressed gas to a safe level. It would also make it possible to obtain one or two stages of compression.
(See page 71.)

Shoulder Joint for Protective Suit

A new shoulder joint allows a full range of natural motion. The wearer senses little or no resisting force or torque.
(See page 64.)

Improved Helmet-Padding Material

New foamed polyimide material forms a very effective padding for helmets. Such helmets can be used by firefighters, police, offshore-drilling and construction workers, miners, race-car drivers, and others in sports and hazardous occupations.
(See page 50.)

Power-Conserving Stepping-Motor Drive Circuits

Two improved drive circuits for a sinusoidally commutated stepping motor include feedback loops to reduce unnecessary power consumption by reducing drive-current amplitude when the motor operates under high load.
(See page 30.)

Making Skew-Resistant Fabrics for Composite Layups

A modified weaving process bonds warp and fill yarns locally by applying an adhesive to them. The amount of adhesive and the number of bond points are controlled to prevent skewing.
(See page 73.)

Low-Dielectric-Constant Polyimide Fibers

These fibers have high thermal stability and good tensile properties. Potential applications include use in printed circuits and in aircraft composites.
(See page 49.)

Thermalite Apparatus

This portable apparatus measures thermal properties of materials. Prior systems for this type of measurement involved complex laboratory equipment. From these measurements, one can determine thermal diffusivity, thickness, integrity of a subsurface bond, presence or absence of surface coating, uniformity, damage, anisotropy, and corrosion.
(See page 44.)

Reconfigurable Full-Page Braille Displays

Electrically actuated braille display cells could be arrayed together to form full-page displays. The proposed cells should be cheap enough for mass production and widespread use.
(See page 30.)

HOW YOU CAN BENEFIT FROM NASA's TECHNOLOGY TRANSFER SERVICES

If you're a regular reader of TECH BRIEFS, then you're already making use of one of the low- and no-cost services provided by NASA's Technology Transfer Program. But a TECH BRIEFS subscription represents only a fraction of the technical information and applications/engineering services offered by this Program. In fact, when all of the components of NASA's Technology Transfer Network are considered, TECH BRIEFS represents the proverbial tip of the iceberg.

We've outlined below NASA's Technology Transfer Network—named the participants, described their services, and listed the individuals you can contact for more information relating to your specific needs. We encourage you to make use of the information, access, and applications services offered.

How You Can Access Technology Transfer Services At NASA Field Centers:

Technology Utilization Officers & Patent Counsels—Each NASA Field Center has a Technology Utilization Officer (TUO) and a Patent Counsel to facilitate technology transfer between NASA and the private sector.

If you need further information about new technologies presented in NASA Tech Briefs, request the Technical Support Package (TSP). If a TSP is not available, you can contact the Technology Utilization Officer at the NASA Field Center that sponsored the research. He can arrange for assistance in applying the technology by putting you in touch with the people who developed it. If you want information about the patent status of a technology or are interested in licensing a NASA invention, contact the Patent Counsel at the NASA Field Center that sponsored the research. Refer to the NASA reference number at the end of the Tech Brief.

Ames Research Ctr.
Technology Utilization Officer: Geoffrey S. Lee
Mail Code 223-3
Moffett Field, CA 94035
(415) 604-4044
Patent Counsel:
Darrell G. Brekke
Mail Code 200-11
Moffett Field, CA 94035
(415) 604-5104

Lewis Research Center
Technology Utilization Officer: Anthony F. Ratajczak
Mail Stop 7-3
21000 Brookpark Road
Cleveland, OH 44135
(216) 433-5568
Patent Counsel:
Gene E. Shook
Mail Code LE-LAW
21000 Brookpark Road
Cleveland, OH 44135
(216) 433-5753

John C. Stennis Space Center
Acting Technology Utilization Officer:
Richard A. Galle
Code HA-30
Stennis Space Center, MS 39529
(601) 688-1929

John F. Kennedy Space Center
Technology Utilization Officer: James A. Aliberti
Mail Stop DE-TDO
Kennedy Space Center, FL 32899
(407) 867-3017
Patent Counsel:
Bill Sheehan
Mail Code DE-TDO
Kennedy Space Center, FL 32899
(407) 867-2544

Langley Research Ctr.
Technology Utilization Officer: Joseph J. Mathis, Jr.
Head, TU & AO Office
Mail Stop 200
Hampton, VA 23681-0001
(804) 864-2484
Patent Counsel:
Dr. George F. Helfrich
Mail Stop 212
Hampton, VA 23681-0001
(804) 864-9260

Goddard Space Flight Center
Technology Utilization Officer: Dr. George Alcorn
Mail Code 702
Greenbelt, MD 20771
(301) 286-5810
Patent Counsel:
R. Dennis Marchant
Mail Code 204
Greenbelt, MD 20771
(301) 286-7351

Jet Propulsion Lab.
NASA Resident Office
Technology Utilization Officer: Arif Husain
Mail Stop 180-801D
4800 Oak Grove Drive
Pasadena, CA 91109
(818) 354-4862
Patent Counsel:
Thomas H. Jones
Mail Code 180-801G
4800 Oak Grove Drive
Pasadena, CA 91109
(818) 354-5179

Technology Utilization Mgr. for JPL:
Wayne Schober
Mail Stop 122-116
4800 Oak Grove Drive
Pasadena, CA 91109
(818) 354-2240

Technical Information/Inquiries:
1-(800) 832-4575

George C. Marshall Space Flight Center
Technology Utilization Officer: Ismail Akbay
Code PR-61
Marshall Space Flight Center,
AL 35812
(205) 544-2223
(800) 437-5186
Patent Counsel:
Robert L. Broad, Jr.
Mail Code CC01
Marshall Space Flight Center,
AL 35812
(205) 544-0021

Dryden Flight Research Facility
Project Manager, Technology Transfer Office: Yvonne Kellogg
Mail Stop D-2131
P.O. Box 273
Edwards, CA 93523-0273
(805) 258-3720

Lyndon B. Johnson Space Center
Technology Utilization Officer: Richard B. Ramsell
Mail Code IC-4
Building 4 South
Houston, TX 77058
(713) 483-3809
Patent Counsel:
Edward K. Fein
Mail Code AL3
Houston, TX 77058
(713) 483-4871

NASA Headquarters
Technology Utilization Officer: Leonard A. Ault
Code CU
Washington, DC 20546
(202) 358-0721
Associate General Counsel for Intellectual Property: Jack Mannix
Code GP
Washington, DC 20546
(202) 358-2424

How You Can Utilize **NASA's Regional Technology Transfer Centers (RTTCs)**—A nationwide network offering a broad range of technology transfer and commercialization services.

You can contact NASA's network of RTTCs for assistance in solving a specific technical problem or locating technology or markets that match your interests. The RTTCs are experienced in working with industry to define technology needs and acquire and commercialize applicable technology. User fees are charged for most services. For more information, call 1-800-472-6785 and you will be connected to the RTTC in your geographical region (or you may call or write directly to the RTTC in your region).

REGIONAL TECHNOLOGY TRANSFER TRANSFER CENTERS (RTTCs)

RTTC Directors

NORTHEAST
Dr. William Gasko
Center tor Technology Commercialization
Massachusetts Technology Park
100 North Drive
Westborough, MA 01581
(508) 870-0042

MID-ATLANTIC
Ms. Lani S. Hummel
University of Pittsburgh
823 William Pitt Union
Pittsburgh, PA 15260
(412) 648-7000
(800) 257-2725 (toll-free US)

SOUTHEAST
Mr. J. Ronald Thornton
Southern Technology Application Center
University of Florida
College of Eng.
Box 24
One Progress Boulevard
Alachua, FL 32615
(904) 462-3913
(800) 225-0308 (outside FL)

MID-CONTINENT
Mr. Gary Sera
Texas Engineering Extension Service
Texas A&M University System
301 Tarrow Street
College Station, Texas 77843-8000
409-845-8762

MID-WEST
Dr. Joseph W. Ray
Great Lakes Industrial Technology Center
25000 Great Northern Corporate Center
Suite 260
Cleveland, OH 44070-5310
(216) 734-0094

FAR-WEST
Mr. Robert Stark
Technology Transfer Center
University of Southern California
3716 South Hope Street,
Suite 200
Los Angeles, CA 90007-4344
(213) 743-6132
(800) 642-2872 (CA only)
(800) 872-7477 (toll-free US)

If you are interested in information, applications, research, training, and services relating to satellite and aerial data for Earth resources, contact NASA's transfer point for earth observing technology: **Earth Data Analysis Center, University of New Mexico, 2500 Yale Blvd. S.E., Suite 100, Albuquerque, NM 87131-6031; Dr. Stan Morain, Director (505) 277-3622.**

If you represent a public sector organization with a particular need, you can contact NASA's Application Team for technology matching and problem solving assistance. Staffed by professional engineers from a variety of disciplines, the Application Team works with public sector organizations to identify and solve critical problems with existing NASA technology. **Technology Application Team, Research Triangle Institute, P.O. Box 12194, Research Triangle Park, NC 27709; Dr. Doris Rouse, Director, (919) 541-6980**

A Shortcut To Software: **COSMIC®**—For software developed with NASA funding, contact COSMIC, NASA's Computer Software Manage-ment and Information Center. New and updated programs are announced in the Computer Programs section. COSMIC publishes an annual software catalog. For more information call or write: COSMIC®, 382 East Broad Street, Athens, GA 30602 John A. Gibson, Director, (706) 542-3265; FAX (706) 542-4807.

If You Have a Question..**NASA Center For AeroSpace Information** can answer questions about NASA's Technology Transfer Network and its services and documents. The CASI staff supplies documents and provides referrals. Call, write or use the feedback card in this issue to contact: NASA Center For AeroSpace Information, Technology Transfer Office, 800 Elkridge Landing Rd, Linthicum Heights, MD 21090-2934. Walter M. Heiland, Manager, (410) 859-5300, Ext. 245.

Which gets your data faster and easier?

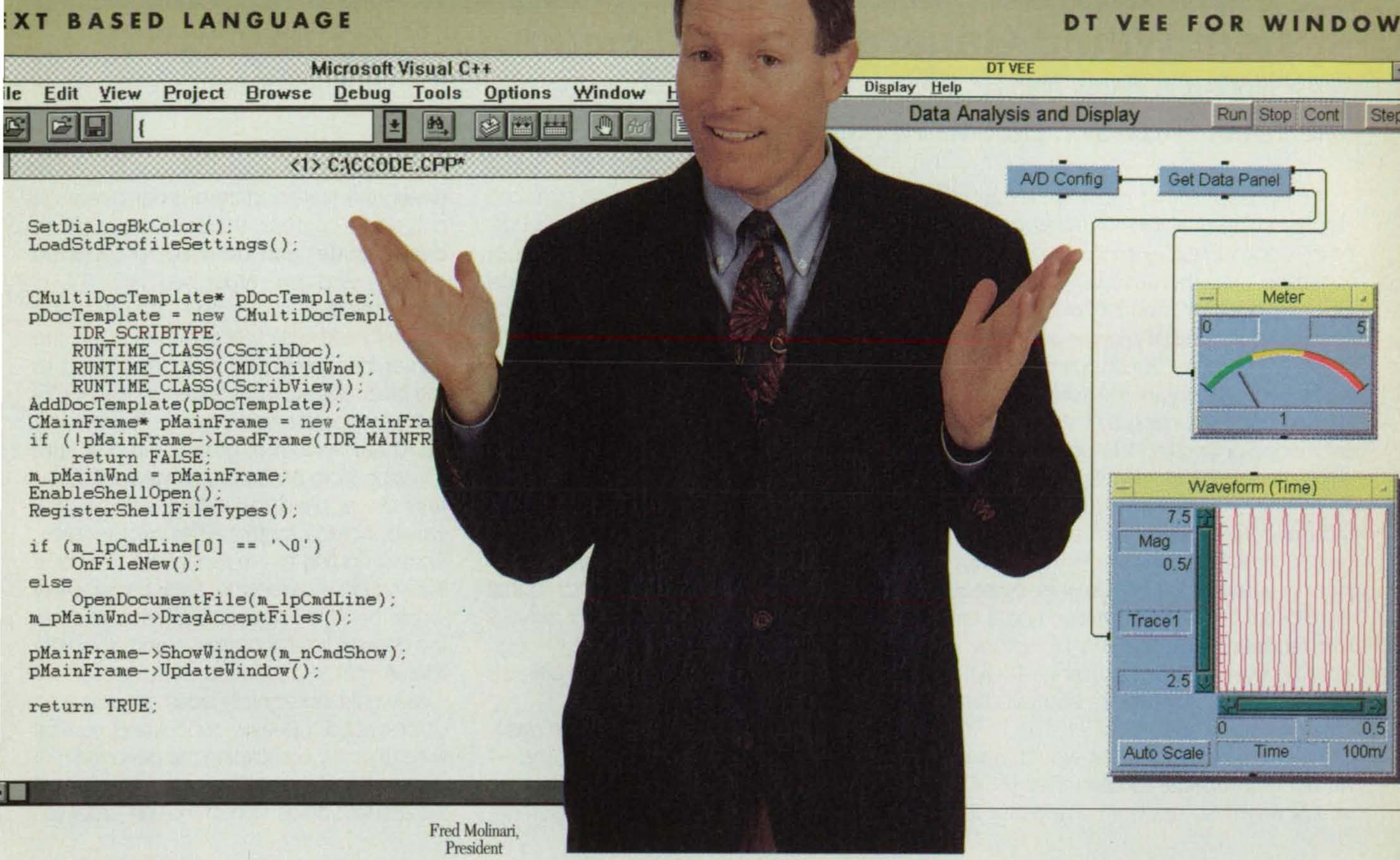

Fred Molinari,
President

DT VEE for Windows: the Obvious Choice

GET DATA FAST AND EASY!

A complete application in three simple steps

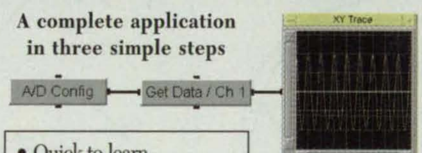

- Quick to learn, easy to use
- Powerful data analysis and display
- 100% Windows: simplified interface, DDE
- Flexible application development and maintenance
- No time-consuming compiling—ready to run

Half Price! All VEE Products
Limited Time Offer. Call Today!

Speed your application development with DT VEE™ for Windows.™ DT VEE is a complete graphical programming approach that lets you create sophisticated data acquisition applications without ever writing code.

With DT VEE, you easily create, debug, and document. Program development is intuitive—simply connect function-specific objects in a logical sequence and run. It's that easy.

With more than 180 analysis functions, comprehensive display capabilities, and full hardware support, DT VEE has everything you need for data acquisition. DT VEE is based on HP VEE for Windows,™ and is backed by the Hewlett-Packard and Data Translation commitment to quality.

Call 1-800-525-8528 today (In USA and Canada).
***FREE* DT VEE evaluation version available.**

DATA TRANSLATION® **World Headquarters: (508) 481-3700, UK Headquarters: (0734) 793838, Germany Headquarters: (07142) 95 31-0, Italy Headquarters: (030) 2425696. Sales Office** Argentina (1) 322-3791; Australia 2699-8300; Austria (222) 367660; Belgium (02) 466.81.99; Brazil 011-564-6024; Canada (800) 525-8528, (800) 268-0427; China (1)-8318811-52 Denmark 42 27 45 11; Finland (0) 3511800; France (1) 69.07.78.02; Greece (1) 361-4300; Hong Kong 515-0018; India 22-2831040; Israel 09-545685; Japan (03) 5379-1971, (03) 5489-3871, (03) 5689-8000; Korea (2) 718-9521; Malaysia (3) 248-6786; Mexico 575-6091; Netherlands (70) 399-6360; New Zealand (9) 415-8362; Norway (22) 43 41 50; Portugal (1) 793483 Singapore 773 4300; South Africa (12) 803-7680/93; Spain (1) 555-8112; Sweden 08-765 02 80; Switzerland (1) 908-1360; Taiwan (2) 3039836; Thailand (02) 281-9596; Turkey (212) 288-6213 4/27/

For More Information Write In No. 615

System Would Generate Virtual Heads-Up Display

Color alphanumerical and/or graphical information would be overlaid on the visual field.

NASA's Jet Propulsion Laboratory, Pasadena, California

A proposed helmet-mounted electronic display system would superimpose full-color alphanumerical and/or graphical information onto the observer's visual field. The displayed information would be projected directly onto the observer's retinas, giving the observer the illusion of a full-size computer display in the foreground or background. Depending on the chosen optical modulator and modulation scheme, the display could be stereoscopic, holographic, or in the form of a virtual image. The system could be used, for example, by a pilot to view navigational information while looking outside or at instruments, by security officers to view information about critical facilities while looking at visitors, or possibly even in stock-exchange facilities to view desktop monitors and overhead displays simultaneously.

The system (see figure) would include an acousto-optical tunable filter (AOTF), which would act as both a spectral filter and a spatial light modulator, as explained below. In general, an AOTF includes a bulk acousto-optical crystal and a thin piezoelectric transducer, driven by an electrical radio-frequency source, which launches either longitudinal or shear acoustic waves into the bulk acousto-optical crystal. The induced acoustic wave propagates through this bulk medium and modulates the index of refraction in the medium. Light that enters the AOTF interacts with the acoustic field such that light within a narrow wavelength passband is diffracted into +1 and −1 orders. The polarization of the diffracted light is perpendicular to that of the incident light. Part of the light remains undiffracted and passes straight through the device: this light is said to be diffracted to zero order.

Whether the input light within the passband is diffracted into the +1 or the −1 order depends on the polarization of the input. Typically, the angular separation between the first- and zero-order beams is only a few degrees; therefore, a polarizing beam splitter can be used to separate the first- and zero-order beams.

The middle wavelength of the passband for first-order diffraction depends on the carrier frequency of the signal applied to the piezoelectric transducer on the AOTF. In the proposed system, the AOTF would be illuminated with red, green, and blue light (possibly from an He/Cd "white-light" laser) and the applied radio-frequency signal would include three carrier frequencies, corresponding to the red, green, and blue illumination wavelengths. Each carrier signal would be amplitude-modulated to encode the desired spatial pattern along a vertical line. A mirror oscillating about a vertical axis would horizontally scan the resulting color-coded, spatially modulated vertical lines, thereby completing the generation of a raster-scan output. To reduce the effect of wavelength dispersion of the first-order dif-

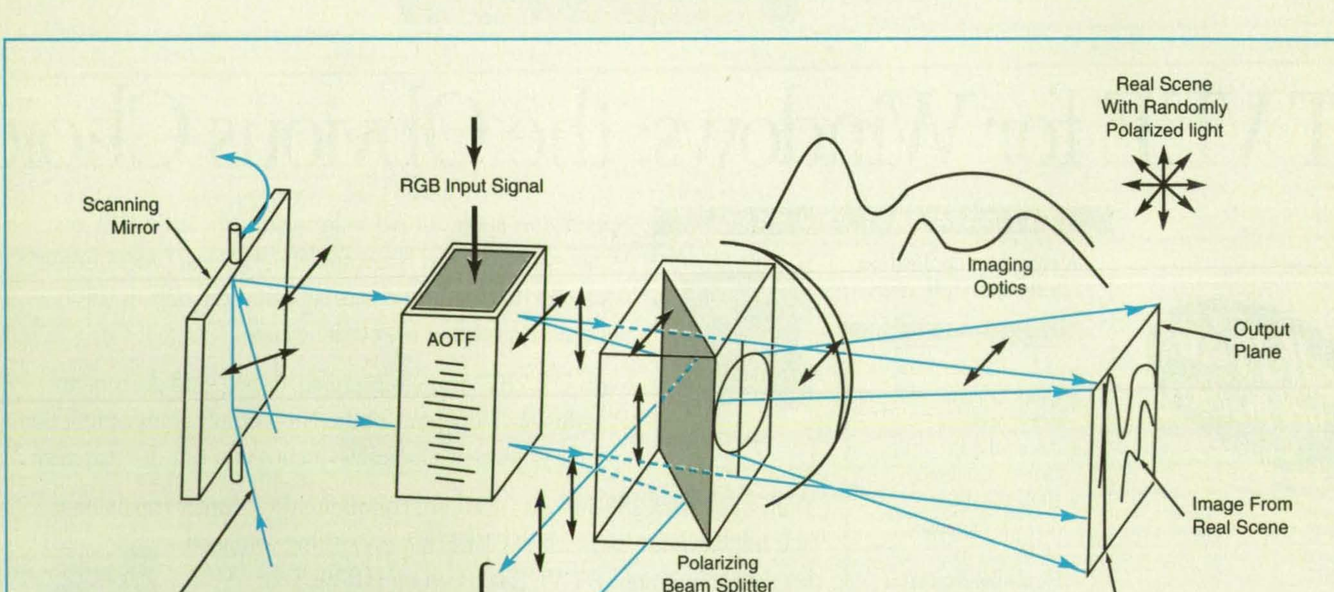

The **Virtual Heads-Up Display System** would frequency- or time-multiplex red, green, and blue (RGB) signals into an AOTF to form spectrally and spatially encoded vertical scan lines. A pulsed, linearly polarized RGB source would illuminate the AOTF periodically as each acoustically encoded vertical scan line filled the aperture of the AOTF. An oscillating scanning mirror would map each vertical scan line into the correct horizontal position in the output plane. A polarizing beam splitter would be used to remove the unused first-order-diffracted light and to overlay a real scene on the output plane.

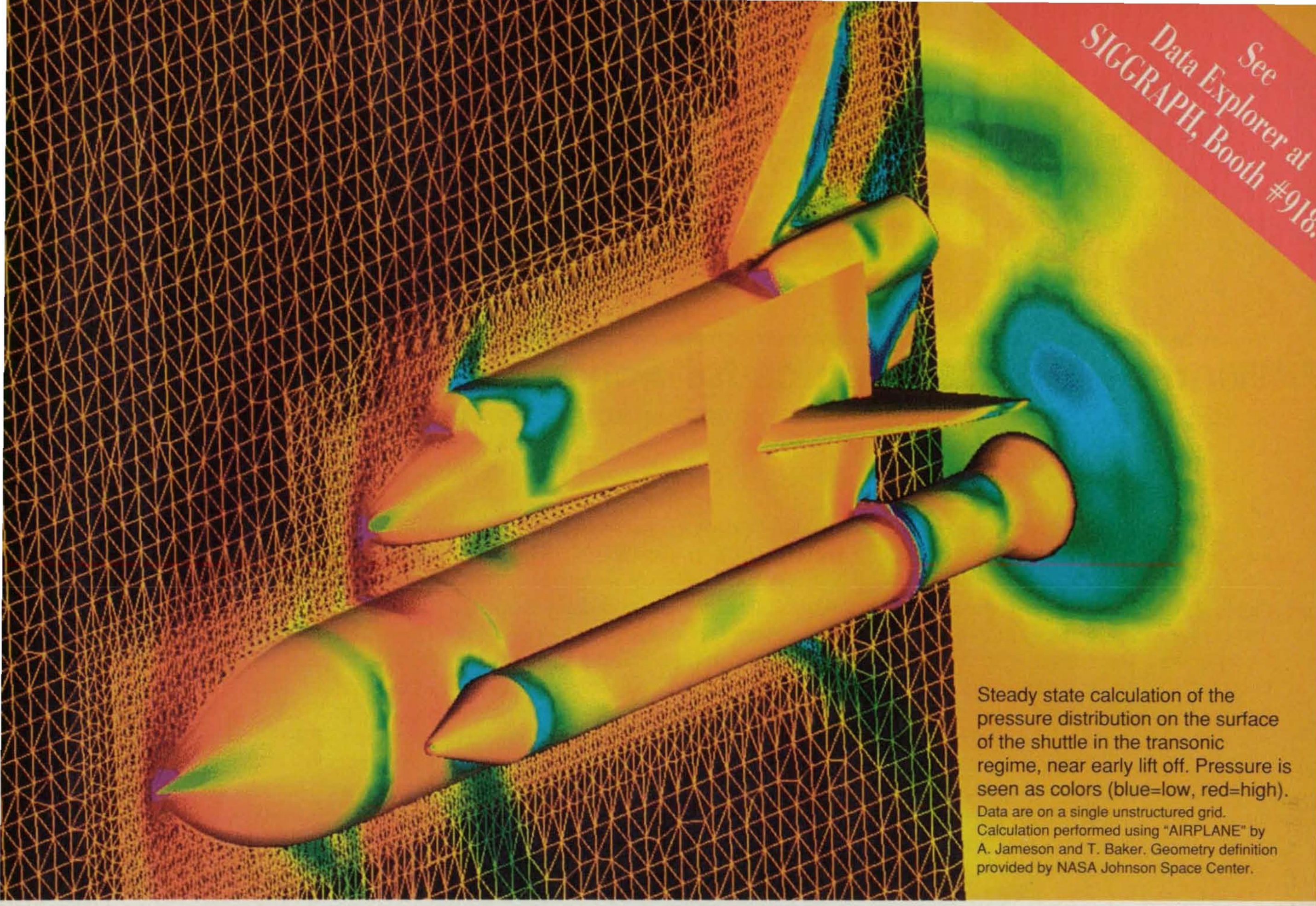

Steady state calculation of the pressure distribution on the surface of the shuttle in the transonic regime, near early lift off. Pressure is seen as colors (blue=low, red=high). Data are on a single unstructured grid. Calculation performed using "AIRPLANE" by A. Jameson and T. Baker. Geometry definition provided by NASA Johnson Space Center.

Boldly go where no visualization software has gone before.

Try IBM Visualization Data Explorer, the advanced visualization software for your SGI, Sun, HP or IBM RISC System/6000™ workstation...*free for 60 days.*

IBM Visualization Data Explorer™ gives you new control over your data...and new insights into their meaning. Yet Data Explorer is easy to use because it lets you visualize data in ways you've never dreamed of–without getting bogged down in the technology.

Here are just a few of the things you can do with Data Explorer:

- Freely combine different visual techniques within the same image.
- Quickly correlate data from various sources, such as simulations and observations, and view them together.
- Directly produce exciting animations from time series without production nightmares.

Data Explorer also has a powerful, extensible tool kit that provides fast access to a broad range of sophisticated functions, both visual and computational.

Whether you're a visualization novice or expert, you can try Data Explorer on your workstation, free for 60 days, no strings attached. **Call: (800) 388-9820.** Or write IBM Visualization Systems, T.J. Watson Research Center, P.O. Box 704, Yorktown Heights, NY 10598.

IBM®

fraction patterns, the spatial modulation patterns would be devised so that the first-order-diffracted light would be discarded via the polarizing beam splitter, and the zero-order beam would carry the spatially and spectrally encoded information to the output plane.

This work was done by James L. Lambert of Caltech for **NASA's Jet Propulsion Laboratory**. *For further information,* ***write in 13*** *on the TSP Request Card.*

This invention is owned by NASA, and a patent application has been filed. Inquiries concerning nonexclusive or exclusive license for its commercial development should be addressed to the NASA Patent Counsel, NASA Resident Office–JPL [see page 20].

Refer to NPO-18736.

Window-Based Graphics for Scheduling

XOPPS can be used in conjunction with project-management software.

The XOPPS computer program generates window-based graphics for scheduling and planning projects. XOPPS provides easy and fast on-screen "what-you-see-is-what-you-get" (WYSIWYG) editing capabilities. The display includes a canvas area that contains the full image of the schedule being edited. The canvas also contains a header area for text and a schedule area for plotting graphical representations of milestone objects in a flexible timeline.

XOPPS is object-oriented, but it is unique in its capability for creating objects that have date attributes. Each object on the screen can be treated as a unit for moving, editing, and the like. There is a mouse interface for simple control of the location of a pointer. The user can position objects to pixel resolution, but objects with associated dates are positioned automatically in their correct timeline positions in the schedule area.

A page with horizontal lines across it is superimposed on the schedule area. The program provides capabilities for multiple pages and for editing the number of lines per page and the line grid. The text on a line can be edited, and a line can be moved, all objects on the line moving with it. The timeline display can be edited to plot any time period in a variety of formats from fiscal year to calendar year and days to years. Text objects and image objects (rasterfiles and icons) can be created for placement anywhere on the page. Milestone event objects with single associated dates (and optional text and milestone symbols) and activity objects with start and end dates (and optional completion dates) contain unique editing panels for entering data. A representation for schedule slips is also provided, with the capability to convert a milestone event to a slip automatically. A milestone schedule on another computer can be saved in an ASCII file to be read by XOPPS. The program can print a schedule into a PostScript file. Dependences between objects can also be displayed on the chart through the use of precedence lines.

This program is not intended to replace a commercial scheduling/project-management program. Because XOPPS includes an ASCII file interface, it can be used in conjunction with project-management software to produce schedules with an appearance of quality.

XOPPS is written in C language for Sun-series workstations running SunOS. This software package requires MIT's X Window System, Version 11 Revision 4, with OSF/Motif 1.1. A sample executable code is included. XOPPS requires 375K of main memory and 1.5 Mb of free disk space for execution. The standard distribution medium is a 0.25-in. (6.35-mm) streaming-magnetic-tape cartridge in UNIX tar format. XOPPS was developed in 1992, based on the Sunview version of OPPS (NPO-18439) developed in 1990. It is a copyrighted work with all copyright vested in NASA.

This program was written by Cassie Mulnix and Kevin Miller of Caltech for **NASA's Jet Propulsion Laboratory**. *For further information,* ***write in 29*** *on the TSP Request Card.*

NPO-19156

Fully Three-Dimensional Virtual-Reality System

A virtual space traveler would perceive orientation without reference to a ground plane.

NASA's Jet Propulsion Laboratory, Pasadena, California

A proposed virtual-reality system would present visual displays to simulate free flight in three-dimensional space. The system, called a virtual space pod, would be a testbed for control and navigation schemes. Unlike most virtual-reality systems, the virtual space pod would not depend for orientation on a ground plane, which could hinder free flight in three dimensions.

The virtual traveler (the person occupying the pod) would don video goggles and sit in a comfortable chair equipped with a joystick on each armrest (see figure). The virtual traveler would see a virtual scene (e.g., interstellar, aerial, or underwater scene) in the goggles. The orientation of the virtual traveler's head would be measured, and the scene as presented to the virtual traveler would be changed accordingly. A ball on the end of each joystick could be pushed, pulled, and turned, providing a total of six degrees of freedom.

In a representative scenario, the virtual traveler would be asked to navigate to a red star, visible in the goggles about 60° above and 45° to the left of dead center. The virtual traveler would press button A (one of three buttons on the outside of the armrest), causing navigation circles to appear on the field of stars. The navigation circles would be three blue and three yellow circles surrounding the virtual traveler, with major tick marks every 30° and minor tick marks every degree. The blue circles would be fixed to the global (e.g., interstellar or Earth-based) coordinate system, while the yellow circles would lie in a coordinate system attached to, and moving with, the space pod. The circles would help the virtual traveler visualize the orientation of the pod.

The virtual traveler would twist the joystick ball to the left and back to make the yellow circles start to move within the blue ones; this would make the red star start to move toward front and center. The vir-

tual traveler would then push the ball slightly forward and simultaneously pull it up a little, causing the pod to begin moving virtually toward the red star; the virtual traveler would see other stars in the peripheral field of view start to slide past slowly.

As the destination star approached front and center, the virtual traveler would slowly relax the twist and upward pull on the ball, then push the ball forward, accelerating the pod. When the pod was up to speed, the virtual traveler would release the ball, then twist it slightly to align a horizontal yellow navigation circle with the most nearly horizontal-looking blue circle. The pod would then be on course, and the virtual traveler would see peripheral stars rushing by.

The star would grow in size and several orbiting planets would appear. The virtual traveler could then change course to explore a planet. The virtual traveler would pull back on the ball to decelerate the pod to a stop. The virtual traveler would then press button B to obtain red navigation circles aligned with the coordinate system fixed to one of the planets (or to a local coordinate system in a terrestrial setting). The virtual traveler would then use the joystick to orient the yellow circles with the red ones and proceed to a planet.

VIRTUAL TRAVELER IN SPACE POD

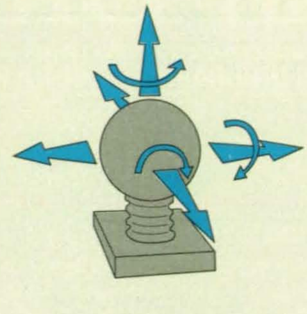

DETAIL OF JOYSTICK, SHOWING TRANSLATIONAL AND ROTATIONAL DEGREES OF FREEDOM OF BALL

The Space Pod would provide comfortable seating, convenient controls, and dynamic virtual-space images for a virtual traveler. The controls would include buttons plus joysticks with six degrees of freedom.

This work was done Brian C. Beckman of Caltech for **NASA's Jet Propulsion Laboratory**. *For further information,* ***write in 102*** *on the TSP Request Card.*

This invention is owned by NASA, and a patent application has been filed. Inquiries concerning nonexclusive or exclusive license for its commercial development should be addressed to the Patent Counsel, NASA Resident Office-JPL [see page 20]. Refer to NPO-18733.

Program Supports Scientific Visualization

GVS helps to convert data outputs to graphical displays.

The primary purpose of the General Visualization System (GVS) computer program is to support scientific visualization of data generated by the panel-method computer program PMARC_12 (inventory number ARC-13362) on the Silicon Graphics Iris workstation. GVS enables the user to view PMARC geometries and wakes as wire frames or as light shaded objects. In addition, geometries can be color-shaded according to such parameters as pressure coefficients or velocities. Screen objects can be interactively translated and/ or rotated to facilitate viewing. Keyframe animation is also available for studying unsteady cases. The purpose of scientific visualization is to enable investigators to gain insight into the phenomena they are examining. Therefore, GVS emphasizes analysis, not artistic quality. GVS uses existing IRIX 4.0 image-processing software tools to provide for conversion of SGI RGB files to other formats.

GVS is a self-contained program that contains all the necessary interfaces to control interaction with PMARC data. This includes (1) the GVS Tool Box, which supports color histogram analysis, lighting control, rendering control, animation, and positioning; (2) GVS on-line help, which enables the user to gain access to control elements and get information about each control simultaneously; and (3) a limited set of basic GVS data-conversion filters, which provide for the display of data in simpler formats. Specialized controls for handling PMARC data include animation and wakes, and visualization of off-body scan volumes.

GVS is written in C language for use on SGI Iris-series workstations running IRIX. It requires 28 Mb of random-access memory for execution. Two separate GVS documents are available. The basic document price for ARC-13361 includes only the GVS User's Manual, which outlines major features of the program and provides instruction on the use of GVS with PMARC_12 data. Programmers interested in modifying

GVS for use with data in formats other than that of PMARC_12 may purchase a copy of the draft GVS 3.1 Software Maintenance Manual separately, if desired, for $26. An electronic copy of the User's Manual, in Macintosh Word format, is included on the distribution medium. Purchasers of GVS are advised that if they attempt to change and/or extend GVS, they do so at their own risk. In addition, GVS includes an on-line help system and sample input files. The standard distribution medium for GVS is a 0.25-in. (6.35-mm) streaming-magnetic-tape cartridge in IRIX tar format. GVS was developed in 1992.

This program was written by Stephan Keith of Sterling Software for **Ames Research Center**. *For further information,* ***write in 67*** *on the TSP Request Card.*
ARC-13361

Computer Modeling of Atomization

Mathematical models developed from first principles have been partially verified by experimental data.

Marshall Space Flight Center, Alabama

Improved mathematical models based on fundamental principles of conservation of mass, energy, and momentum have been developed for use in computer simulation of atomization of jets of liquid fuel in rocket engines. These models can also be used to study atomization in terrestrial applications; they could prove especially useful in designing improved industrial sprays — humidifier water sprays, chemical process sprays, and sprays of molten metal, for example.

The difficulty in computer simulation of atomization arises from the relatively large number of parameters that influence it. Most of the older mathematical models of atomization in rocket engines depend on empirical correlations obtained from cold-flow experiments. Because the present improved mathematical models are based on first principles, they are only minimally dependent on empirical correlations and are better able to represent the hot-flow conditions that prevail in rocket engines and that are too severe to be accessible for detailed experimentation.

One of the improved mathematical models, called the "primary atomization model," comprises linear and nonlinear submodels through which one can study the influence of various parameters on the atomization process. These parameters include free-stream values of velocities, Reynolds numbers, and Weber numbers. One of these submodels (a linear wave model) has been found to predict drop-size distributions and intact-liquid-core lengths that agree well with those observed in cold-flow experiments. Another, nonlinear submodel predicts the formation of satellite drops in the breakup of low-speed jets.

The deformation and breakup of droplets affects the efficiency of spray combustion. There are two mechanisms of such deformation and breakup: shear breakup and bag breakup. These mechanisms are represented by another of the improved models, called the "secondary atomization model" or, alternatively, the "droplet deformation and breakup" model. This model is based on the equations for the energy balance of liquid drops. It can be coupled with the primary atomization model to obtain a more-realistic simulation of the atomization process.

Another model represents the flow field that results from impingement of a cylindrical jet; this model can predict the sizes of drops produced by impingement. Still another model that represents swirling jets can predict the cone angles and thicknesses of hollow conical sprays.

The primary atomization model can be coupled with a model that represents the dynamics of a chemically reacting flow to obtain a model and computer code for embedding a jet in an overall chemically reacting flow field (e.g., a spray of fuel into a combustion chamber). The overall model accounts for the strong mutual coupling between the liquid and gas phases. The liquid- and gas-phase equations are coupled through initial and boundary conditions. In this representation, the differential equations that describe the dynamics of the liquid-jet core are solved by marching in space on an adaptive grid that conforms to the shape of the jet. Another grid for computation of the dynamics of the gas phase is then adapted to the shape of the liquid core. The interface between the liquid and gas is modeled as a sliding wall that moves with the velocity of the jet; this defines the boundary condition for velocity of the gas. Droplets that leave the interface are tracked by solving the Lagrangian equations of their motions. The exchanges of mass, momentum, and energy between the droplets and the gas are represented as source and sink terms in the equations for the dynamics of the gas phase. A global model of chemistry represents the combustion process.

This work was done by M. Giridharan, E. Ibrahim, A. Przekwas, S. Cheuch, A. Krishnan, H. Yang, and J. Lee of CFD Research Corp. for **Marshall Space Flight Center**. *For further information,* ***write in 90*** *on the TSP Request Card.*
MFS-28721

Electronic Components and Circuits

Reconfigurable Full-Page Braille Displays

Relative simplicity and low cost may result in widespread use.

Langley Research Center, Hampton, Virginia

Electrically actuated braille display cells of a proposed type could be arrayed together to form full-page braille displays. Like other braille display cells, these would provide changeable patterns of bumps driven by digitally recorded text stored on magnetic tapes or in solid-state electronic memories.

These cells would differ from cells in current use that contain sets of pins that are raised to form the dots of braille characters. One of the disadvantages of the cells in current use is that each pin must be actuated independently by a magnetic, piezoelectric, or pneumatic device; this makes the cells and the displays that contain them bulky and expensive. Furthermore, the pin-based braille cell display units are generally limited to single lines of 20 to 40 characters each because of the complexity and cost of the pin mechanisms. Display units that contain the proposed cells would not only display full pages of text but should also be cheap enough for mass production and widespread use.

The proposed cells would contain an electrorheological fluid. The viscosity of such a fluid increases in a strong electrostatic field. Cornstarch in corn oil, zeolite in silicone oil, and aluminum dihydrotripolyphosphate in mineral oil are among the materials that exhibit the electrorheological effect.

The figure shows the part of a proposed cell that would actuate one dot of a braille character. The electrorheological fluid would flow from a manifold through an entrance orifice into a chamber at the position of the dot. In the absence of electrical excitation, the relatively large exit orifice in the chamber would let the fluid flow out with little restriction so that little pressure would build up in the chamber. However, when a voltage was applied between a common electrode and an individual electrode at the exit orifice, the viscosity of the fluid between the electrodes would rise enough to restrict the flow and build up the pressure in the chamber. A diaphragm on the outer surface of the chamber would then bulge out, creating a bump that the reader would perceive as a dot in a braille character. When the voltage was removed from the electrodes, the flow would resume and the diaphragm would relax.

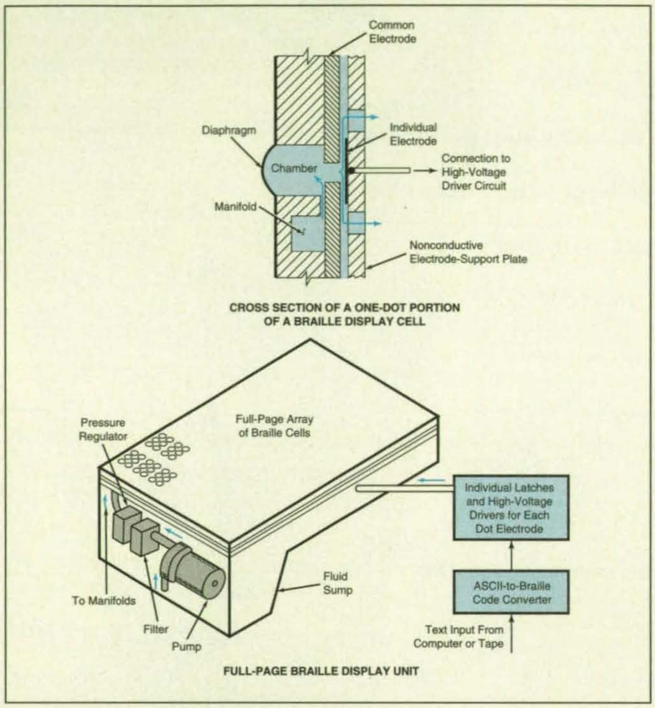

Fluid Would Be Pumped continuously into the manifold, from which it would flow into chambers like this one, each representing a braille dot. A high voltage applied to the electrodes would raise the viscosity of the fluid, causing the pressure in the chamber to increase and the diaphragm to bulge, thereby forming a braille dot.

The cells would be laid out with the dots in the groups of six that constitute the matrices of the braille characters. A pageful of characters would be arranged on a platen equipped with a fluid reservoir, pump, and control-logic circuits. The control-logic circuits would read out text from a cassette tape player or computer memory as ASCII or other digital code and convert it into braille code for high-voltage drivers on the dot chambers.

This work was done by H. Douglas Garner of **Langley Research Center**. *No further documentation is available.*

Inquiries concerning rights for the commercial use of this invention should be addressed to the Patent Counsel, Langley Research Center [see page 20].
Refer to LAR-14860.

Power-Conserving Stepping-Motor Drive Circuits

Motor currents are reduced when loads are reduced.

Marshall Space Flight Center, Alabama

Two improved drive circuits for a sinusoidally commutated stepping motor include feedback loops that reduce the unnecessary consumption of power by reducing the drive-current amplitude, I, when the motor operates under a light load. The basic design strategy is to attempt to supply only a little more current than the minimum needed to overcome friction in the lightly loaded condition. Older drive circuits of this type supply current at a constant high value of I, regardless of

The Company that Wrote the Book on PC Data Acquisition Announces a New Chapter.

ISO 9001 CERTIFIED — KEITHLEY METRABYTE

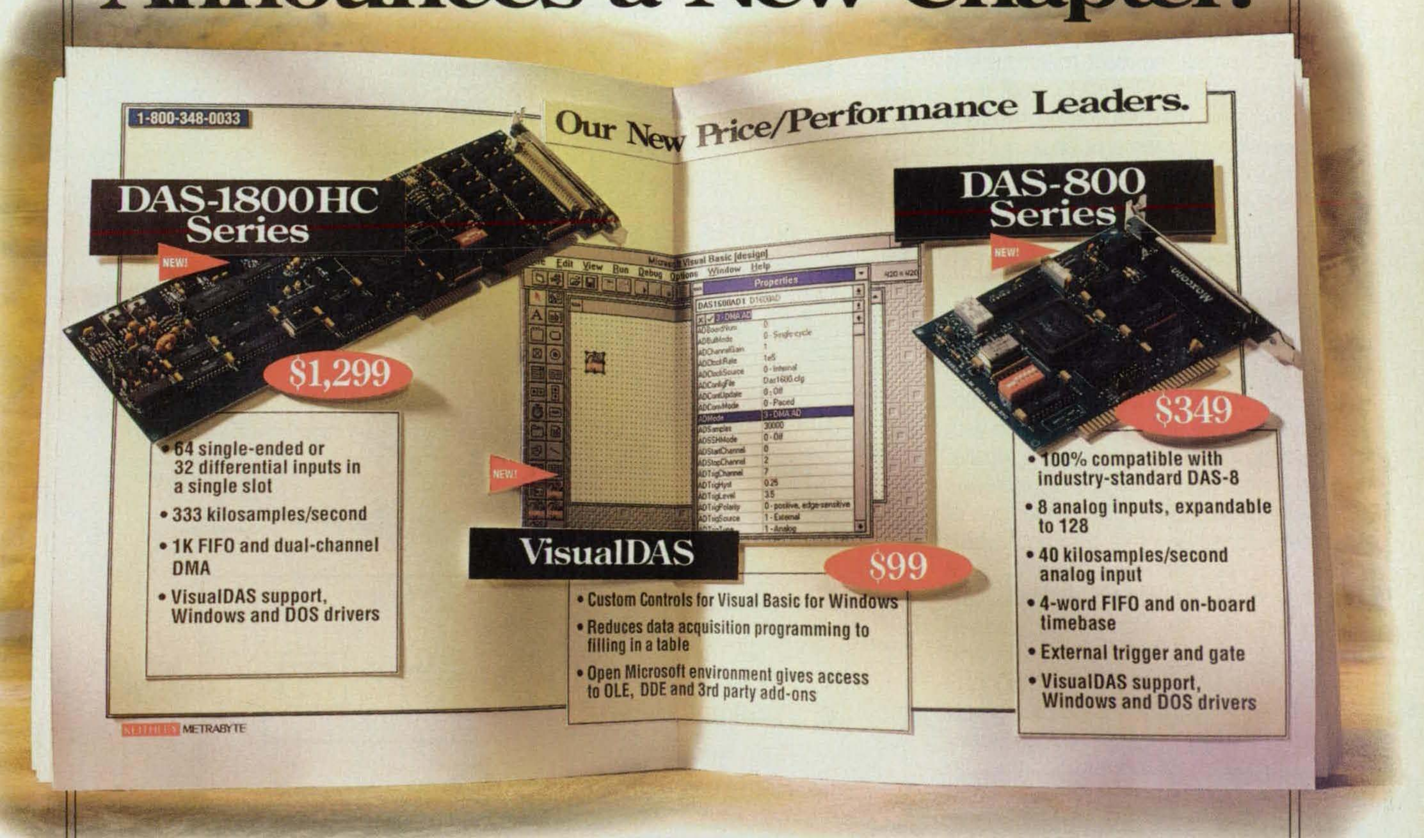

Here's the story: Keithley MetraByte once again sets the standards in PC data acquisition by introducing new, powerful price/performance leaders.

World Class Technical Support

A novel approach to value. Breakthrough performance. World-class support. Unbelievable prices. Only Keithley MetraByte provides this winning combination in a product line built for your applications. So whether you monitor temperatures or high-speed waveforms, are in R&D or on the factory floor, we have the products and support you need.

Hardware and software integration. Our software and hardware are designed to work together. Our software solutions range from easy, point-and-click packages to in-depth programming tools. And comprehensive *drivers* let you program in virtually any language, under Windows or DOS.

Pick up a bestseller today. Call 1-800-348-0033 to order our new DAS products or to get a copy of our catalog. You won't be able to put it down.

1-800-348-0033

Systems Integrator inquiries welcome

KEITHLEY METRABYTE

Keithley MetraByte, 440 Myles Standish Blvd., Taunton, MA 02780. Tel 508-880-3000 FAX 508-880-0179

Windows and Visual Basic are trademarks of Microsoft Corporation.

load, so that the power dissipated remains constant at a high value of I^2R (where R is the effective electrical resistance of the motor).

Figure 1 illustrates schematically a sinusoidally commutated, two-phase stepping motor, in which drive currents of $I \sin(x)$ and $I \cos(x)$ are supplied to phases A and B, respectively, to position the rotor at the commanded angle x. When the actual rotor angle differs from x by an amount θ, the motor exerts a torque, $-KI \sin(\theta)$ (where K is the torque constant of the motor), that urges the rotor toward angle x. When the motor is lightly loaded, θ remains small, so that the torque remains small, even though I remains large, and the motor thus operates inefficiently. When the motor is more heavily loaded, θ increases, resulting in more efficient operation in that the same I generates more torque.

The motor includes Hall-effect devices that measure the actual angle $(x + \theta)$ of the rotor. The improved drive circuits use the outputs of these sensors plus the angle-command signals to make I increase with θ. The first of the improved drive circuits, shown at the top of Figure 2, includes two pairs of multipliers. The lower pair of multipliers, together with a subtractor, produces a signal proportional to $\sin(x + \theta)\cos(x) - \cos(x + \theta)\sin(x)$, which equals simply $\sin(\theta)$. This signal is processed through an absolute-value circuit and summed with a dc bias, yielding a signal $D + |C \sin(\theta)|$, where D is the dc bias and C is a constant. Then by use of the upper pair of multipliers, I is made proportional to this signal. Thus, I increases with θ and increases with the load. D is chosen so that the minimum value of I (at $\theta = 0$) is sufficient to overcome bearing friction and other losses in the motor.

The second of the improved drive circuits, shown at the bottom of Figure 2, differs from the first circuit in that it makes I vary in proportion to $|\theta|$ instead of to $|\sin(\theta)|$. It includes an oscillator (typically with a frequency of 5 kHz) that generates in-phase and quadrature carrier signals. By use of trigonometric identities and other concepts similar to those of the first circuit, this circuit produces intermediate signals proportional to $\cos(x + \theta - \omega t)$ and to $\cos(x - \omega)$ (where $\omega = 2\pi \times$ frequency and t = time). These signals are processed through squaring circuits, yielding two square waves, at frequency $\omega/2\pi$, the phases of which differ by θ. These square waves are processed through the circuit shown in dashed outline, to obtain a dc signal $|C\theta|$. This signal is added to a dc bias, and the sum signal is used as before to multiply the amplitude of the angle-command signals.

This work was done by Frank J. Nola

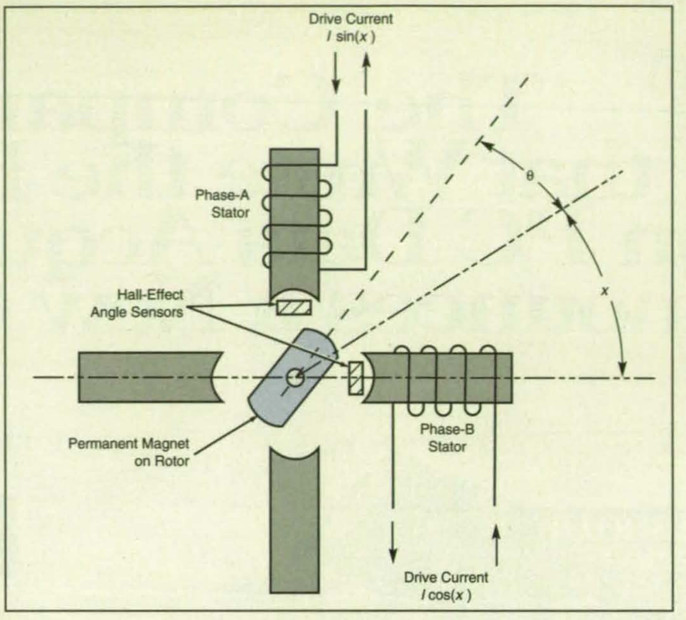

Figure 1. In this **Sinusoidally Commutated Two-Phase Stepping Motor**, the magnetic field generated by the drive currents in the phase-A and phase-B stator windings urges the rotor toward commanded angle x.

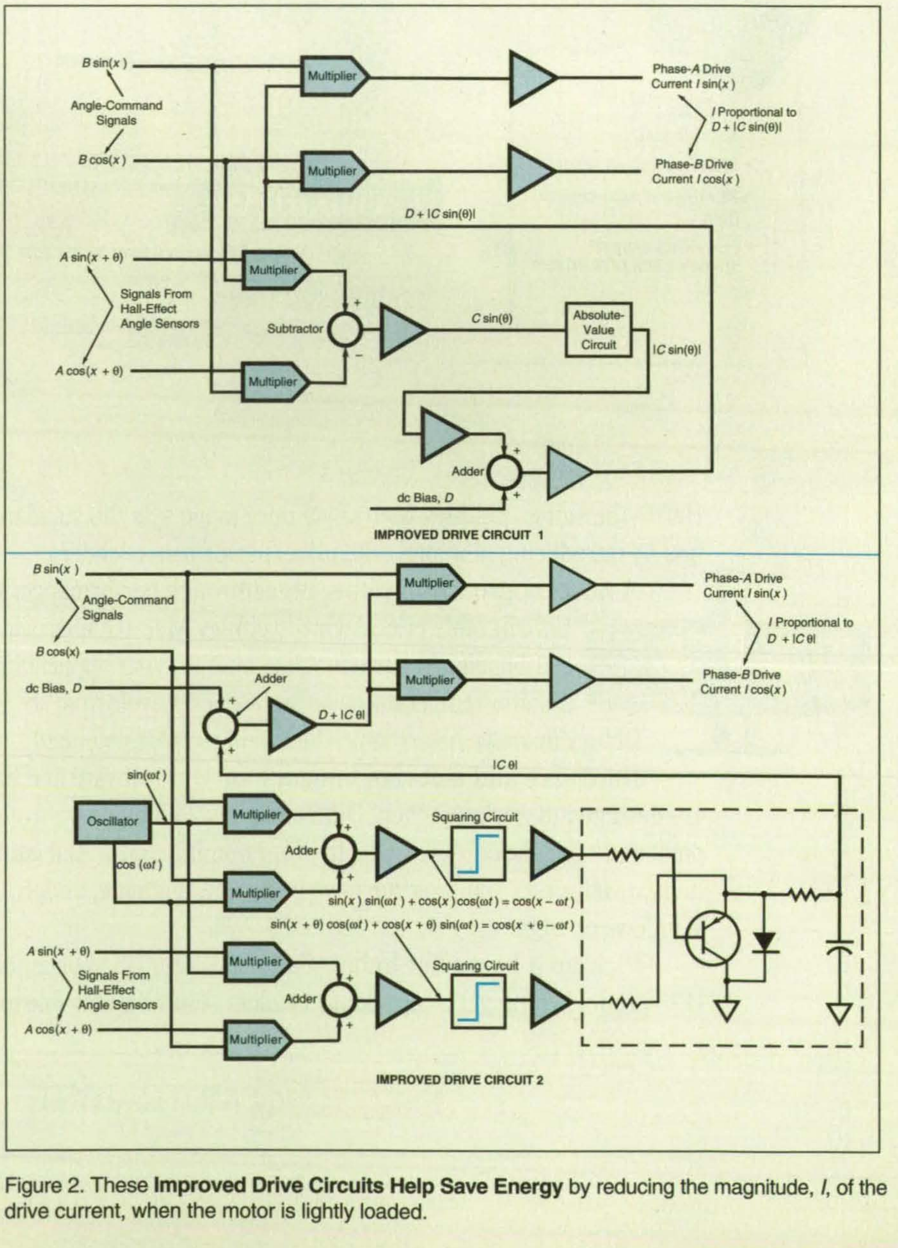

Figure 2. These **Improved Drive Circuits Help Save Energy** by reducing the magnitude, I, of the drive current, when the motor is lightly loaded.

Engine development

Measure casting temperatures

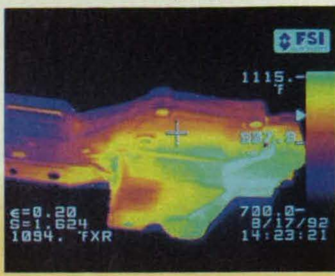

Defects in composite materials

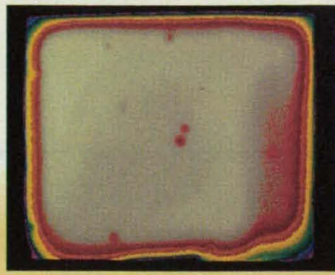

Moisture content in paper

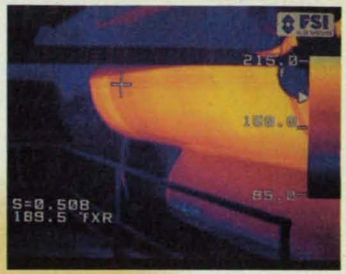

Monitor soldering processes

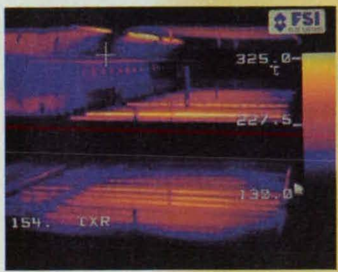

Injection mold performance

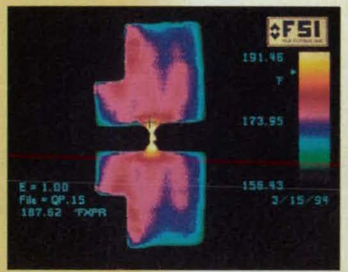

FLIR SYSTEMS POINTS OUT YOUR DEFECTS WITH WARMTH AND SENSITIVITY.

Evaluate wax injection presses

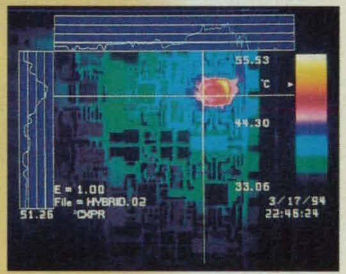

Hybrid circuit failure analysis

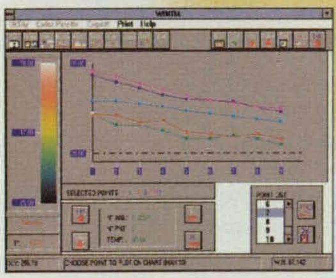

Analyze trend data

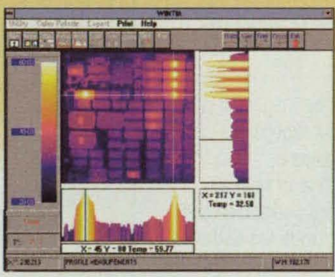

Post-processing thermal analysis

A variety of desktop, portable and hand-held systems to fit your needs

Our infrared (IR) imaging products detect and measure a variety of thermal conditions through easy-to-use, non-contact infrared imaging technology.

What's more, we have the industry's broadest selection of IR products: the IQ Series of real-time image processing systems; the hand-held Prism infrared cameras; Windows™-based image analysis software; and a full range of accessories. So whether you work in R&D, process monitoring and control or non-destructive testing, let our skilled applications engineers help you solve your problems. Call FLIR Systems at 1-800-322-3731 for more information or to arrange for a sample IR analysis at your site or in our laboratory.

FSI
FLIR SYSTEMS™

16505 SW 72nd Ave., Portland, OR 97224, (503) 684-3731, Fax (503) 684-3207

For More Information Write In No. 696

and David E. Howard of **Marshall Space Flight Center**. For further information, **write in 40** on the TSP Request Card.

Inquiries concerning rights for the commercial use of this invention should be addressed to the Patent Counsel, Marshall Space Flight Center [see page 20]. Refer to MFS-28854.

Isolation Amplifier Based on Sigma-Delta Modulation

Relatively imprecise digital pulses convey an analog signal with relatively high precision.

Lyndon B. Johnson Space Center, Houston, Texas

An improved isolation amplifier transmits a dc or low-frequency analog signal by use of digital pulses. Even though the instantaneous amplitudes of the pulses can be relatively imprecise, the output signal approximates the input signal with a precision greater than that achievable in older isolation amplifiers in which the input signals are chopped into square waves and transmitted by transformer or capacitive coupling.

The improved isolation amplifier implements a sigma-delta modulation scheme, in which the input voltage, v_{in}, is summed with a precise positive or negative reference voltage ($\pm V_{ref}$), and the output waveform is reconstructed with the help of $\pm V_{ref}$ sources on the other side of the electrical isolation barrier. The overall precision of this isolation amplifier is limited only by the dc performances of the operational amplifiers in it and by the precision of the $\pm V_{ref}$ sources on both sides of the electrical isolation barrier.

This isolation amplifier (see figure) includes a two-stage operational-amplifier integrator, a comparator, and a flip-flop clocked by a crystal-controlled oscillator. At the input terminal of the integrator, v_{in} is summed with either V_{ref} or $-V_{ref}$, depending on the output of the flip-flop. The output of the integrator is fed to the comparator, and the output of the comparator is fed to the D input of the flip-flop. These components function together as a control loop that strives to maintain zero net voltage at the input terminal of the integrator. Provided that the clock frequency greatly exceeds the limiting frequency of the control loop, the average (that is, doubly integrated) value of the resulting train of V_{ref} and $-V_{ref}$ pulses closely approximates v_{in}.

The pulses and clock are transmitted across the barrier by use of optocouplers (alternatively, transformer or capacitive coupling could be used). The pulses are then fed to a second flip-flop, clocked by the optically-coupled version of the crystal-controlled oscillator output. The output of this second flip-flop controls an electronic switch that reconstructs the V_{ref} and $-V_{ref}$ pulses by alternatively making contact with the V_{ref} and $-V_{ref}$ sources on its side of the barrier. The pulses are then low-pass-filtered, yielding an output voltage v_{out} that closely approximates the input voltage.

This circuit could be used wherever a conventional amplifier is needed. This includes medical instrumentation, switching-type power supplies, and other applications in which input voltages must be measured in the presence of large common-mode voltages.

This work was done by Daniel N. Harres of McDonnell Douglas Corp. for **Johnson Space Center**. *For further information,* ***write in 34*** *on the TSP Request Card.*
MSC-22132.

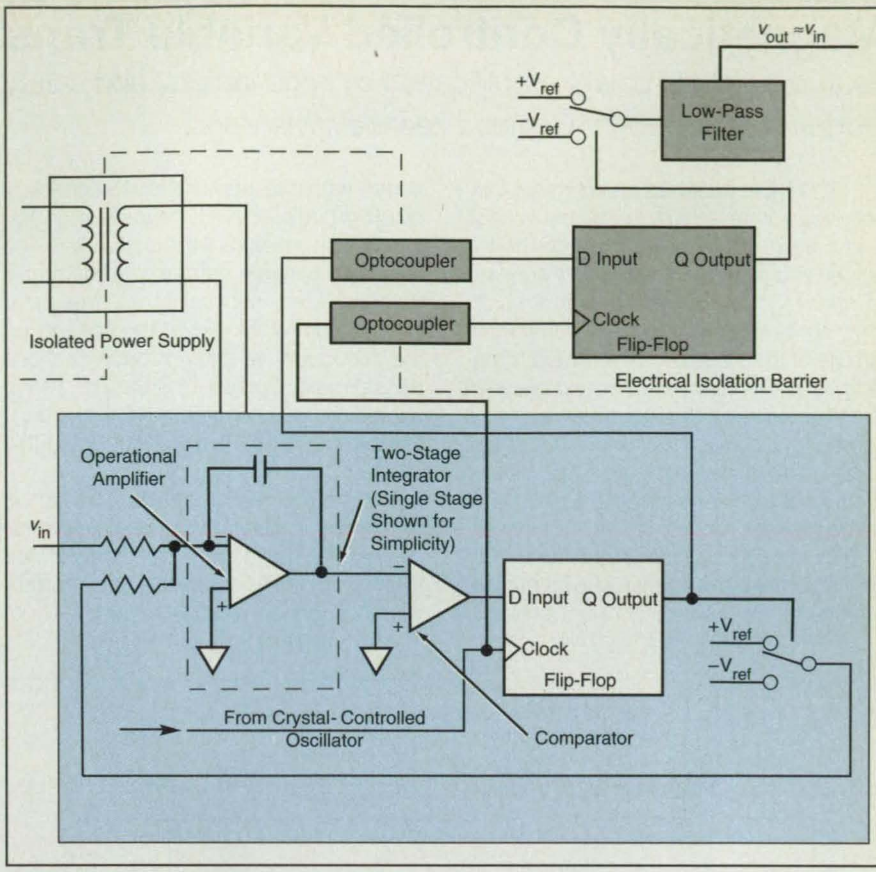

This **Isolation Amplifier**, shown here in simplified form, implements a sigma-delta modulation scheme in which the input waveform is reconstructed approximately at the output by low-pass-filtering a train of V_{ref} and $-V_{ref}$ pulses.

Bypassing an Open-Circuit Power Cell

A battery can continue to function at reduced voltage when one cell fails.

Goddard Space Flight Center, Greenbelt, Maryland

A collection of bypass circuits enables a battery that consists of a series string of cells to continue to function when one of its cells fails in an open-circuit (high-resistance) condition. The basic idea is simply to shunt the current around the defective cell to prevent the open circuit from turning off the battery altogether. Thus, the battery can continue to function at reduced voltage, as though the cell had failed in the short-circuit condition.

A bypass circuit like either one shown in the figure is connected in parallel with each cell in the series string. The circuit consists of an initially open bypass switch in a latching relay. The relay includes a latching coil in series with a diode, and a resetting coil that is normally not connected to a source of power.

As long as the cell functions normally, the polarity of its voltage is opposite that of the diode, and no appreciable current flows in the latching coil. When the cell fails in the open-circuit condition, the polarity of the voltage generated by the other cells matches that of the diode, so that current flows through the latching coil. This current actuates the relay, causing the bypass switch to close. The bypass switch remains closed, serving as a shunt around the defective cell, until the relay is reset by supplying current to the resetting coil.

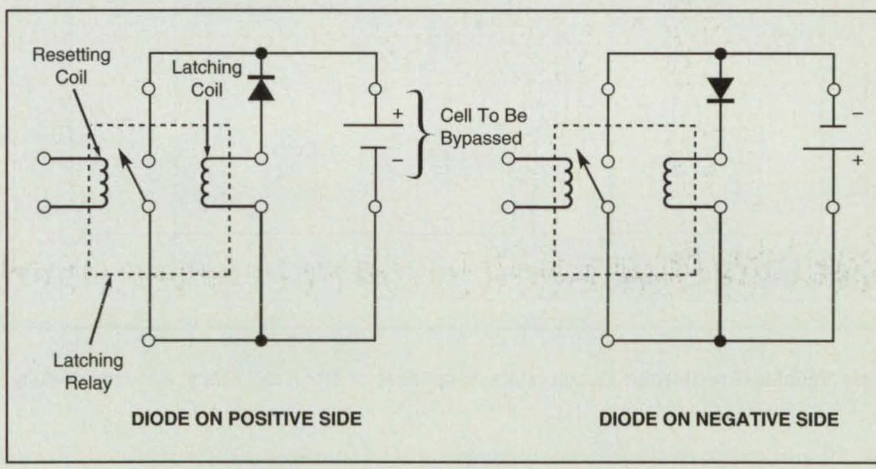

These **Bypass Circuits** dissipate little power and are nearly immune to false activation.

This work was done by Harry E. Wannemacher of McDonnell Douglas Corp. for **Goddard Space Flight Center**. *No further documentation is available.*
GSC-13480

Magnetically Controlled Variable Transformer

Features include power amplification by large factors, and safety.

Goddard Space Flight Center, Greenbelt, Maryland

The figure illustrates an improved variable-transformer circuit, the output voltage and current of which can be controlled by use of a relatively small current supplied at relatively low power to control windings on its magnetic cores. Transformer circuits of this type have been called "magnetic amplifiers" because the ratio between the controlled output power and the power that drives the control current of such a circuit can be large. This ratio— the power gain — can be as large as 100 in the present circuit.

This circuit contains a two-core variably saturable transformer with its primary and secondary windings connected in series with the primary and secondary windings, respectively, of a linear (in the sense of nonsaturable) transformer. The two-core variably saturable transformer comprises two identical transformers that include control windings; the voltage on the secondary winding of each of these transformers decreases with the degree of saturation, which increases with the control current (which is direct current in this case).

The control windings are connected electrically in series, with polarities chosen so that ac voltages transformed into them from the primary and secondary windings cancel wholly or partly. Thus, unlike in some prior magnetically controlled variable transformers, large ac voltages do not appear at the control-winding terminals, and controllability and safety are thus enhanced.

The numbers of turns in the primary and secondary windings are chosen, along with the polarities of the secondary windings, so that in the absence of control current, the combined voltages on the secondary windings of the two-core variably saturable transformer are equal in magnitude and opposite in polarity to the voltage on the secondary winding of the linear transformer. Thus, at zero control current, the net output (load) voltage, which is the sum of the secondary-winding voltages, is zero. This is an advantage over some prior circuits, in which large ac output voltages are generated at zero control currents.

As the control current is increased from zero, the degree of saturation increases, with corresponding reduction in the amplitude of the secondary-winding voltage of the variably saturable transformer. Because this voltage no longer cancels the secondary-winding voltage of the linear transformer, the net output voltage increases. This increase can continue until the control current becomes large enough to produce full saturation. Leakage reactance limits the output power at full saturation, but this is not a serious disadvantage, inasmuch as leakage reactance at saturation also limits the output power of a conventional transformer.

The techniques described herein can also be applied to multiphase systems and can be used over a wide range of frequencies. Reference: Patent 4,907,246 March 6th, 1990 "Magnetically Controlled Variable Transformer."

This work was done by Charles T. Kleiner of **Goddard Space Flight Center**. *For further information,* ***Circle 98*** *on the TSP Request Card.*
GSC-13247

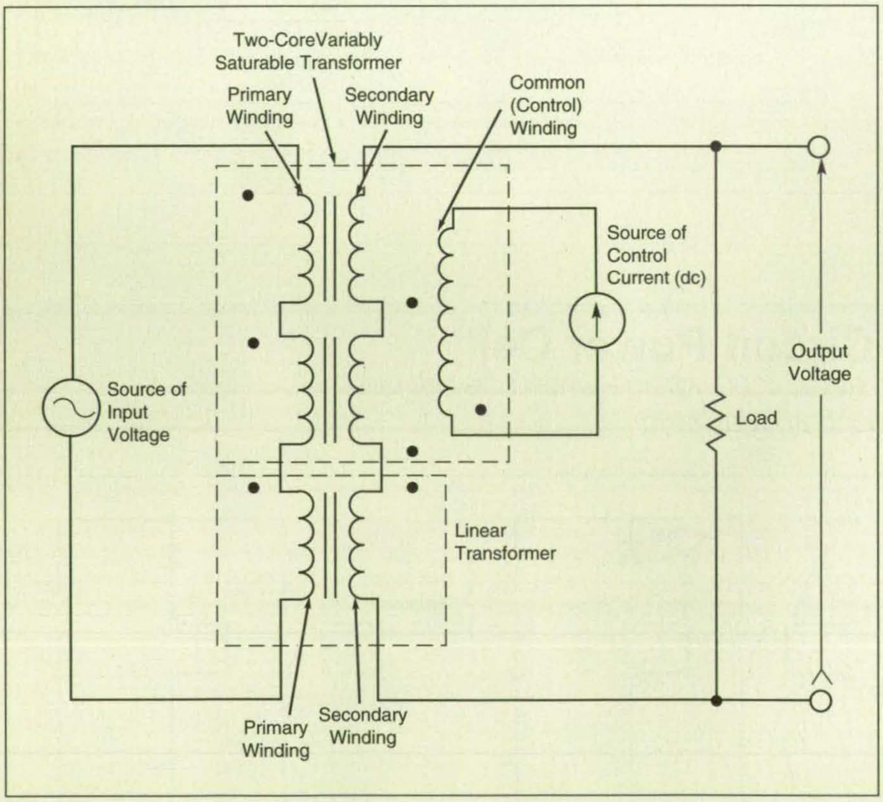

This **Variable-Transformer Circuit** offers advantages of efficiency, safety, and controllability

Electromagnetic Flaw Detector Is Easier To Use

Calibration is ordinarily not needed, and readings can be interpreted with relative ease.

Langley Research Center, Hampton, Virginia

The electromagnetic flaw detector illustrated schematically in the figure is based on the eddy-current principle. It nondestructively detects cracks, voids, and other flaws that introduce electrical discontinuities into specimens of electrically conductive materials. The circuitry associated with this flaw detector is simpler than that of older eddy-current flaw detectors. Unlike older eddy-current nondestructive testers, this electromagnetic flaw detector can be used with little or no calibration, without having to perform tedious null balance adjustments, and without the difficulty of interpreting readouts in the form of complex-impedance-plane displays.

The electromagnetic probe includes a magnetizing coil wound on the outside of a hollow magnetic-flux-focusing core made of soft iron or other conductive highly magnetically permeable material. A pickup coil is placed inside the core. The core concentrates the magnetic field generated by passing electrical current through the magnetizing coil and thereby nearly completely shields the pickup coil from the magnetic field.

The magnetizing coil is excited by a sinusoidal current, the frequency of which is chosen so that the characteristic attenuation length (skin depth) of electromagnetic waves in the specimen material is commensurate with the depths and/or sizes of flaws to be detected. When the electromagnetic probe is held up in midair, away from any specimen, there is some leakage of magnetic flux to the pickup coil. Consequently, a voltage is induced in the pickup coil and is conveniently read out on an ac voltmeter.

When the probe is placed on or sufficiently close to a flat surface of a conductive specimen that does not contain flaws, the eddy current induced by the concentrated magnetic field prevents most of the leakage flux from reaching the pickup coil. The readout voltage therefore becomes much smaller than the midair value; for practical purposes it falls to a background or null level. Thus, without calibration and by virtue of the basic principle of operation, this instrument automatically gives a null readout for a flawless specimen.

When a specimen contains a flaw, the eddy-current pattern is altered in a way that allows some leakage flux to reach the probe, causing the readout voltage to rise above the null or background level. The size of the readout voltage depends on the size, shape, and location of the flaw; in some cases, readout voltages can even exceed the midair value.

This work was done by C. Gerald Clendenin and Min Namkung of **Langley Research Center***; John W. Simpson of Lockheed Engineering & Sciences Co; and James P. Fulton, Buzz Wincheski, and Ronald G. Todhunter of Analytical Services and Materials, Inc. For further information,* ***write in 85*** *on the TSP Request Card.*

This invention is owned by NASA, and a patent application has been filed. Inquiries concerning nonexclusive or exclusive license for its commercial development should be addressed to the Patent Counsel, Langley Research Center [see page 20]. Refer to LAR-15046.

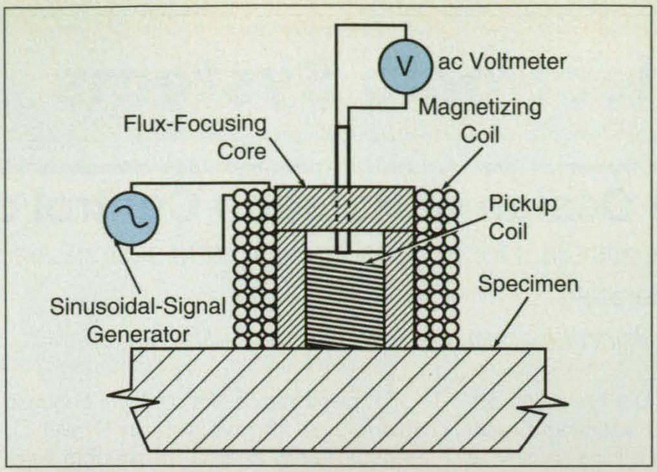

This **Electromagnetic Flaw Detector** operates on an eddy-current principle. In comparison with older eddy-current instruments, it is much easier to use because it requires no calibration, no tedious adjustments, and no interpretation of complicated two-dimensional readouts.

Sequential Design of Rotation Control of Flexible Structure

Linear quadratic controllers for rotation tracking and suppressing vibrations are designed separately.

NASA's Jet Propulsion Laboratory, Pasadena, California

An improved procedure has been devised for designing and adjusting a linear quadratic control system for a somewhat flexible rotating structure like a large radio antenna, a large telescope, or a robot arm. The basic purpose of the control system is to make the structure track the desired rotation (for example, to rotate at a specified rate to track a celestial object or to slew to a new observing direction) and to suppress vibrations, which could be excited by wind or other external phenomena or by changes in angle and angular-velocity commands.

A linear quadratic control system is a feedback control system in which (1) a feedback control vector **u** is the product of a control-gain matrix K and an state vector **x** and (2) the control gains are chosen to minimize a quadratic performance index, J, given by

$$J = \int_0^\infty (\mathbf{x}^T Q \mathbf{x} + \mathbf{u}^T R \mathbf{u}) dt$$

where t is time, the superscript T denotes the vector transpose, R is a positive definite input-weight matrix, and Q is a positive semidefinite state-weight matrix.

The performance of a controller depends strongly on the weights in R and Q. Heretofore the choices of weights have been largely arbitrary. The improved procedure also involves arbitrary choice of some weights, but it provides for systematic choice of others. Furthermore, the improved method involves division of the overall control problem into several smaller ones: as a result, the order of the mathematical model of the control system, the complexity of the control system, and the amount of computation needed to design and adjust the control system are all reduced.

The improved procedure consists of the following steps:

1. On the basis of the mathematical model of the dynamics of the structure to be controlled, construct a state-space matrix representation of the structure and divide it into tracking and flexible parts. (There is also a part in which both tracking and flexible behaviors overlap, but in practice it is small.) A separate controller will be designed for each part (see figure).
2. Arbitrarily choose an initial set of reasonably small weights for the tracking part.
3. Choose an initial set of weights for the flexible part, wherein each vibrational mode is weighted separately, and modify these weights so that the closed-loop performance of the overall control system that minimizes J is maximized or altered in some desired way. For example, choose the weights to impose the required shift in a pole in the transfer function or to suppress the resonant peak in another mode to the required level without depreciating other properties of the closed-loop transfer function of the overall system. Disregard the modes for which the weighting does not improve the closed-loop performance of the overall system.
4. Given the weights thus determined for the flexible part, modify the weights of the tracking part to improve the tracking performance.
5. Adjust the weights of the flexible part, if necessary.

This work was done by Wodek Gawronski of Caltech for **NASA's Jet Propulsion Laboratory**. *For further information,* ***write in 104*** *on the TSP Request Card.*
NPO-18843

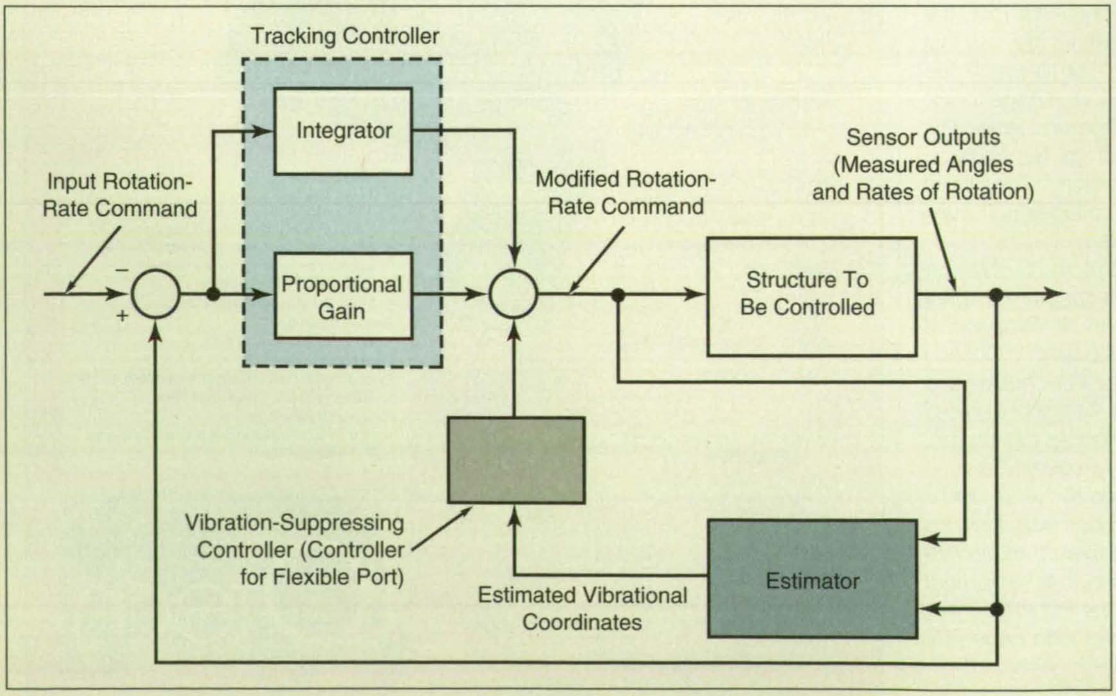

The **Control System Is Divided** into a tracking part and a vibration-suppressing part.

Multiple-Symbol, Partially Coherent Detection of MPSK

A combination of coherent-reception and incoherent-reception decision rules would be used.

NASA's Jet Propulsion Laboratory, Pasadena, California

A proposed method of reception of multiple-phase-shift-keyed (MPSK) radio signals would involve multiple-symbol, partially coherent detection. Instead of attempting to determine the phase of the transmitted signal during each symbol period as in coherent detection, the receiver would acquire signal data during a multiple-symbol observation interval, then produce a maximum-likelihood-sequence estimate of the phases transmitted during the interval.

The ideal case of phase-coherent detection of MPSK is based on exact knowledge of the phase of the carrier signal. The rule for deciding the identity of a received symbol ("decision rule" for short) that yields the lowest bit-error probability in coherent detection is based on a correlation metric and leads to bit-by-bit decisions. A typical receiver includes a carrier-phase-tracking loop that estimates the carrier phase. In practice, the estimate is degraded by additive noise, which is always present, and detection is therefore partially coherent.

Ordinarily, one continues to use the ideal coherent-detection correlation metric in the presence of noise, even though this metric is not optimum for partially coherent detection: Because the error in the estimated carrier phase introduces memory, any metric that leads to bit-by-bit detection cannot be optimum. Instead, one must resort to sequence estimation in which the length of the sequence is the number of symbol periods during which the phase error can be assumed constant.

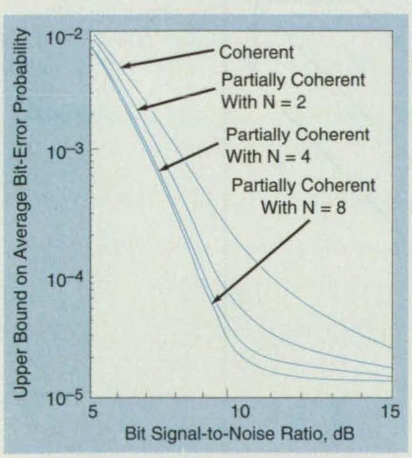

These **Upper Bounds on Average Bit-Error Probability** were computed for an example of binary PSK with a tracking-loop signal-to-noise ratio of 10 dB.

In the proposed method, the receiver would generate maximum-likelihood estimates of sequences of N symbols each. The optimum decision metric used in the receiver would be a weighted sum of the coherent-detection metric and the noncoherent-detection metric, which is optimum for differential detection of MPSK. According to theory and computer simulations, the bit-error rate of this receiver would be less than that of a receiver based on the coherent-detection metric. The average bit-error probability of this receiver would decrease with increasing N (see figure) toward a lower limit ("error floor") associated with noise. The bit-error performance would also be relatively insensitive to the error in the estimate (computed from measurements) of the loop signal-to-noise ratio, which would be used in computing the decision metric.

This work was done by Marvin K. Simon and Dariush Divsalar of Caltech for **NASA's Jet Propulsion Laboratory.**

For further information, ***write in 76*** *on the TSP Request Card.*
NPO-18932

Three-Dimensional Vertical-Bloch-Line Memory System

Advantages include high storage density, high speed, nonvolatility, and insensitivity to ionizing radiation.

NASA's Jet Propulsion Laboratory, Pasadena, California

In a proposed magnetic memory system without moving parts, data would be stored in a stack of two-dimensional vertical-Bloch-line (VBL) memory chips or modules (see Figure 1). The three-dimensional configuration would provide high volumetric storage density. In some versions, a high rate of transfer of data into and out of the system would be achieved by operating all the layers in parallel. Like other VBL memory systems, this one would also offer the advantages of nonvolatile storage and relative insensitivity to disruption by ionizing radiation. In some respects, this system would be similar to the one described in "Three-Dimensional Magnetic-Bubble Memory System" (NPO-18533), *NASA Tech Briefs*, Vol. 17 No. 12 (December 1993), page 32.

Each VBL module in this memory system would be similar to the module described in "Vertical-Bloch-Line Memory" (NPO-18467), *NASA Tech Briefs*, Vol. 17, No. 6 (June 1993), page 42. The VBL's would be stored in a linear array of parallel stripe domains called "minor loops." The VBL's would be propagated around the loops by applying a global pulsed magnetic field. During readout, a reading/writing gate at one end of each stripe domain would convert the presence or absence of a VBL pair in the minor loop (representing binary 1 or 0) into the presence or absence of a magnetic bubble. To write a datum into the minor loop, a reading/writing gate would convert a magnetic bubble (if present) into a VBL pair. Magnetic bubbles would propagate to or from the reading/writing gates along adjacent regions called "major lines."

In the version of the system shown in Figure 1, the magnetic bubbles in either major line would be propagated to the

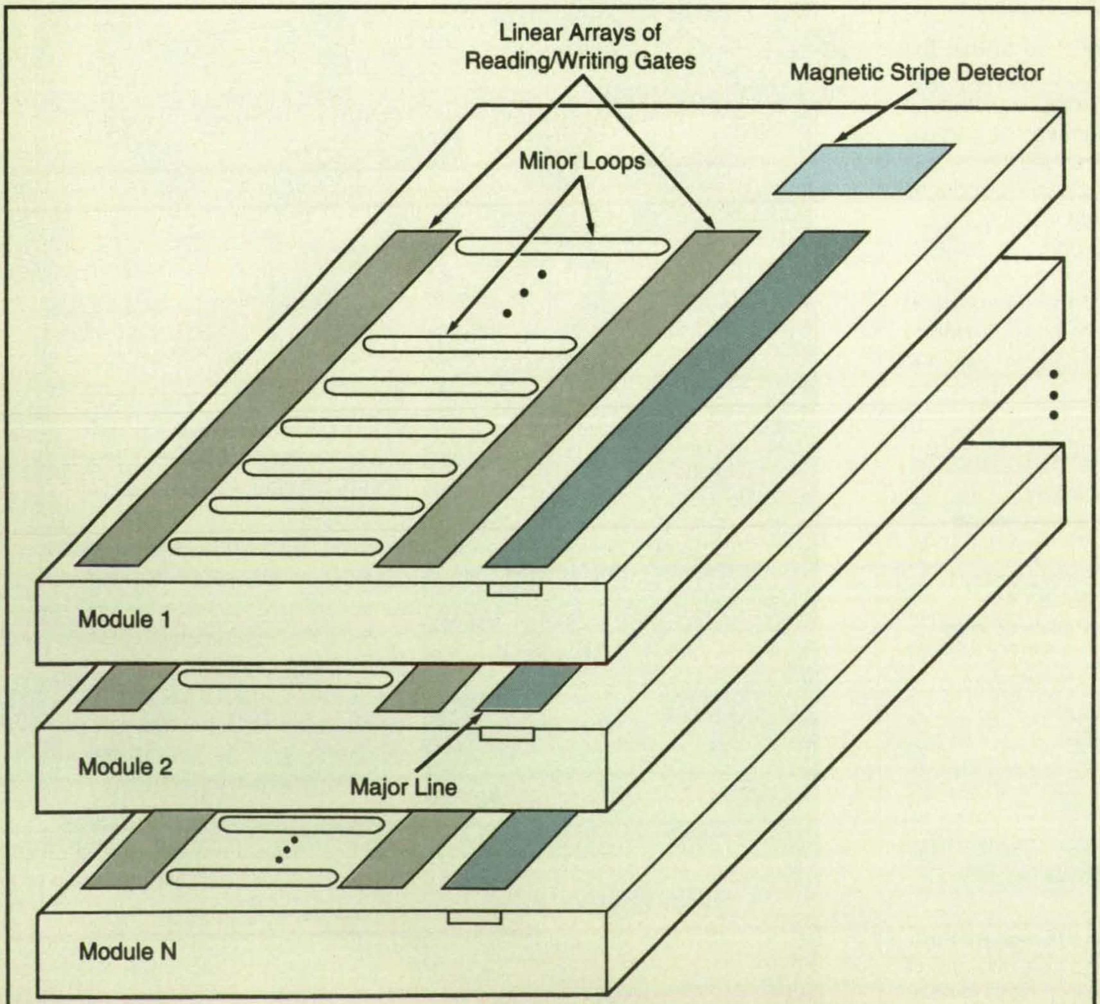

Figure 1. **Planar VBL Memory Modules Would Be Stacked** to achieve high storage density. In this version with magnetic-stripe readout, all *N* modules could be operated simultaneously, yielding an overall input and output data rate *N* times that of a single module.times as great as that attainable with magnetic-stripe readout.

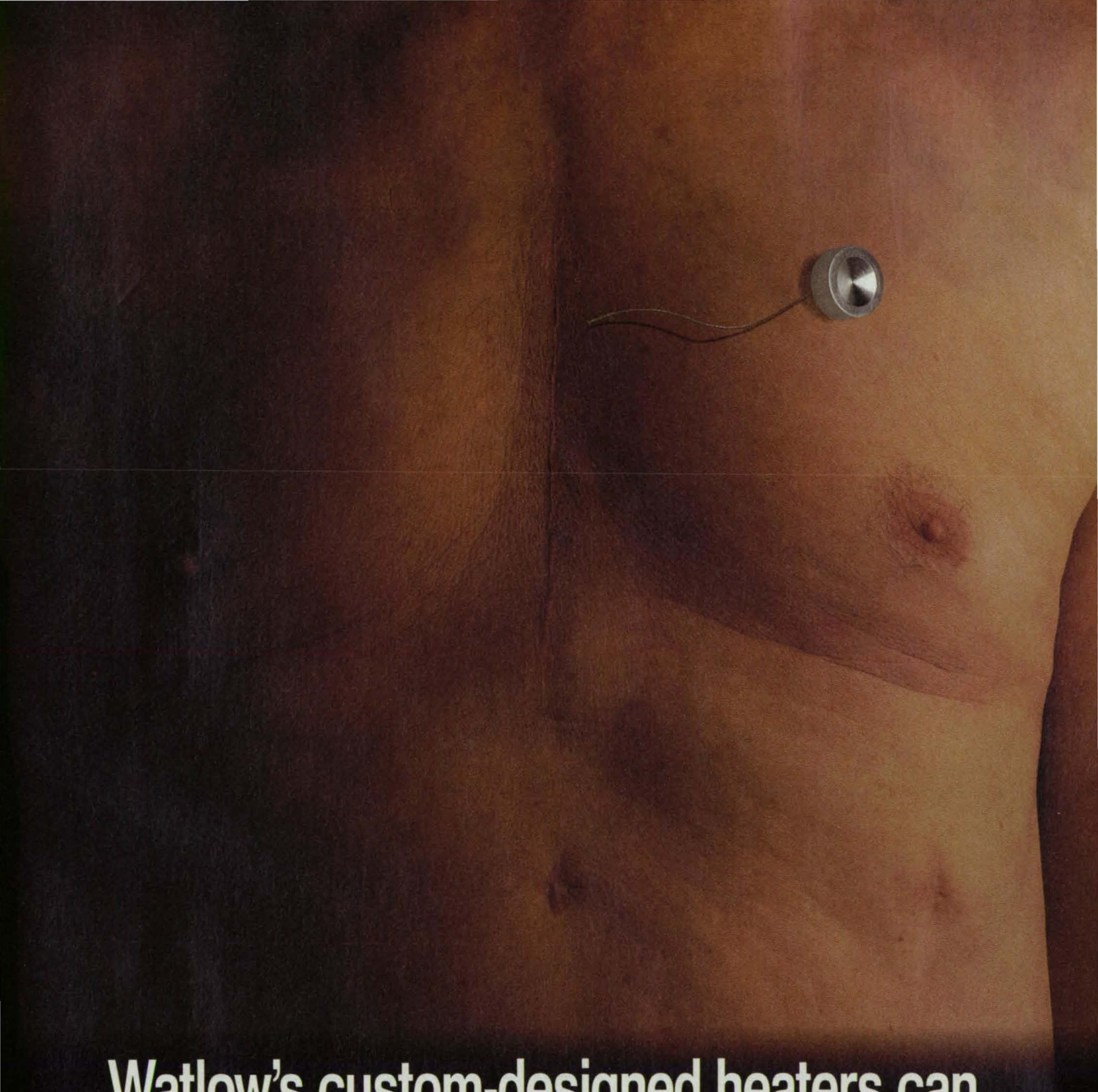

Watlow's custom-designed heaters can get straight to the heart of any heating problem.

Someday, the human heart may get an assist from a permanently implantable blood pump that's fully capable of keeping pace with the natural heart, regardless of stroke volume, heart rate or aortic load.

Stirling Technology Co., working with the National Heart, Lung and Blood Institute, is developing such a device right now that is powered by a thermal battery. And its heat source? Two special Watlow curved cartridge heaters.

Special applications like this are nothing new to Watlow's in-house team of engineers. With over 250,000 designs on file, Watlow has come up with the ideal heating solution for virtually every kind of application imaginable. From the ordinary to the extraordinary, no one delivers better than Watlow. So next time you have a special heat application, make sure you call Watlow. It'll be just what the doctor ordered.

For more information about this application or to get the Watlow catalog FREE of charge, call us at 314-878-4600 or request by FAX at 314-878-6814.

WATLOW

For More Information Write In No. 628

output end of the line, where they would be expanded into magnetic stripes, which would be detected via the magnetoresistive effect. By operating all *N* modules in the stack simultaneously, data could be transferred out at a rate *N* times that of a single module.

Alternatively, the magnetic bubbles could be read out via the Faraday effect: Laser diodes and a polarizer at the top of the stack would generate polarized light, which would pass through the stack at each readout location along the major line, then would pass through an analyzer into a photodetector. Because the light would go through all the modules, the photodetector could detect only the net change in polarization and thus could read out the data from only one module at a time. The total rate of transfer of data out of the memory in this version would be *M* times the data-output rate of a single module with magnetic-stripe readout, where *M* is the number of minor loops.

A system containing modules like the one shown in Figure 2 would transfer data out at the highest rates. Instead of propagating the magnetic bubbles along the major line to a stripe detector for serial detection, a module according to this version would include either *M* or 2*M* Hall-effect sensors on the output major line — one or two for each minor loop. This would enable simultaneous readout from all minor loops, with a resultant modular data-output rate *M* times that of the equivalent module with magnetic-stripe readout. Because all *N* modules in the stack could be operated simultaneously in this version, the overall data-output rate would be *MN* times that of a single module with magnetic-stripe readout.

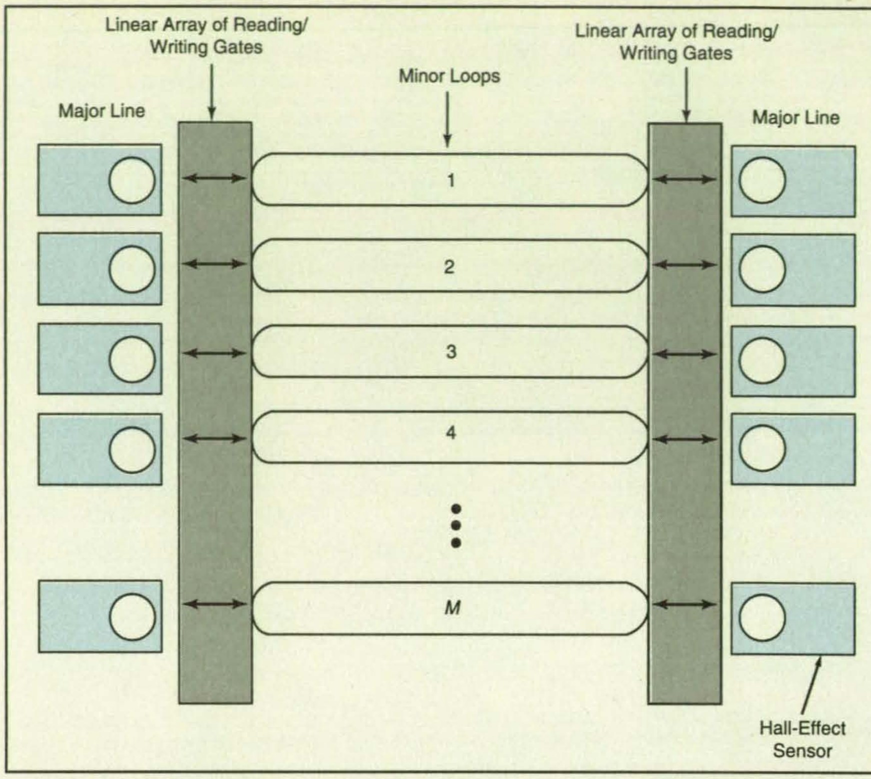

Figure 2. **Hall-Effect Sensors** would read out data from all minor loops simultaneously, resulting in an overall data-output rate *M* times as great as that attainable with magnetic-stripe readout.

This work was done by Romney R. Katti, Jiin-chuan Wu, and Henry L. Stadler of Caltech for **NASA's Jet Propulsion Laboratory**. *For further information,* ***write in 58*** *on the TSP Request Card.*

In accordance with Public Law 96-517, the contractor has elected to retain title to this invention. Inquiries concerning rights for its commercial use should be addressed to

William T. Callaghan, Manager
Technology Commercialization
(M/S 79-23)
Jet Propulsion Laboratory
4800 Oak Grove Drive
Pasadena, CA 91109

Refer to NPO-18867 volume and number of this NASA Tech Briefs *issue, and*

Low-Power CMOS Digital Autocorrelator Spectrometer

Total dc power needed is only 6 W.

NASA's Jet Propulsion Laboratory, Pasadena, California

A prototype digital autocorrelator spectrometer circuit has been designed and built as an assembly of a few very-large-scale integrated (VLSI) complementary metal oxide/semiconductor (CMOS) circuit chips. The spectrometer contains 128 frequency channels and can operate at a clock rate of as much as 40 MHz — suitable for sampling an input signal up to a bandwidth of 20 MHz. The outstanding design feature of this circuitry is low power: it consumes only 6 W.

Autocorrelator spectrometers are based on a Fourier-transform relationship between the power spectrum of the input signal in the frequency domain and the autocorrelation function of the input signal in the time domain. Digital autocorrelator spectrometers offer advantages over analog filter bank spectrometers: these advantages include the inherent stability of digital circuits, flexibility in reconfiguring the bandwidth and frequency resolution between observations, reliability, small size, small mass, and relatively low cost when the number of frequency channels exceeds 50.

In the prototype spectrometer circuit (see figure), the input signal is first amplified, then digitized to 2 bits (1 magnitude bit, 1 sign bit) and sampled at the Nyquist rate. The sampled signal is fed into the autocorrelator. In the autocorrelator chip, the signal is delayed by use of a shift register; then it is multiplied by the undelayed signal, using relatively simple logic circuits. The output of the multiplier is accumulated in a binary counter to obtain the autocorrelation value for the delay channel. The outputs from each delay channel counter are fed, via interface circuitry, to an external computer. The computer converts the counter values into autocorrelation coefficients and computes a power spectrum at N points on the frequency domain.

Digitizing the input signal to only 2 bits degrades the signal-to-noise ratio by 13

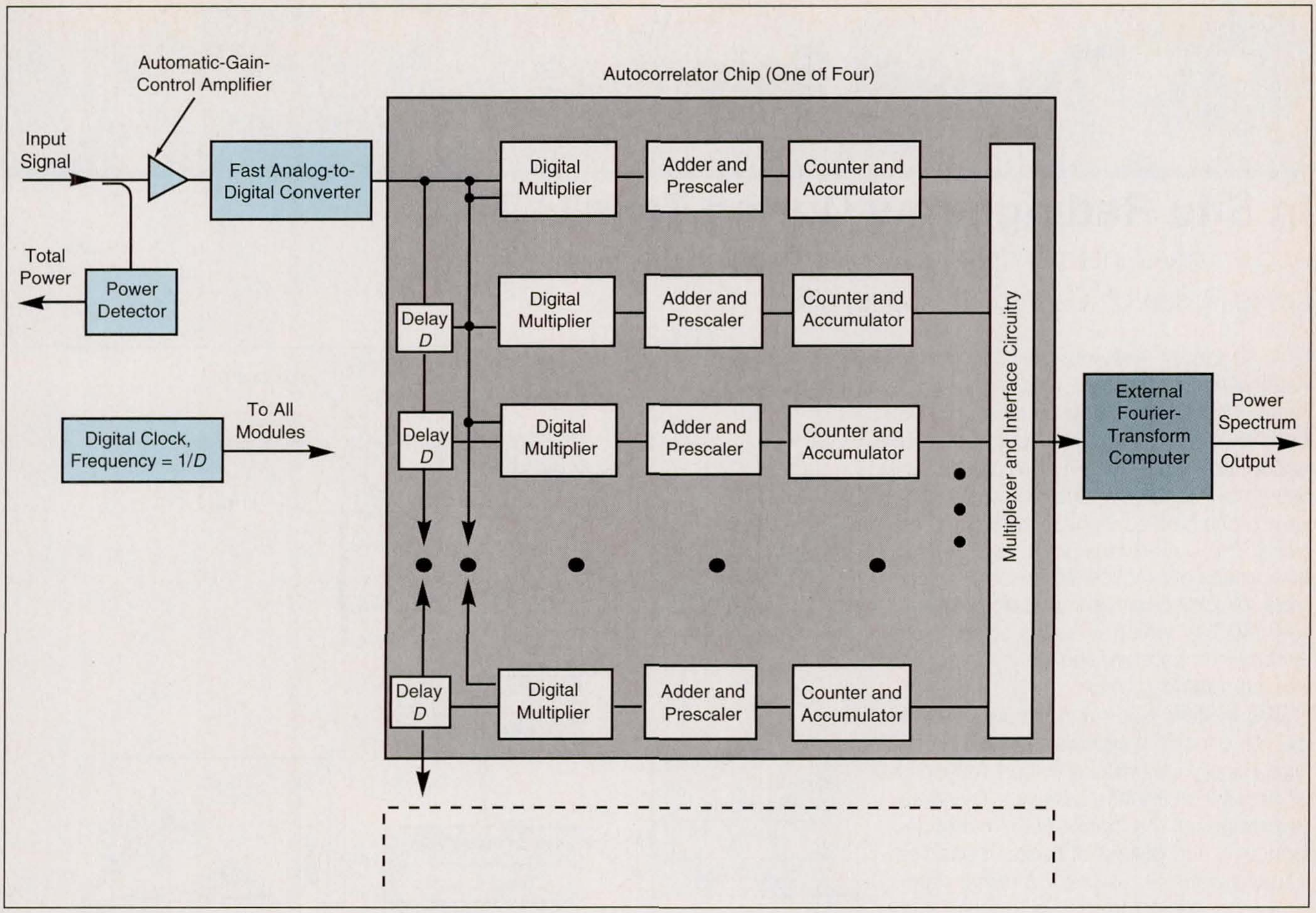

The **Digital Autocorrelator Spectrometer** consists of four 32-channel autocorrelator chips that collectively produce a 128-point spectrum of the input signal as computed by the use of Fourier transform.

percent. However, it offers an important design advantage in that it reduces the number of digital operations needed, thereby accelerating the multiplication and addition processes and making it possible to analyze wide bandwidth signals. This also reduces the dc power consumption which is important for space-borne applications.

The prototype digital autocorrelator spectrometer includes two hardware modules. One module contains an input automatic-gain-control (AGC) amplifier and a low-power 2-bit analog-to-digital converter; the other module contains four 32-channel correlator chips that are cascaded to obtain a total of 128 channels. Each correlator chip measures 5.24 by 4.32 mm and is contained in a 48-pin quad flat pack for surface mounting on a printed-wiring board.

This work was done by Kumar M. Chandra and William J. Wilson of Caltech for **NASA's Jet Propulsion Laboratory**. *For further information,* ***write in 1*** *on the TSP Request Card.*
NPO-18993

In Situ Radiography During Tensile Tests

Accumulated internal damage can be monitored during loading.

Lewis Research Center, Cleveland, Ohio

A laboratory system for testing specimens of metal-, ceramic-, and intermetallic-matrix composite materials incorporates both an electromechanical tensile-testing subsystem and either of two imaging subsystems that take x-ray photographs of specimens before, during, and after tensile tests. The system has been used to test specimens of reaction-bonded silicon nitride reinforced with silicon carbide fibers (SiC/RBSN), which is being considered for high-temperature service in advanced aircraft turbine engines.

The system (see figure) provides data on the effects of preexisting flaws (e.g., high-density impurities and local variations of density) on fracture behavior. By creating images of the matrix, fiber/matrix debonding, and pullout of fibers, it enables experimenters to monitor internal damage as it accumulates in a specimen during a tensile test. In addition, it can be helpful in estimating interfacial shear strength between the fibers and the matrix by the matrix-crack-spacing method.

The x-ray source in one imaging subsystem operates at a maximum power of 3.2 kW, a maximum voltage of 160 kV, or a maximum current of 45 mA with either a 400-μm or 3-mm focal spot. This imaging subsystem operates in a near-contact mode. The other imaging subsystem contains a source with a 10-μm focal spot and operates in a projection mode. The x-ray images are recorded on films. The electromechanical tensile-testing subsystem includes a 250-kN load frame, a 100-kN electric actuator, a 50-kN load cell, and a digital control subsystem.

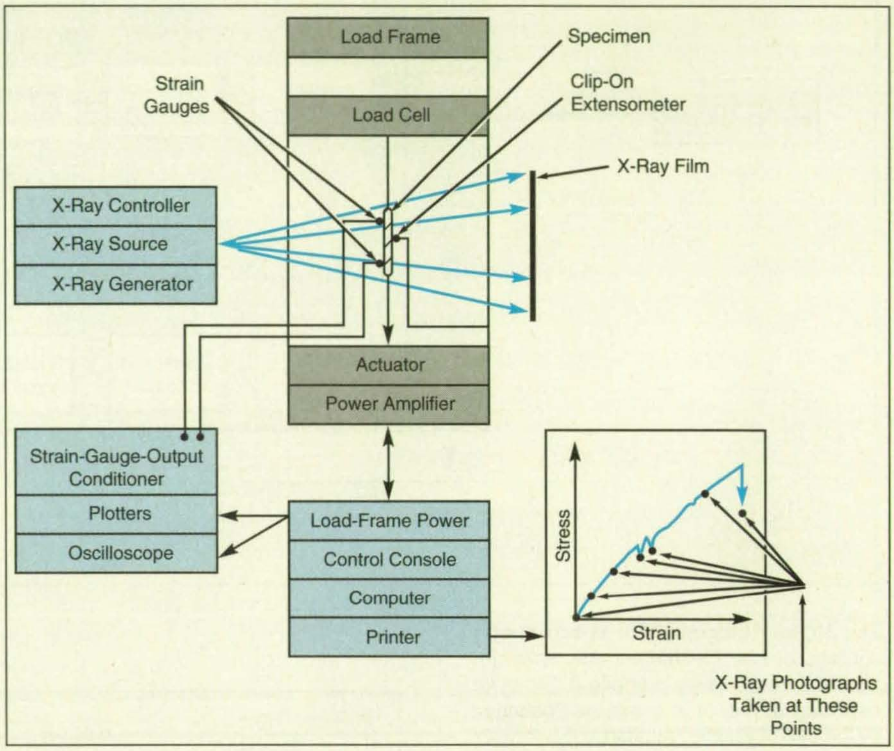

The **X-Ray Source Illuminates** a specimen in a load frame while the specimen is pulled. X-ray images on film can be correlated with stress-vs.-strain data from the tensile test.

Room temperature tensile tests can be done under load control or displacement control. For example, in the case of the SiC/RBSN specimens, some were tested under load control at 4.54 kg/min, and others were tested under displacement control at 25 μm/min. These low rates were chosen to limit changes during 25- to 35-second exposures of the radiographic films, making it unnecessary to hold loads or displacements during the exposures. Typically, x-ray photographs of a specimen are taken before the tensile test, at various stress and strain levels during the test, and after the specimen has failed at the end of the test. During the test, axial strains in the specimen are monitored by use of two adhesively bonded strain gauges and a clip-on extensometer.

This work was done by George Y. Baaklini of **Lewis Research Center** *and Ramakrishna T. Bhatt of the U.S. Army Aviation Systems Command. For further information,* ***write in 44*** *on the TSP Request Card.*
LEW-15684

Thermalite Apparatus

This portable apparatus measures thermal properties of materials.

Langley Research Center, Hampton, Virginia

The thermalite is a portable apparatus that nondestructively determines the thermal-diffusion properties of a specimen. It is based on the heat-pulse method; that is, it applies a pulse of heat to the specimen, then computes the relevant thermal properties of the specimen from time-resolved measurements of the thermal response of the specimen to the heat pulse. Prior systems for measurements of this type involved complex laboratory equipment that included laser scanners, infrared cameras, and such contact temperature sensors as thermocouples. These systems are not portable, are expensive, and are not

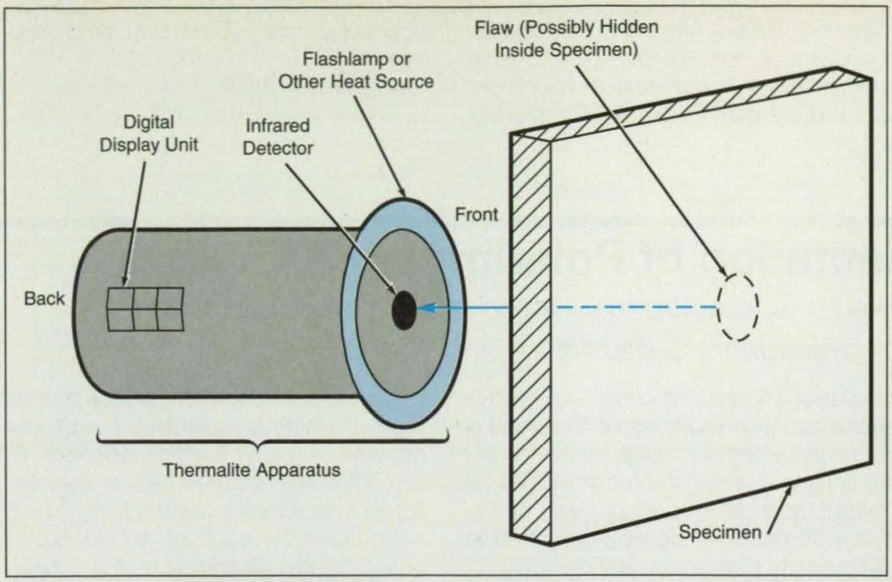

Figure 1. The **Thermalite Apparatus** can be used to assess a flaw in a specimen.

very practical for use in the field.

The thermalite apparatus is self-contained and can be calibrated and tested by contrast with a stored thermal pattern as a standard. It can determine the emissivity of the specimen through heating of the surface of the specimen by use of a pulsed source that could be a flashlamp or an inductive multifrequency device that is capable of heating to varying degrees at varying depths. The apparatus aligns itself and is able to determine vector heat flow through a linear or a two-dimensional pattern of sensors.

Figure 1 illustrates the use of the thermalite apparatus to measure thermal properties of a specimen that contains a flaw. The thermalite presents a quantitative digital display of the effective thermal properties of the specimen. Heat is injected into the specimen by the heating source in the thermalite, and the thermal response of the specimen is detected by the thermal sensor in the thermalite. A digital display unit indicates quantitatively the thermal properties of the specimen determined from its thermal response.

Figure 2 outlines the operation of the electronic subsystems of the thermalite apparatus. The microprocessor in a logic microprocessor/bus controls the other subsystems and, through the bus, communicates with the other subsystems. The sequence of operations is started by discharging a charged capacitor to energize the heat source, which in this case is a flashlamp. (The capacitor is subsequently recharged by a recharging circuit.) The flash heats the specimen, and the evolution of the temperature at the heated spot on the specimen is measured by an infrared detector. The output of the detector is digitized and stored in memory.

More than one sensor can be set into the front of the thermalite apparatus. Multiple sensors enable measurement of the vector flow of heat from the center of the heated spot out to the periphery of the measurement area. The thermalite apparatus can be rotated to exploit this vector-measurement capability to measure anisotropy of thermal diffusion in the sample. From measurements with the thermalite apparatus, one can compute such properties of the specimen as thermal diffusivity, thickness, integrity of a subsurface bond, presence or absence of surface coating material, uniformity, damage, anisotropy, and corrosion.

This work was done by Joseph S. Heyman, William P. Winfree, K. Elliott Cramer, and Joseph N. Zalemeda of **Lang-**

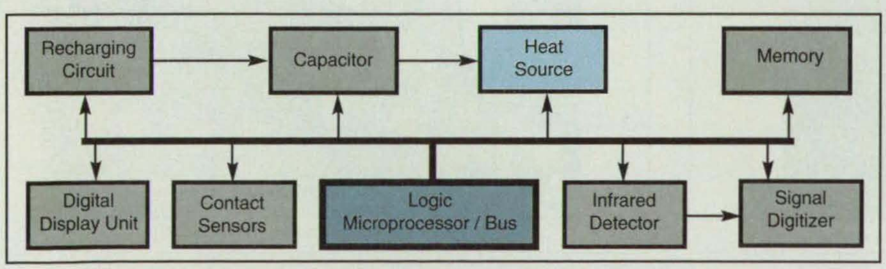

Figure 2. The **Logic Microprocessor/Bus** controls and communicates with the other subsystems of the electronic system of the thermalite apparatus.

ley Research Center. *For further information,* ***write in 23*** *on the TSP Request Card.*

This invention is owned by NASA, and a patent application has been filed. Inquiries concerning nonexclusive or exclusive license for its commercial development should be addressed to the Patent Counsel, Langley Research Center [see page 20].

Refer to LAR-14559.

Unsupervised Segmentation of Polarimetric SAR Data

A method is being developed towards automated real-time identification of Earth terrain.

NASA's Jet Propulsion Laboratory, Pasadena, California

A method of unsupervised segmentation of polarimetric synthetic-aperture-radar (SAR) image data into classes involves the selection of the classes on the basis of a multidimensional fuzzy clustering of logarithms of the parameters of the polarimetric covariance matrix. The data in each class represent parts of the image wherein polarimetric SAR backscattering characteristics of the terrain are regarded as homogeneous. It is desired to have each class represent a type of terrain, sea ice, or ocean surface that could be distinguished from other types (to the extent possible) via its backscattering characteristics.

Most of the methods used previously to segment polarimetric SAR data have involved supervised classification, in which the SAR data are correlated with ground truth from selected training areas that contain the various types of terrain, ice, or water that one seeks to identify. Supervised classification can be hampered by the sparsity of ground truth and/or the cost of collection of ground truth, and by the rapid evolution of the ground truth (even while the classification is being performed, and especially in the case of sea ice). Supervised classification also entails substantial intervention by technicians in the acquisition and interpretation of data, and is therefore time consuming.

In contrast, unsupervised classification does not require training areas, is a nearly automated computerized process, and provides a nonsubjective selection of image classes that are naturally well separated by the radar. By coupling unsupervised segmentation techniques with look-up tables of backscattering characteristics for different types of natural terrain, it may be possible to develop algorithms of automated real-time identification of Earth terrain from polarimetric SAR images.

In the present method of unsupervised classification, a multidimensional cluster analysis of the SAR data is first performed to define the radar characteristics of various image classes, followed by the labeling of each pixel into an image class using a Bayesian algorithm that maximizes the posterior distribution of the classes given the SAR observations. The feature vector $\mathbf{x}_C$ used for clustering is defined as

$$\mathbf{x}_C = \begin{pmatrix} 10\log_{10}(<|HH|^2>) \\ 10\log_{10}(<|HV|^2>) \\ 10\log_{10}(<|VV|^2>) \\ 10\log_{10}(|<HHVV^*>|) \\ 10^{\frac{\arg<HHVV^*>}{\log(10)}} \end{pmatrix}$$

and corresponds to ten times the logarithm of the components composing the covariance matrix $\mathbf{C}_l$ of the data

$$\mathbf{C}_l = \begin{pmatrix} <|HH|^2> & 0 & <HHVV^*> \\ 0 & <|HV|^2> & 0 \\ <HH^*VV^*> & 0 & <|VV|^2> \end{pmatrix}$$

where each pair of letters denotes a complex backscattering amplitude, the first letter in each pair denotes the receiving polarization, the second letter in each pair denotes the transmitting polarization, and < > denotes a spatial average operator. $\mathbf{C}_l$ completely characterizes the first-order statistical charactristics of class l.

Optimum selection of the classes is based on the minimization of an objective function defined to maximize the distance between cluster centers, while minimizing the size (in the polarimetric feature space) of each cluster. The algorithm is "fuzzy" in that the optimization accounts for the possible partitioning of each sample point into several classes, according to some distribution function that is iteratively updated; i.e., each sample element may be a mixture of different types of terrain instead of a pure sample of one class. Only a small number of sample points are needed to define the cluster centers for an entire SAR scene.

The advantages of performing this computation in the logarithmic rather than the linear domain are twofold. The first advantage arises in connection with the fact that in traditional methods, clustering is driven mainly by the amplitude variance of the SAR signal. Because of image speckle, the amplitude variance is proportional to its mean in magnitude-squared detection. As a result, more clusters are selected in the high-backscatter regions than in the low-backscatter regions. However, in the log domain, the statistical characteristics of speckle are those of additive noise, with the power level not varying much across the image, and therefore speckle does not

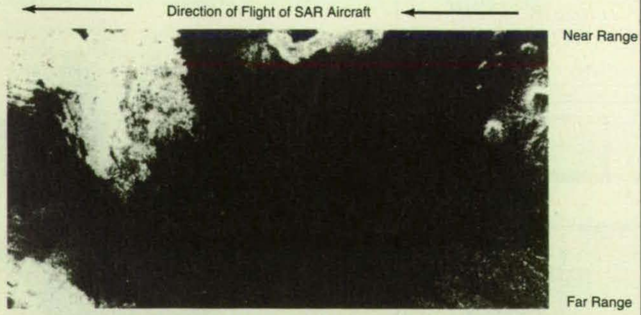

Composite SAR Image : HH, VV, and HV Images Superimposed

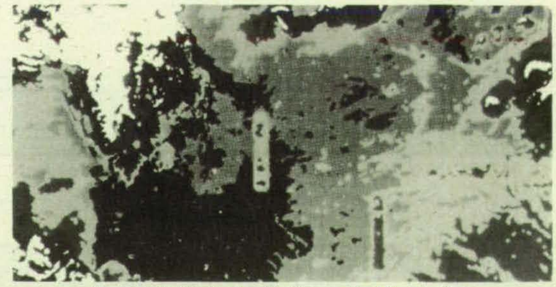

Segmentation Map Produced by Unsupervised Classification

The **Segmentation Map** contains 6 classes: class 1 (phase II lava), class 2 (phase III lava), class 3 (phase I lava), class 4 (alluvial fan and cobble), class 5 (alluvial fan only), and class 6 (dry lake bed). These images represent an area of 12×5 km.

impair the selection of centers of clusters.

The second advantage arises in connection with the fact that in the linear domain, the cross-polarized terms (i.e., *HV*) are often several orders of magnitude smaller than the copolarized terms (i.e., *HH* or *VV*), and clustering is driven mainly by the copolarized terms unless an arbitrary weighting of the signals in different channels is used. The optimal weighting may vary with the type of target or the environmental conditions. In the log domain, the differences between the backscatter levels of the cluster center are independent of the differences between the absolute magnitudes in the channels. Weighting of the signals in the channels is therefore not necessary.

The figure shows the result obtained by applying this method to a four-look polarimetric SAR image of the Pisgah lava flows in the Mojave Desert, Nevada. Image classes identified by unsupervised classification of the data match very well with lava flows of different ages, and different types of sedimentary floors.

This work was done by Eric J. Rignot, Pascale Dubois, Jakob van Zyl, Ronald Kwok, and Rama Chellappa of Caltech for **NASA's Jet Propulsion Laboratory**. *For further information,* ***write in 17*** *the TSP Request Card. NPO-18591*

Refined Estimation of Thermal Tensile Stresses in Bolts

Elasticity of the bolted material and radial thermal expansion are also taken into account.

Langley Research Center, Hampton, Virginia

Thermal changes in the tensile stresses and strains in a bolt and in the corresponding compressive stresses and strains in bolted material can be estimated somewhat more accurately by use of equations that incorporate two refinements over the previous equations. Heretofore, the elasticity of the bolt, the thicknesswise thermal expansion of the bolted material, and the possibly different lengthwise thermal expansion of the bolt were taken into account, but the bolted material was otherwise assumed to be perfectly rigid (that is to expand or contract thermally but not to yield under stress) and the effects of radial thermal expansion were neglected. In the refined equations, the elasticity of the bolted material and the effect of differential radial thermal expansion between the bolt and the nut or threaded hole that it engages are also taken into account. The refined equations can improve the design and analysis of bolted joints that are assembled at one temperature (e.g., room temperature) and in which a specified minimum tension must be maintained (and/ or a specified maximum tension not exceeded) at a higher or lower operational temperature.

The refined equations are derived according to a linearized, small-perturbation approach that starts with the previous equations. The stress and strain effects of the elasticity of the bolted material and the differential radial thermal expansion (if the temperature increases) or contraction (if the temperature decreases) are taken into account by use of additive terms.

To represent the effect of elasticity in the bolted material, the compressive force on the bolted material is assumed equal to the tensile force in the bolt and is assumed to be distributed evenly over an annulus that ranges from the bolthole out to three times the diameter of the bolthole; that is, the bolted material is represented as a hollow cylinder with a length equal to the effective thickness and an outer diameter three times that of the bolthole. This mathematical model is a generally accepted approximation.

If the bolt engages either a nut or a threaded hole in the bolted material and if the coefficient of thermal expansion of the bolted material or nut differs from that of the bolt, then the effect of differential radial thermal expansion (or contraction) can be surprisingly large. This is because the contact between the two threads under lengthwise tension forces the relative radial motion of the threads to be accompanied by a relative axial motion proportional to the tangent of the angle between the thread face and the local radius. Thus, the length of the bolt changes, adding to or subtracting from the net stress and strain depending on the sign of the change in temperature.

The following example is illustrative: Suppose that a nut made of the bolted material is used, and that the angle between the thread face and the local radius is the standard 30°. Suppose, further, that both the bolt and the bolted material have the same modulus of elasticity, E_S. Then the net tensile force (F) in the bolt or, equivalently, the net compressive force on the bolted material is given by

$$F = \frac{8}{9}\left(1 \frac{D}{2L\sqrt{3}}\right)(a_m - a_s) A_t E_s \Delta T$$

where D is the effective diameter of the bolt; L is the thickness of the bolted material; a_m and a_s are the coefficients of thermal expansion of the bolted material and bolt, respectively; A_t is the effective tensile-stress area of the bolt; and ΔT is the increase in temperature. The force in the bolt is positive (tensile) when for a positive ΔT (temperature increase) a_m is greater than a_s, or when for a negative ΔT (temperature decrease) a_m is less than a_s. Note also that a negative force can be interpreted as a reduction in the bolt tension from the bolt tension that was developed during assembly.

This work was done by Larry C. Rash of Calspan Corp. for **Langley Research Center**. *For further information,* ***write in 61*** *on the TSP Request Card. LAR-14913*

Multilayer Badges Indicate Depths of Ion Sputter Etches

Visible erosion of laminar thin films quickly determines the ion etch depth.

Lewis Research Center, Cleveland, Ohio

Multilayer badges have been devised to provide rapid, in-place indications of ion sputter etch rates. These badges were conceived for use in estimating the ion erosion of molybdenum electrodes used in inert-gas ion thrustors. The multilayer badge concept, for example, could be adapted to measure ion erosion in industrial sputter etching processes used for the manufacturing of magnetic, electronic, and optical devices.

Each badge contains many alternating layers of copper and molybdenum with thicknesses of ~600 Å. As shown in Figure 1, the badge has a mask to facilitate counting of the layers. After the badge and the molybdenum workpiece have been exposed to the ion beam, the badge is viewed through a microscope. The depth to which the workpiece has been sputter-etched is estimated from a count of the number of molybdenum and copper layers that are exposed after etching. The contrast between the copper and molybdenum eases the counting of the layers. From published ion sputter yields at 300 eV, copper is etched at a rate about 2.6 times as fast as than molybdenum. The equivalent molybdenum ion etch depth is the sum of the depth of the molybdenum layers plus the sum of the depth of the copper layers divided by 2.53 to 2.74 depending on the type of inert gas ions used.

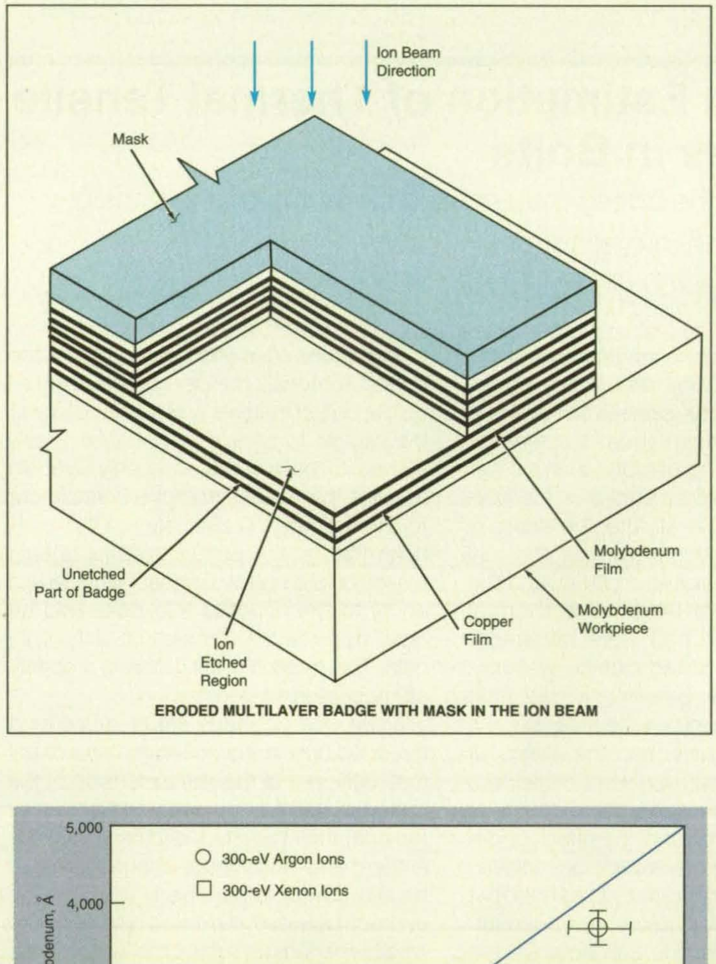

Figure 1. The **Multilayer Erosion Badge** is etched when bombarded by energetic ions. Badge layers are exposed using a mask. The contrast between layers facilitates counting of layers to determine the etch depth.

Figure 2 shows the results of calibration measurements of the depth of erosion of bulk molybdenum specimens versus the depth of erosion determined from the laminar-thin-film badges for 300 eV argon, krypton, and xenon ions. The multilayer badge etch depth results were within ±800 Å of the results obtained from ion etching bulk molybdenum. The multilayer badge concept could just as easily be performed to indicate the erosion of other bulk materials — silicon, germanium, or aluminum, for example — under bombardment by inert gas ions.

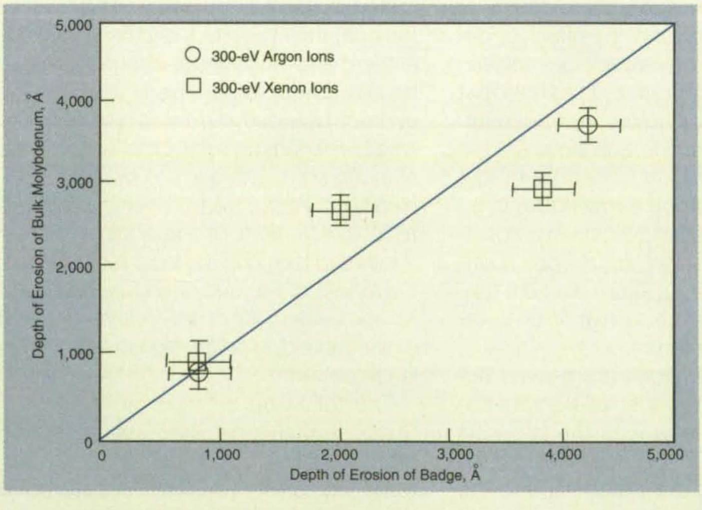

Figure 2. The **Straight Line** compares the ion etch depth obtained using polished bulk molybdenum versus etch depths from multilayer badges.

This work was done by J. R. Beattie, J. N. Matossian, and H. L. Garvin of Hughes Research Laboratories for **Lewis Research Center**. *For further information,* ***write in 32*** *on the TSP Request Card.*
LEW-15599

Low-Dielectric-Constant Polyimide Fibers

These fibers also have high thermal stability and good tensile properties.

Langley Research Center, Hampton, Virginia

A need for materials that have low (< 3) dielectric constants has grown in the aerospace and electronic industries in recent years. These materials have been used as coatings, films, matrix resins, and fibers in various applications. In experiments performed at NASA Langley Research Center, low-dielectric-constant polyimide fibers were produced by use of resin extrusion.

In the experiments, resins derived from 2,2-bis(3,4-dicarboxyphenyl) hexafluoropropane dianhydride (6FDA) and 2,2-bis[4-(4-aminophenoxy)phenyl]hexafluoropropane (4-BDAF) were used to make polyimide fibers in two different methods. In one method, filaments of polyamic acid were formed by the extrusion of an N,N-dimethylacetamide solution of the polyamic acid into 71-percent aqueous ethylene glycol. These filaments were washed in water, dried in vacuum at a temperature of 80 °C, and thermally imidized to the polyimide-fiber form. The other method involved the extrusion of an N,N-dimethylacetamide solution of the polyimide into 71-percent aqueous ethylene glycol. The resulting polyimide filaments were also washed in water and dried in vacuum at 80 °C.

The tensile properties of the fibers (see table) were found to be in the range of properties of standard textile fibers. The highest tensile properties were exhibited by polyimide fibers produced from polyimide wet gel filaments that were stretched at 288 to 289 °C, the tensile properties increasing with the stretch ratio. The results of thermal gravimetric analysis indicated a polymeric material of high thermal stability. Polyimide fibers made by either method have dielectric constants similar to that of the corresponding polymer; namely, 2.50 at a frequency of 10 GHz.

Properties	From Polyamic Acid Solution		Polyimide Fibers Produced From a Polyimide Solution	
	Polyamic Acid Fibers	Polyimide Fibers		
Stretch Temperature	Ambient	—	Ambient	289 °C
Stretch Ratio	1.1	—	1.0	2.3
Cross-Sectional Shape of Fiber	Round	Round	"C" Shape	Dumbbell
Cross-Sectional Area of Fiber, μm^2	350	230	990	240
Percent Solid Fibers*	46	46	13	0
Breaking Tenacity, kpsi (MPa)	13 (90)	24 (165)	6 (41)	36 (250)
Percent Elongation to Break	7	110	9	22
Initial Modulus, kpsi (GPa)	490 (3.4)	430 (3.0)	180 (1.2)	770 (5.3)

*(Number of solid-core fibers ÷ Total number of fiber ends examined) × 100.

Tensile and Geometric Properties of low-dielectric-constant polyimide fibers made by the two methods are compared.

These aromatic polyimide fibers should prove useful in industrial and aerospace applications in which fibers are required to have dielectric constants less than 3, high thermal stability, and tensile properties in the range of those of standard textile fibers. Potential applications include use in printed circuit-boards and in aircraft composites.

This work was done by William E. Dorogy, Jr., of Lockheed Engineering & Sciences Co. and K. Mason Proctor and Anne K. St. Clair of **Langley Research Center**. *For further information,* ***write in 33*** *on the TSP Request Card.*

This invention is owned by NASA, and a patent application has been filed. Inquiries concerning nonexclusive or exclusive license for its commercial development should be addressed to the Patent Counsel, Langley Research Center [see page 20]. Refer to LAR-14526.

Composite Solid Electrolyte for Lithium Cells

Features include high ionic conductivity and strength.

NASA's Jet Propulsion Laboratory, Pasadena, California

A composite solid electrolyte material consists of very small (0.05 μm) α-alumina particles, each coated with thin layer of LiI, bonded together with a polymer electrolyte or other organic binder. This electrolyte material offers significant advantages over other solid electrolytes in lithium cells and batteries:

- The lithium transference number (t_{Li^+}) is close to unity (see table): as a result, concentration polarization is eliminated, with consequent enhancement of the discharge-current and power capacity.
- The salt anion (I^-) is compatible with lithium, resulting in a chemically stable system.

- Because of this compatibility and because of an improved lithium-transport mechanism, the electrical resistance of the interface between the Li and this solid electrolyte (interface resistance) is smaller, by a factor of 10, than that in the case of older polymeric electrolytes.
- In comparison with polymeric electrolytes, the composite solid electrolyte has greater mechanical strength, and, unlike polymeric electrolytes, it can be used at temperatures above 100 °C.
- The ionic conductivity of the composite solid electrolyte at 20 to 120 °C is similar to or greater than that of the older polymeric electrolytes.

The composite solid electrolyte will enable the development of Li/TiS_2 or other batteries with overall power densities greater than 100 W/kg (pulse power capability of 1 kW/kg) and specific energy of 100 W•h/kg.

In a typical older polymeric electrolyte like polyethylene oxide, Li^+ cations complexed (bound) to the polyethylene oxide or other organic polymer have low mobility (transference number = 0.3 to 0.5), whereas the uncomplexed anions move faster; this leads to high concentration polarization and high interface resistance. Moreover the BF_4^- AsF_6^-, ClO_4^- or $CF_3SO_3^-$ anions contained in such a polymer degrade the lithium because they are not chemically compatible with it. In addition, when heated above 100°C, a typical older polymeric electrolyte becomes soft and begins to flow.

In initial experiments on the composite solid electrolyte, it was found that by mixing LiI and Al_2O_3 powders and pressing them into a pellet, one obtained a solid electrolyte with a conductivity an order of magnitude greater than that of pure LiI, which itself has good ionic conductivity and low electronic conductivity (its lithium-transference number is close to 1). This enhanced conductivity is due to the presence of Al^{3+} cations at the LiI/Al_2O_3 interface, which cations cause an increase in the concentration of Li^+ vacancies. The Li^+ conduction occurs in the LiI mainly at the LiI/Al_2O_3 interface. Unfortunately, a pellet of pressed LiI/Al_2O_3 is very brittle and has low resistance to mechanical shock, and its other mechanical properties are generally poor.

The composite solid electrolyte retains the vacancy conduction mechanism for Li^+ and is expected to exhibit the flexibility of polymeric electrolytes. The polymer in the composite solid electrolyte can serve two purposes: it can be used as a binder alone, the conduction taking place only in the Al_2O_3 particles coated with solid LiI; or it can be used as both a binder and as a polymeric electrolyte, providing ionic conductivity between the solid particles that it binds together.

This work was done by Emmanuel Peled, Ganesan Nagasubramanian, Gerald Halpert, and Alan I. Attia of Caltech for **NASA's Jet Propulsion Laboratory**. *For further information,* ***write in 68*** *on the TSP Request Card.*

This invention is owned by NASA, and a patent application has been filed. Inquiries concerning nonexclusive or exclusive license for its commercial development should be addressed to the Patent Counsel, NASA Resident Office– JPL [see page 20]. Refer to NPO-18694.

Composition of Solid Electrolyte	Temperature, °C	Bulk Conductivity, $\Omega^{-1}cm^{-1}$	Lithium-Transference Number (t_{Li^+})	Interface Resistance $\Omega \cdot cm^2$
Composite Solid Electrolytes				
$(LiI)_1$ $(PEO)_3$ $(Al_2O_3)_{0.3}$ $(Triglym)_{0.3}$	116 90	10^{-3} 2×10^{-4}	0.8 + 0.05 0.9 + 0.05	2.5 10
$(LiI)_1$ $(PEO)_{1.65}$ $(Al_2O_3)_{0.39}$	103	10^{-4}	1 + 0.05	25
Polymeric Electrolytes				
$(PEO)_8$ NaI 10% Al_2O_3	120	3×10^{-4}		
$(PEO)_8$ LiClO 10% Al_2O_3	118	10^{-3}	0.22	25
$(PEO)_{4.5}$ LiSCN	115	10^{-4}	0.5	72

Note: "PEO" means "polyethylene oxide."

Electrochemical Properties of thin films of composite solid electrolytes are shown in comparison with those of older polymeric electrolytes.

Improved Helmet-Padding Material

The material is very resistant to ignition and combustion.

Lyndon B. Johnson Space Center, Houston, Texas

Polyimide of the chemical formula shown in the figure can be foamed into lightweight padding material for use in helmets. In comparison with older padding materials, this one exhibits increased resistance to ignition, combustion, and impact, and it outgasses less. Helmet components made of this polyimide have been foamed in thicknesses of ¼ to ⅜ in. (6.4 to 9.5 mm) and ½ in. (12.7 mm) and molded in various shapes and sizes to accommodate the individuals wearing the helmet in manned tests at the NASA/JSC Crew and Thermal Systems Division.

MAKE THE SPARCSTATION™ YOU ALREADY HAVE AS FAST AS THE SPARCSTATION YOU'D LIKE TO HAVE.

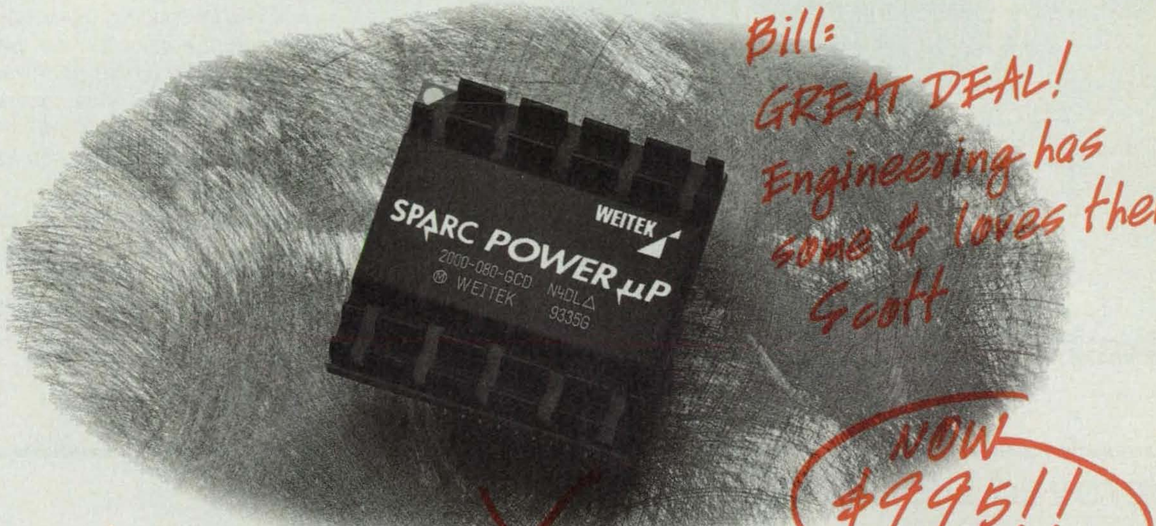

~~$1,500~~

This is all it costs to make your present workstations as fast as the SPARCstation 10.

Good Reviews!

BEST PRODUCT

If you're looking for an economical and efficient way to boost the speed of your present workstations, look no further.

For just $1,500, WEITEK will get everyone running considerably faster in practically no time at all.

The 80 MHz WEITEK SPARC POWER™ µP CPU upgrade can improve the performance of your SPARCstation 2™ or IPX™ systems to match that of the SPARCstation 10™ Model 30.

SPARC Compliant SCD v7

And SPARC POWER µP is easy enough to install yourself in minutes. It's 100% pin-for-pin and binary-compatible with existing systems and software. And it's backed by all the benefits of SunService's SunSpectrum℠ maintenance.

SunService A Sun Microsystems, Inc. Business

For more information, call us or return the accompanying reply card via mail or fax.

Join the thousands of SPARCstation 2 and IPX users who already enjoy the performance of the WEITEK SPARC POWER µP.

WEITEK

TO ORDER YOUR SPARC POWER µP, CALL 1-800-758-7000, Oper. 15.

For More Information Write In No. 614

Multiple Pages Intentionally Left Blank

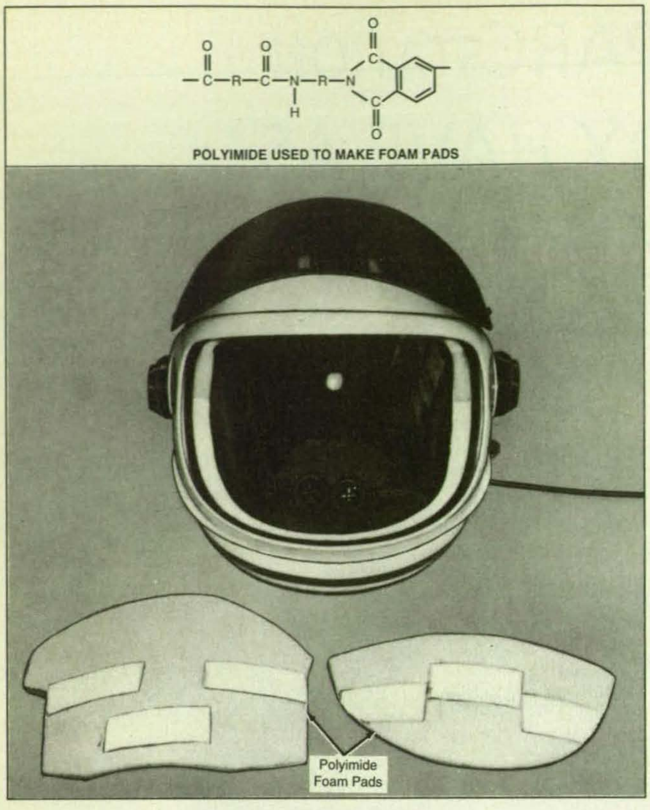

Foam of the Polyimide shown at the top offers increased resistance to ignition, combustion, and impact, as well as decreased outgassing and toxicity.

This polyimide foam satisfies the offgassing and toxicity requirements of NASA/ JSC criteria (NHB80601B). Helmets that contain this improved padding material could be used by firefighters, police, offshore drilling technicians, construction workers, miners, and race-car drivers. This improved foam could also be used in a variety of other applications.

This work was done by Frederic S. Dawn of **Johnson Space Center** *and Fred R. Weiss and John D. Eck of Lockheed Engineering & Sciences Co. No further documentation is available.*

This invention is owned by NASA, and a patent application has been filed. Inquiries concerning nonexclusive or exclusive license for its commercial development should be addressed to the Patent Counsel, Johnson Space Center [see page 20].
Refer to MSC-21842.

Improved Dielectric Films for Capacitors

Blends of cyanoresin and cellulose triacetate have high breakdown strengths plus high dielectric constants.

NASA's Jet Propulsion Laboratory, Pasadena, California

Dielectric films made from blends of some commercially available high-dielectric-constant cyanoresins (see Figure 1) with each other and with cellulose triacetate (CTA) have both high dielectric constants and high breakdown strengths. The dielectric constants can be as high as 16.2. Unoptimized cast films — with thicknesses ranging from 2 μm to 30 μm — have breakdown strengths ranging from 4.5 kV/mil (1.710^8 V/m) to 9.4 kV/mil (3.710^8 V/m). Optimized films made of cyanoresin/CTA blend are projected to have breakdown strengths >15 kV/mil (5.9 V/m). These films could be used to produce high-energy-density capacitors.

In experiments, acetonitrile, chloroform, and dichloromethane were used as solvents in casting films made of various blends of different cyanoresins. Of the blends tested, the only one that exhibited properties suitable for use in capacitors was a mixture of 80 weight percent high-molecular-weight cyanoethyl hydroxyethyl cellulose (CRE) and 20 weight percent high-molecular-weight cyanoethyl cellulose. This blend, which was not optimized, exhibited an electrical breakdown strength of 4.5 kV/mil (1.710^8 V/m) (dc voltage), a dielectric constant of 16, and a dielectric loss of 0.04. The x-ray diffraction spectrum of this film showed that it was amorphous.

Because of the thermal, morphologi-

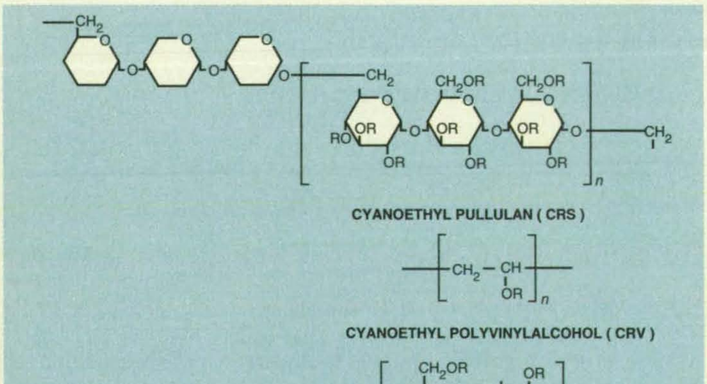

Figure 1. These **Cyanoresins** were tested for use in making dielectric films.

Figure 2. **Thermomechanical Analysis** performed on a CRE/CTA (1:1) film yielded this plot.

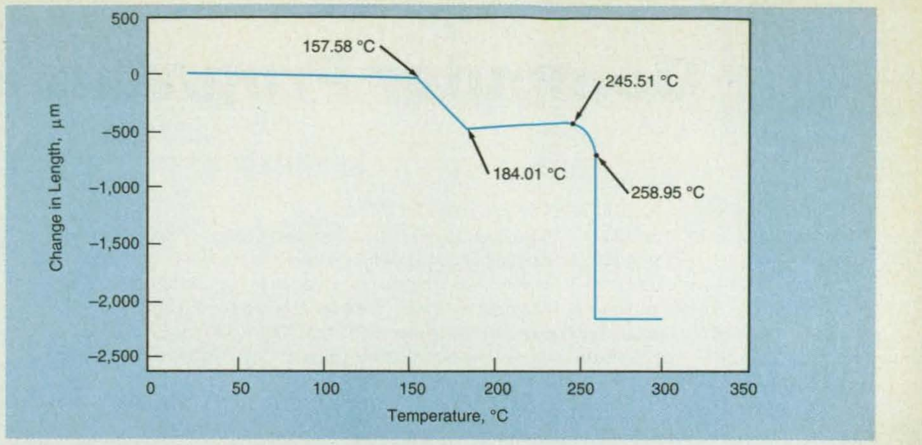

cal, and mechanical properties and the film processability of the various cyanoresins, only the high-molecular-weight CRE polymer has the potential to make high-dielectric-constant and high-breakdown-strength film when blended with semicrystalline cellulose triacetate (CTA) polymer. In an experiment, a roll of about 100 g of CRE/CTA (1/1) film was made by use of a 5-in. (12.7-cm) laboratory drum caster. Chloroform and dichloromethane were used as solvents for CRE and CTA, and 2-methoxyethanol was used as a releasing compound to ensure the lift-off of film from the casting drum. The concentration of the polymer in solution was adjusted, in the range of 5 to 10 percent by weight, to obtain the desired viscosity of the solution for drum casting. The temperature of the casting drum was 30 °C, and the speed at which the film was produced was only a few feet (about 1 meter) per minute. After lift-off from the drum, the film was dried by passing it through an electric oven at a temperature of about 150 °C. After drying, the film was wound onto a cord under tension to orient it.

The x-ray diffraction spectrum showed that the film had an oriented amorphous molecular structure. Thermomechanical analysis showed that the film had a glass-transition temperature of 157.7 °C (see Figure 2). At 184 °C, the film started to crystallize, and the melting temperature of the film was ~245.5 °C. The results of the thermomechanical analysis indicate that the film should be able to withstand temperatures up to 150 °C.

The oriented amorphous CRE/CTA film had a dielectric constant of 7.87 and a dielectric loss of 0.031 at a frequency of 1 kHz and an average dc breakdown strength of 9.42 kV/mil (3.710^{8} V/m). On the basis of these observations plus observations of polycarbonate film, it is expected that if the molecular structure of the film is optimized with biaxial orientation (by inducing crystallinity), the film should display a breakdown strength in excess of 15 kV/mil (5.910^{8} V/m).

This work was done by Shiao-Ping S. Yen and Carol R. Lewis of Caltech and Peter J. Cygan and T. Richard Jow of the U.S. Army LABCOM for **NASA's Jet Propulsion Laboratory.** *For further information,* ***write in 73*** *on the TSP Request.*

This invention is owned by NASA, and a patent application has been filed. Inquiries concerning nonexclusive or exclusive license for its commercial development should be addressed to the Patent Counsel, NASA Resident Office– JPL [see page 20]. Refer to NPO-18913.

Computer Programs

COSMIC: Transferring NASA Software

COSMIC, NASA'S Computer Software Management and Information Center, distributes software developed with NASA funding to industry, other government agencies and academia.

COSMIC's inventory is updated regularly; new programs are reported in *Tech Briefs*.For additional information on any of the programs described here, write in the appropriate TSP number.

If you don't find a program in this issue that meets your needs, call COSMIC directly for a free review of programs in your area of interest. You can also purchase the annual *COSMIC Software Catalog*, containing descriptions and ordering information for available software.

COSMIC is part of NASA's Technology Transfer Network.

COSMIC® —
John A Gibson, Director
Phone (706) 542-3265;
FAX (706) 542-4807
The University of Georgia,
382 East Broad Street,
Athens, Georgia 30602

Computer Programs

These programs may be obtained at a very reasonable cost from COSMIC, a facility sponsored by NASA to make computer programs available to the public. For information on program price, size, and availability, write in the reference number on the TSP and COSMIC Request Card in this issue.

Mathematics and Information Sciences

Software for Monitoring VAX Computer Systems

VAXCMS generates charts that summarize performance data.

The VAX Continuous Monitoring System (VAXCMS) computer program was developed at NASA Headquarters to aid system managers in monitoring the performances of VAX computer systems through the generation of graphic images that summarize trends in performance metrics over time. Since its initial development, VAXCMS has been extensively modified at the NASA Lewis Research Center. Data are produced by using the VMS MONITOR utility subprogram to collect the performance data. This data is then fed through custom-developed linkages to the Computer Associates' TELL-A-GRAF computer-graphics software to generate the chart images for analysis by the system manager. The VMS ACCOUNTING utility subprogram is also used to gather interactive process information.

The charts that are generated by VAXCMS are as follows: (1) central-processing-unit (CPU) modes for each node during the most recent 4-month period; (2) CPU modes for a cluster as a whole, by use of a weighted average of all the nodes in the cluster based on processing power; (3) percent of primary memory in use for each node during the most recent 4-month period; (4) interactive processes for all nodes during the most recent 4-month period; (5) daily, weekly, and monthly summaries of performance for CPU modes, percent of primary memory in use, and page fault rates for each node; and (6) plots of daily disk performance data in the form of average disk input/output response times based on input/output operation rates and lengths of queues.

VAXCMS is written in DCL and VAX FORTRAN for use with DEC VAX-series computers running VMS 5.1 or later. This program requires the TELL-A-GRAF graphics software package to generate plots of system data. A FORTRAN compiler is required. The standard distribution medium for VAXCMS is a 9-track, 1,600-bit/in. (630-bit/cm) magnetic tape in DEC VAX BACKUP format. It is also available on a TK50 tape cartridge in DEC VAX BACKUP format. An electronic copy of the documentation in ASCII format is included on the distribution medium. Portions of this code are copyrighted by David Lavery and are distributed with his permission. These portions of the code may not be redistributed commercially.

This program was written by Les Farkas and Ken Don of **Lewis Research Center**, *David Lavery of NASA Headquarters, and Amy Baron of Washington University. For further information,* ***write in 3*** *on the TSP Request Card. LEW-14950*

File-Sectioning and Reducing Program

Large ASCII files are split into smaller, more manageable files.

The SPLIT computer program accepts inputs in the form of any large ASCII-type file and splits or rewrites the input into smaller, more-easily-managed files. The number of lines in the files thus created is designated by the user. These smaller files can then be edited, printed, or copied onto floppy disks without file-size complications, inasmuch as all editors, printers, and floppy drives have inherent file-size limits. File order is maintained by the program in naming each output file with the original filename plus a sequentially numbered filename extension. There is no limit on the size of the input file. SPLIT is completely menu-driven and includes input prompts for the user.

SPLIT is written in FORTRAN 77 for IBM PC-series and compatible computers running MS-DOS. The standard distribution medium for this program is a 5.25-in. (13.34 cm), 360K MS-DOS-format diskette. Documentation is included in the price of the program. SPLIT was developed in 1992.

This program was written by R. A. Akian of Rockwell International Corp. for **Marshall Space Flight Center**. *For further information,* ***write in 12*** *on the TSP Request Card.*
MFS-29863

Machinery

Geodetic and Astrometric VLBI Program

MODEST estimates propagation delays and geodetic and astrometric parameters.

Observations of extragalactic radio sources in the gigahertz region of the radio-frequency spectrum by two or more antennas separated by a baseline as long as the diameter of the Earth can be

When it comes to electromagnetic design software, Integrated Engineering Software leads the way in solving your problems. Quickly. Easily.

What You can Expect from IES Software

- Shorter time to market
- High quality designs
- Simplified analysis
- Enhanced productivity
- Real dollar savings

Discover the Power of Parametrics

Explore dozens of design possibilities with our latest optimization feature, Parametrics. With Parametrics, you can customize countless "what if" scenarios to your exact specifications, giving you the capacity to change and refine your designs. Effortlessly. Accurately.

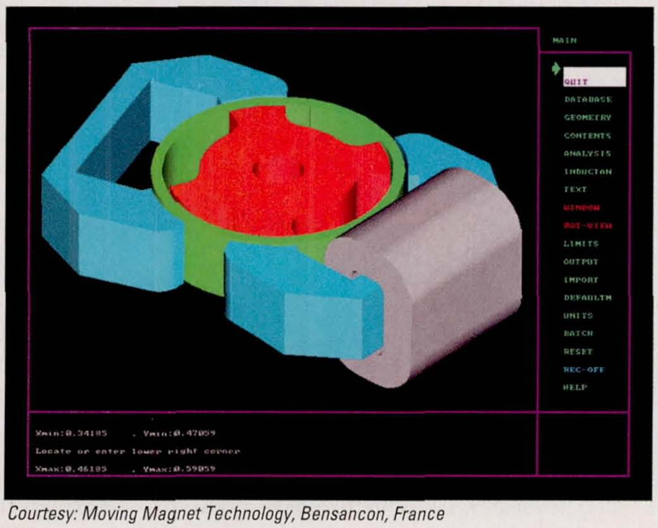

Courtesy: Moving Magnet Technology, Bensancon, France

Our User-Friendly Software just got Friendlier

IES software accelerates computer-aided engineering into a new dimension of speed, simplicity and performance by running under the Microsoft Windows and Windows NT environments. For the past ten years, our programs have been synonymous with design innovation due to the Boundary Element Method (BEM)'s meshless analysis. This theoretical base combined with Windows technology and power ensures that no other product will have you up and running faster.

Expand Your Fields of Analysis

Put our competitive edge to work for you with KELVIN

Built around the same principles of integration, KELVIN, our new 2D/RS Thermal Analysis program, combines ease of use and convenience with smart thermal solutions. Seamlessly import your electromagnetic designs into KELVIN to handle all your thermal analysis needs.

Depend on our products to get you back to the business of quality designs

Call today for your 30-day no-charge software evaluation.

INTEGRATED
ENGINEERING SOFTWARE

TEL: (204) 632-5636 FAX: (204) 633-7780
e-mail: info@integrated.mb.ca

For More Information Write In No. 467

reduced, by the techniques of radio interferometry, to yield time delays and their rates of change. The very-long-baseline interferometric (VLBI) observables can be processed by the MODEST software to yield geodetic and astrometric parameters of interest in such applications as geodynamics and the tracking of geophysical satellites and spacecraft. As the accuracy of radio interferometry has improved, increasingly complete models of the delay and delay-rate observables have been developed. MODEST is a delay-model (MOD) and parameter-estimation (EST) program that takes into account such delay effects as those related to geometry, the clock, the troposphere, and the ionosphere.

MODEST includes all known effects at the centimeter level in its mathematical model. As the field evolves and new effects are discovered, these can be included in the model. In general, the model includes contributions to the observables from the orientation of the Earth, motion of the antenna, behavior of the clock, atmospheric effects, and structure of the radio source. Within each of these categories, a number of unknown parameters can be estimated from the observations. Since all parts of the time-delay model contain nearly linear parametric terms, a square-root-information filter (SRIF) linear least-squares algorithm is employed in estimation of parameters.

Flexibility (via dynamic allocation of memory) in the MODEST code ensures that the same executable code can process a wide array of problems. These range from a few hundred observations on a single baseline that yield estimation of tens of parameters to global solutions for the estimate of tens of thousands of parameters from hundreds of thousands of observations at antennas widely distributed over the surface of the Earth. Depending on the availability of memory disk storage, large problems can be subdivided into more tractable pieces that are processed sequentially.

MODEST is written in FORTRAN 77, C language, and VAX Assembler for DEC VAX-series computers running VMS. It requires 6 Mb of random-access memory for execution. The standard distribution medium for this package is a 1,600-bit/in. (630-bit/cm), 9-track magnetic tape in DEC VAX BACKUP format. It is also available on a TK50 tape cartridge in DEC VAX BACKUP format. Instructions for use and sample input and output data are available on the distribution media. This program was released in 1993 and is a copyrighted work with all copyright vested in NASA.

This program was written by Ojars J. Sovers, Richard P. Branson, and John L. Fanselow of Caltech for **NASA's Jet Propulsion Laboratory**. *For further information,* ***write in 45*** *on the TSP Request Card.*
NPO-18818

US/SPINSIM

This program simulates the exoatmospheric motion of the spinning upper stage of a rocket.

The IUS/SPINSIM computer code was written to evaluate a proposed spinning third stage for the Inertial Upper Stage (IUS) Jupiter Mission. The third stage of the IUS was not to have attitude control during the solid-motor burn for this mission. IUS was to be spun up about its principal thrust axis in the desired attitude prior to ignition of its solid motor. IUS/SPINSIM can also be used to evaluate the performances of other spinning stages that utilize fixed-burn motors.

IUS/SPINSIM performs a six-degree-of-freedom simulation for exoatmospheric flight of an IUS. It incorporates the assumption that the stage is released in orbit at or near its desired inertial attitude, and is spinning slowly. The code models three phases: a coast phase, in which further spin-up may occur; a burn phase, during which the burn of a solid rocket motor (SRM) injects the spacecraft into a transfer trajectory; and a final coast phase. IUS/SPINSIM takes into account the effects of the following: a reaction control system (RCS) spinning the vehicle; buildup, decay, and misalignment of thrust in the SRM; changing mass; center of gravity; principal moments of inertia; cross products of inertia; time derivatives of inertia; jet-damping moments; and a mathematical model of gravitation based on an assumed oblate spheroidal shape of the planet.

Numerical integration of the equations of motion via a Runge–Kutta fourth-order integration algorithm and small step sizes is used to track the position, velocity, attitude, and rates of spin of the vehicle. Instead of using Euler angles or a direction-cosine matrix, quarternions are used to model the attitude and spinning of the vehicle. This eliminates the renormalization difficulties associated with either of the other methods. Program input is taken from a file, and output is to a print file and a data file suitable for use in plotting.

The IUS/SPINSIM is written in FORTRAN 77 for DEC VAX-series computers running VMS. The standard distribution medium for this program is a 9-track, 1,600-bit/in. (630-bit/cm) magnetic tape in DEC VAX BACKUP format. It is also available on a TK50 tape cartridge in DEC VAX BACKUP format. This program was developed in 1992.

This program was written by V. A. Dauro of **Marshall Space Flight Center**. *For further information,* ***write in 53*** *on the TSP Request Card.*
MFS-28811

Physical Sciences

Computing Flows of Slush Hydrogen in Pipes

FLUSH computes solid fractions and other parameters under various flow conditions.

Slush hydrogen, a mixture of the solid and liquid phases of hydrogen, is a candidate form of fuel for the National Aerospace Plane (NASP). Advantages of slush hydrogen over liquid hydrogen include greater heat capacity and greater density. However, the practical use of slush hydrogen as a fuel requires systems of lines, valves, and the like that are designed to deliver the fuel in slush form with minimal loss of the solid fraction as a result of pipe heating or flow friction. Engineers involved with the NASP Project developed the FLUSH computer program to calculate the pressure drop and the loss of the solid fraction of slush hydrogen in steady-state, one-dimensional flow.

FLUSH solves the steady-state, one-dimensional energy equation and the Bernoulli equation for flow in a pipe. The program performs these calculations for each two-node element — straight length of pipe, elbow, valve, fitting, or other part of the piping system — specified by the user. The user provides the rate of flow, upstream pressure, initial solid-hydrogen fraction, heat leaks in elements of the plumbing, and such parameters of these elements as lengths and diameters. For each element, FLUSH first calculates the pressure drop, then figures the solid fraction of slush leaving the element. The code employs GASPLUS routines to calculate thermodynamic properties of the slush hydrogen.

FLUSH is written in FORTRAN IV for DEC VAX-series computers running VMS. An executable code is provided on the

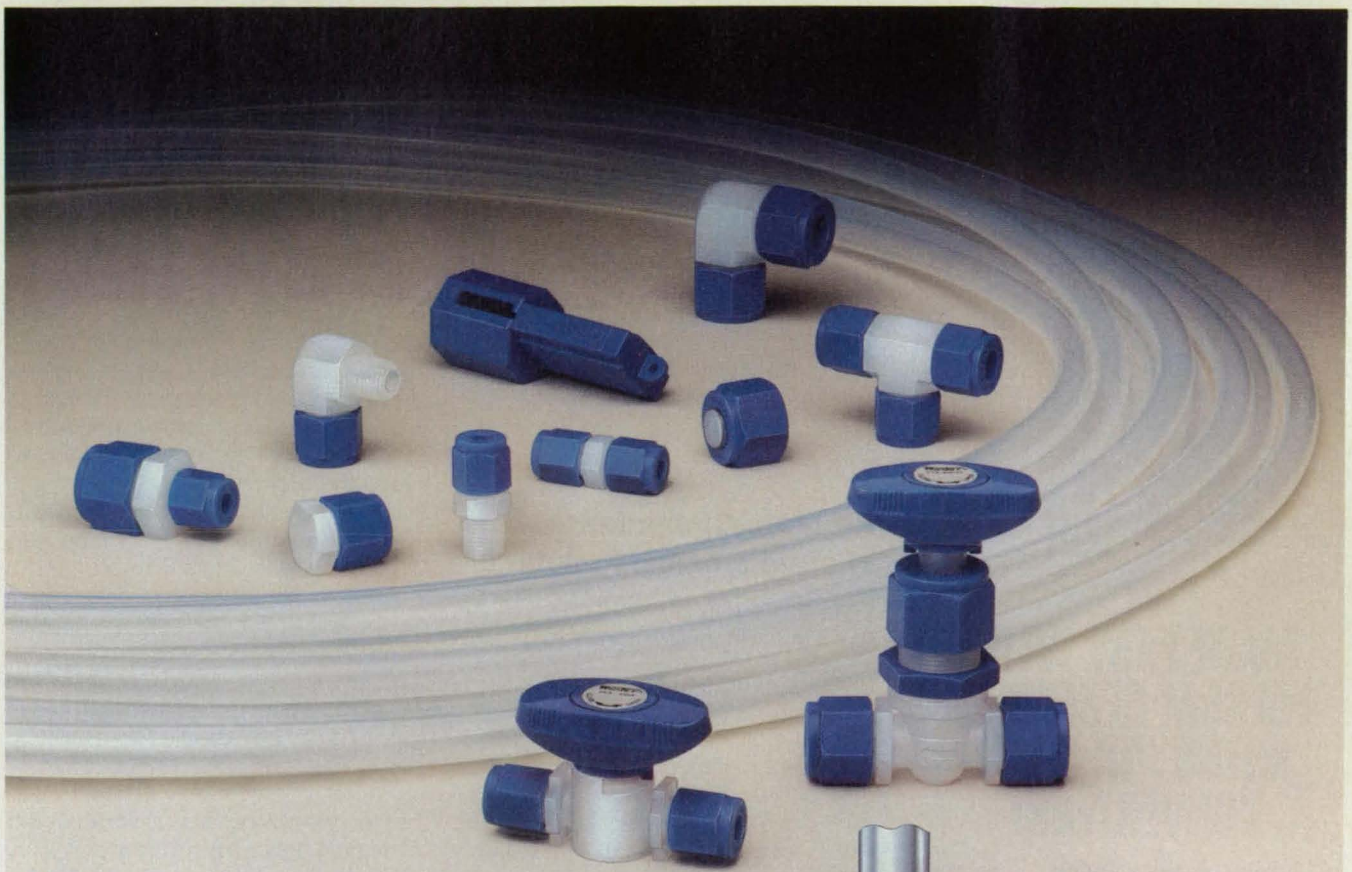

Complete Containment for corrosive and hard-to-handle fluids

***PFA* Fittings, Tubing, and Valves from the SWAGELOK companies let you design leak-tight systems from start to finish.**

SWAGELOK® *PFA* Tube Fittings
- Leak-tight seals with high pressure capability
- 1/4″, 3/8″, and 1/2″ sizes
- Pressures to 275 psig

SWAGELOK *PFA* Tubing
- 1/4″, 3/8″, and 1/2″ sizes
- 0.062″ wall thickness
- 50 ft. and 100 ft. lengths

SWAGELOK Groove Cutter
For grooving *PFA* Tubing used in SWAGELOK *PFA* Tube Fittings.

WHITEY® *PFA* Valves

Needle
- Roddable, straight-through orifice for easy cleaning and high flow (C_V's to 1.39)
- 1/4″, 3/8″, and 1/2″ SWAGELOK Tube Fitting end connections
- Plug tip stem ensures leak-tight shut-off and offers flow control
- Positive stem stop prevents accidental disassembly
- Panel mountable
- Patented stem seal eliminates leakage and requires less operating torque
- Pressures to 180 psig
- Temperatures to 300°F

Plug
- 1/4 turn actuation
- Easily cleaned or purged
- Full flow design ($C_V = 1.8$)
- Compact
- 1/4″ SWAGELOK Tube Fitting end connections
- Pressure rating 60 psig
- Temperatures to 200°F

the SWAGELOK® companies

SWAGELOK Co.
Solon, OH 44139

For More Information Write In No. 403

For More Information Write In No. 417

tape. The GASPLUS physical-properties routines, which are required for building the executable code, are included as one object library on the program medium (full source code for GASPLUS is available separately as COSMIC Program Number LEW-15091). FLUSH is available in DEC VAX BACKUP format on a 9-track, 1,600-bit/in. (630-bit/cm) magnetic tape (standard medium) or on a TK50 tape cartridge. FLUSH was developed in 1989.

This program was written by T. Hardy of **Lewis Research Center**. *For further information,* ***write in 39*** *on the TSP Request Card.*
LEW-15217

Program Computes Thermodynamic Functions

PAC91 is the latest in the PAC (Properties and Coefficients) series.

The two principal features of the PAC91 computer program are to provide means of (1) generating theoretical thermodynamic functions from molecular constants and (2) least-squares fitting of these functions to empirical equations. The coefficients obtained from a least-squares fit can then be used to generate a library of thermodynamic data in a uniform format that is easy to use in other computer codes.

Several large compilations of selected or calculated thermodynamic data currently exist. Nevertheless, there is a continuing need for additional calculations because of the discovery of new species; the revision of existing molecular constants and structural parameters; the need for data at temperatures other than those for which data are already published; the availability of new or revised heats of formation, dissociation, or transition; and the revision of fundamental constants or atomic weights. Calculations may also be needed to compare the results of assuming various possible forms of the partition function. In addition, there is often a preference for thermodynamic data in functional rather than tabular form.

To satisfy these needs, the PAC91 program can perform any combination of the following: (1) calculate thermodynamic functions (heat capacity, enthalpy, entropy, and Gibbs free energy) for any set of 1 to 202 temperatures; (2) obtain a least-squares fit of the first three of these functions (either individually, two at a time, or all three simultaneously) for up to eight temperature intervals; and (3) calculate, as a function of temperature, heats of formation and equilibrium constants from assigned reference elements.

The thermodynamic functions for ideal gases can be calculated from molecular constants by use of one of several variations of the partition function provided by the program. For monatomic gases, one of three partition-function cutoff techniques can be selected by the user, and unobserved but predicted electronic energy levels can be included by the program. For a diatomic or polyatomic gas, one of five partition functions is available. These differ in the correction factors for nonrigid rotation, anharmonicity, and interactions between vibrations and rotations. Excited electronic states can also be included.

Other capabilities of the program include the ability to estimate thermodynamic properties by a group-additivity method, the ability to calculate properties of species with internal rotors, and a method for extrapolation of data to high temperatures. For the purpose of additional processing, known thermodynamic functions for solids, liquids, or gases can be read in directly, or thermodynamic functions can be calculated from heat-capacity equations.

PAC91 is written in FORTRAN 77 to be machine-independent. It requires 1 Mb of random-access memory for execution. It has been tested on a Sun SLC computer running SunOS, a DECstation 3100 computer running ULTRIX, an IBM RS/6000 computer running AIX, and a MicroVAX 3600 computer running VMS. It has not been implemented under DOS. The standard distribution medium for PAC91 is a 0.25-in. (6.35-mm) streaming-magnetic-tape cartridge (Sun QIC-24 format) in UNIX tar format. Other distribution media and formats are available upon request. PAC1 was originally released in 1967 and has been continuously revised, updated, and extended. PAC91, the latest version, was released in 1993. This program is documented in NASA RP-1271.

This program was written by Bonnie J. McBride of **Lewis Research Center** *and Sanford Gordon of Sanford Gordon and Associates. For further information,* ***write in 80*** *on the TSP Request Card.*
LEW-15779

PV·WAVE

Your Decisions Are Only as Good as Your Analysis

Gathering data isn't so hard these days. Real—time information services, data acquisition systems, satellites, MRI scanners, and many other sources of information abound. All capable of generating more data than can be meaningfully interpreted.

Available on UNIX, VMS, Windows® and Windows NT®

That's where PV-WAVE can help. PV-WAVE is designed to interactively manage, analyze, and display large and complex data sets. PV-WAVE is built around a powerful and flexible 4GL designed specifically for interactively analyzing data and building custom data analysis environments. PV-WAVE'S concise language can reduce your coding by up to 80%, so you can generate results quickly.

To do this, the PV-WAVE product family provides integrated mathematics and statistics, advanced graphing and plotting, custom GUI (Graphical User Interface) tools, real-time data monitoring, direct interfaces to SQL databases, connectivity to your existing application software, and even symbolic math capabilities. PV-WAVE readily accepts almost any data format, from rich HDF files, to raw ASCII data, to TIFF or bit-mapped data, and even custom data formats.

Making it a snap to turn even the most complicated data sets into practical knowledge.

So call us today, and learn how technical and financial customers the world over are using PV-WAVE to improve the speed and accuracy of their analyses and decision making.

Turn massive amounts of multi-variable data into easily interpreted images

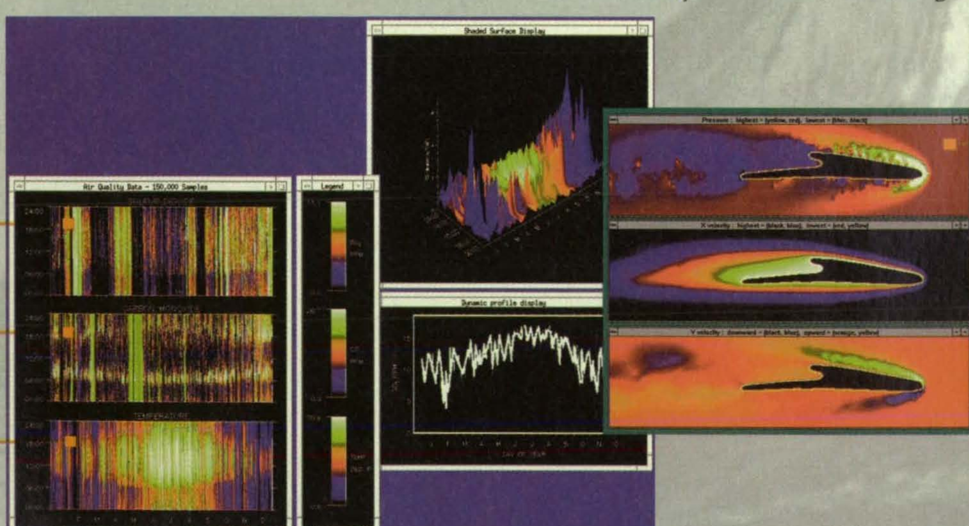

Perform analysis and display of multiple real-time data sources, such as data acquisition systems

For additional information and a product demo, call:

1-800-447-7147

Visual Numerics

PV-WAVE Products
6230 Lookout Rd. • Boulder, Colorado 80301 USA
Tel: 303-530-9000 • FAX: 303-530-9329

Corporate Headquarters
9990 Richmond Avenue, Suite 400 • Houston, Texas 77042-4548 USA
Tel: 713-784-3131 • FAX: 713-781-9260

AD9428

MATHEMATICS YOU CAN SEE!

NEW!

C Numerical Analysis and Presentation Graphics for Windows NT™

See us at Siggraph July 26-28 Orlando, FL

THE PRODUCTIVITY TOOLS YOU NEED FOR C APPLICATION DEVELOPMENT

IMSL C NUMERICAL LIBRARIES

Mathematical functions:

- integration & differentiation
- transforms
- differential equations
- linear systems
- eigensystems
- interpolation & approximation
- nonlinear equations
- optimization
- special functions
- basic matrix/ vector operations

Statistical functions:

- basic statistics
- goodness-of-fit
- cluster analysis
- time series analysis & forecasting
- nonparametrics
- probability distribution & inverses
- random numbers
- analysis of variance
- categorical & discrete data analysis
- factor analysis
- correlation
- regression

The IMSL C Numerical Libraries

C for Yourself! Order Your IMSL Software for the PC Now!

IMSL EXPONENT GRAPHICS FOR C

- Interactive graphics library produces over 30 plots in 2D & 3D with only two function calls.
- Built-in GUI to quickly modify plots, access your data, prototype results & perform "what if" analysis.

IMSL Exponent Graphics

- The only interactive graphics library that is flexible *and* easy to use.

Additional Features of IMSL C Numerics and Graphics:

- Developed in C for native language syntax.
- Copy and paste example code directly into your application for major time savings.
- Windows-based online documentation.

IMSL®

FORTRAN and C application development tools from Visual Numerics

60-day money-back guarantee!

1-800-222-IMSL ext.6495

Tel: 713-954-6495 Fax: 713-781-9260
E-mail: pcsales@houston.vni.com

Save a Bundle – Buy the Bundle!

IMSL NUMERICS & GRAPHICS
Bundle Price: $1,195

All products also available on UNIX workstations.

System Requirements:

- Intel PC
- Microsoft Windows NT 3.1
- Microsoft Visual C++ 1.0
- Math co-processor recommended

For More Information Write In No. 414

Master Card & VISA accepted

AD9484

Safety Retainer for Shackle Bolt

A reusable locking device replaces safety wire.

Lyndon B. Johnson Space Center, Houston, Texas

A retainer for a shackle bolt can be installed quickly and easily. The retainer can be installed on a shackle that is used to lift heavy loads. It ensures that the shackle bolt does not accidentally back out of the shackle.

The retainer replaces safety wire, which must be tied in a time-consuming procedure each time it is installed. The retainer, in contrast, can be assembled in a few seconds. A shackle user who might ignore the requirement for using safety wire would be more likely to use the retainer. Thus, because of its convenience, the retainer promotes greater safety in lifting.

The retainer includes a notched collar through which a tethered pin can be inserted (see figure). The collar is placed over the shackle bolt so that the notch engages one arm of the shackle. The pin is then inserted through holes in the collar and bolt. The pin thus holds the retainer on the shackle bolt. A spring-loaded ball on the pin prevents it from slipping through the collar and bolt holes. The collar can be removed from the shackle just as easily as it was installed: the user depresses the spring-loaded ball so that the pin can be removed. The collar can then be removed from the shackle.

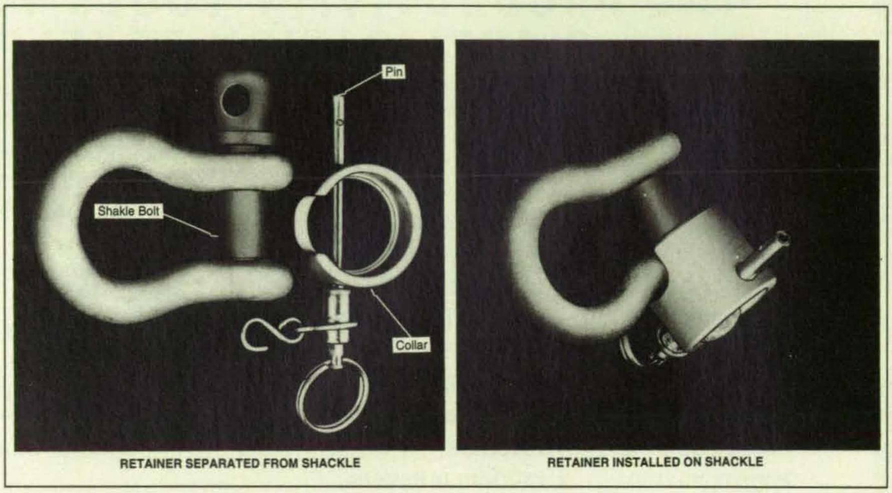

The **Shackle-Bolt Retainer** can be installed and removed quickly.

This work was done by Elwood S. Falls of **Johnson Space Center**. *For further information,* ***write in 41*** *on the TSP Request Card.*
MSC-22256

Shoulder Joint for Protective Suit

Nesting rings are designed for freedom of movement.

Lyndon B. Johnson Space Center, Houston, Texas

A shoulder joint for a protective suit imposes very small resisting forces and torques, allowing the wearer's arm to move almost naturally. The joint also resists damage by abrasion or by penetration of debris. Developed for a space suit, the joint would also offer advantages in a protective garment for underwater work, firefighting, or cleanup of hazardous materials.

The joint includes a series of rings linked by rod-end pivots spaced 90° apart on alternate rings, with rotary bearings at the shoulder, midsection, and upper arm (see figure). Internal laminated pleats between rings seal the joint. The pleats allow the rings to roll concentrically or nest inside one another. In the original space-suit application, the joint withstands an internal pressure of 8.3 psi (57 kPa).

The gimbal action of the rod-end pivots and the rotation of shoulder, midsector, and upper-arm bearings accommodate the full range of natural shoulder motions. Similar principles of design may also be applicable to wrist, hip, and ankle joints.

This work was done by Joseph J. Kosmo of **Johnson Space Center** *and Richard D. Smallcombe of ILC Space Systems. For further information,* ***write in 36*** *on the TSP Request Card.*
MSC-22261

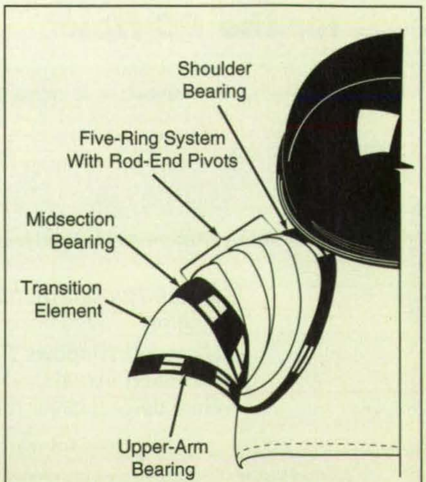

The **Shoulder Joint** allows the full range of natural motion: the wearer senses little or no resisting force or torque.

Simulating Microfracture in Metal-Matrix Composites

Simulation procedures can predict microfracture propagation and heirarchy of fracture modes.

Lewis Research Center, Cleveland, Ohio

Computational procedures have been developed for simulating microfracture in metal-matrix/fiber composite materials under mechanical and/or thermal loads at ambient and high temperatures. These procedures are used to evaluate the microfracture behavior of the composites, establish hierarchies and sequences of fracture modes, and examine the influences of compliant layers and partial debonding on the properties of the composites and on the initiation of microfractures in them.

The procedures are based on finite-element analysis and equations of micromechanics (mechanics of materials at the microscopic matrix/fiber level). The finite-element models used to evaluate microfractures in unidirectional-ply and cross-ply composites contain nine fibers in a 3 × 3 array of unit cells that are subdivided into finite polyhedral volume elements of fiber, interphase, and matrix materials. Each volume element is characterized by the tabulated mechanical properties of its material at the designated temperature at which microfracture is to be simulated.

To prepare for a simulation of fracture, duplicate nodal or grid points of the finite volume elements are placed on both sides of an assumed microcrack. Both points in each resulting pair initially coincide with each other, but there is no connection between them: thus, what is represented initially is a crack of zero width. The load and boundary conditions are applied to the model through uniform boundary displacements. In a typical set of simulations, fracture is initiated at the middle of the fiber in the central cell and is allowed to propagate either through the matrix or along the fiber/matrix interface; fracture is introduced around the fiber, such that the fiber becomes debonded from the matrix around its whole circumference. Similarly, the crack could be initiated in the matrix or at the fiber/ matrix interface.

Resulting nodal forces that correspond to the applied boundary displacements are computed by finite-element analysis. These nodal forces are compared for the reduction in global stiffness as the defect is propagated or perturbed, and the corresponding strain-energy-release rates (SERR's) are computed, as described below. In the case of thermal loads, symmetrical boundary conditions are applied in the middle planes so that the composite is free to move on either side. As before, SERR's are computed to quantify different fracture modes and establish hierarchies thereof.

The SERR is an indicator of the fracture toughness of a material. It gives a measure of the amount of energy required to propagate a crack in a material. In this method, the SERR is computed via a global approach (instead of a traditional local or microfracture approach) in which applied nodal displacements and corresponding nodal forces are used to calculate the work done to propagate the crack. The SERR is calculated as the incremental change in work divided by the incremental change in new surface area that opens up along the path from one fracture mode to another. The applied displacement between two fracture modes is kept the same, while nodal forces required to maintain that displacement change because of the reduction in global stiffness as the fracture propagates. In the case of thermal loads, SERR is calculated by comparing the internal strain energies before and after incremental propagation. The advantage of this global (total) SERR formulation is that it bypasses gradients of stress and other local details that can give rise to inconsistencies. The global SERR shows whether the growth of the crack is stable and which way the crack will grow.

The simulation procedures have been applied to two composites of SiC fibers in Ti matrices: a unidirectional-fiber laminate with a fiber volume fraction of 0.35 and a cross-ply $(0^\circ/90^\circ/0^\circ)$ laminate with a fiber volume fraction of 0.3. The results of the simulations show that interfacial debonding follows fracture of a fiber or matrix, and that thermomechanical cyclic loading severely degrades the integrity of a composite material.

This work was done by Subodh K. Mital of the University of Toledo and Christos C. Chamis and Pascal K. Gotsis of **Lewis Research Center.** *For further information,* ***write in 81*** *on the TSP Request Card.*
LEW-15613

America's Premier Technology Showcase Is

TECHNOLOGY 2004

The Fifth National Technology Transfer Conference & Exposition

November 8-10, 1994
Washington, DC Convention Center

Sponsored by NASA, NASA Tech Briefs, and the Technology Utilization Foundation, in cooperation with the Federal Laboratory Consortium for Technology Transfer

The federal government and its contractors will spend over $75 billion this year on research and development. Technology 2004 will show you how to tap into this tremendous resource and will introduce you to new funding and partnering opportunities.

Technology 2004 will bring together the top technologists and tech transfer agents in US national laboratories, universities, and high-tech industry. It is designed to help companies to quickly and easily find innovative, ready-made ideas they can use to solve engineering problems, create new or improved products, and grow their businesses.

How You Will Benefit:

Practical, Informative Workshops

Defense conversion...technology reinvestment...dual-use inventions. You've heard the buzz words, but what do they mean for your company and your job? How can you take advantage of the federal government's multi-billion-dollar push to commercialize taxpayer-supported technologies and leverage the nation's R&D investment? Technology 2004 workshops will show you how to get started and what's in it for you.

Symposia Spotlighting America's Best New Inventions

Leading technologists from NASA, the departments of Defense and Energy, and other key agencies will unveil commercially-promising innovations and advanced processes in critical areas driving US and world growth markets. Discover how ideas developed for defense and space programs can be reapplied in commercial industries such as biotech, electronics, computing, transportation, and many more.

The World's Largest Technology Transfer Exposition

A "who's-who" of government labs, universities, and high-tech firms will demonstrate their latest inventions and products available for license or sale in the 80,000+ sq. ft. exhibits hall. It's the place to meet the technology vanguard, discuss your needs and capabilities you have to offer, and keep abreast of leading-edge developments across the techno-spectrum.

Free Internet Training Sessions

Daily demonstrations in the exhibits hall will help you to take advantage of the Internet — the worldwide web of computer networks that has been labeled "the on-ramp to the information superhighway." Learn about important resources on the net and how you can access them without spending a lot of time or money. Sessions will begin at 10:30 am each day.

Technology 2004 Program

Tuesday, November 8

8:30 am - 10:00 am
Plenary Session: Government-Industry Partnership Opportunities

10:30 am - 12:30 pm
National Critical Technologies Concurrent Symposia: Advanced Manufacturing; Bio/Medical Technology; Computer-Aided Design; Materials Science; Power & Energy

2:00 pm - 4:00 pm
Concurrent Symposia: Artificial Intelligence; Computers & Software; Electronics; Environmental Tech; Video/Imaging

Exhibition Hours: 10:00 am - 5:00 pm

Wednesday, November 9

8:30 am - 10:00 am
Concurrent Workshops: Business Guide To Tech Transfer Resources; The Defense Technical Application Center (DTAC) Network; Small Business Innovation Research Grants

10:30 am - 12:30 pm
National Critical Technologies Concurrent Symposia: Artificial Intelligence; Materials Science; Test & Measurement; Video/Imaging; Virtual Reality/Simulation

2:00 pm - 4:00 pm
Concurrent Symposia: Computers & Software; Electronics; Environmental Tech; Materials Science; Test & Measurement

7:00 pm - 10:00 pm
Technology Transfer Awards Dinner

Exhibition Hours: 10:00 am - 5:00 pm

Thursday, November 10

8:30 am - 10:00 am
Concurrent Workshops: International Tech Transfer Forum; Licensing Government Patents; The Technology Reinvestment Project

10:30 am - 12:00 pm
Concurrent Workshops: International Tech Transfer Forum (cont.); Cooperative Research & Development Agreements; The DOC Advanced Technology Program

Exhibition Hours: 10:00 am - 3:00 pm

Plus: The LaserTech '94 Photonics Technology Transfer Conference will be held concurrently with Technology 2004 on Wednesday, November 9 from 8:00 am to 4:30 pm. Complete registrants can attend the LaserTech '94 sessions, breakfast, and networking luncheon for an upgrade fee of $35.00.

Coming To Washington, DC This November

Preregister and $ave

	by 10/21	On-site
Complete Registration (includes Technology 2004 symposia and exhibits, awards dinner, and a set of official proceedings)	$250	$295
One-Day Registration	$85	$100
Awards Dinner Only	$50	$60
LaserTech '94 (upgrade for T2004 complete registrants; includes breakfast, lunch, and photonics symposia on 11/9)	$35	$40
Exhibits Only	— No Charge —	

Preregistrants will receive written confirmations via mail along with their name badges and inquiry cards. Badge holders, programs, and dinner tickets must be picked up in person at the Washington, DC convention center (900 Ninth St. NW) beginning at 12:00 pm on Monday, November 7.

Special Hotel Rates

Renaissance Hotel (headquarters)	**$125 single/double**
Grand Hyatt Washington	**$134 single/double**
Henley Park Hotel	**$100 single/$110 double**
Hotel Washington	**$99 single/double (govt. only)**

To make reservations, call the housing bureau at (800) 535-3336 or (202) 842-2930 and identify yourself as a Technology 2004 attendee. A $125 per room deposit is required.

Travel Discounts

Budget Rent-A-Car: Call (800) 772-3773 and refer to the Technology 2004 rate code #VNRD/TNGY. Valid Nov. 1-17.
Amtrak: 10% discount. Call (800) USA-RAIL and refer to the Tech 2004 fare code #X-84E-927. Valid Nov. 6-12.
USAir: Book your ticket on USAir to be entered into a drawing for two round-trip tickets good in the continental US, Canada, the Bahamas, and San Juan. 10% discount off unrestricted coach fares, and 5% off first class. Call (800) 334-8644, refer to gold file #35380094.

Questions? Call Wendy Janiel at (212) 490-3999.

ntb 7/94

TECHNOLOGY 2004 PREREGISTRATION FORM

USE A SEPARATE FORM OR PHOTOCOPY FOR EACH REGISTRANT. BE SURE TO ANSWER ALL QUESTIONS BELOW.

Name ____________________

Title ____________________

Company ____________________

Address ____________________

City/St/Zip ____________________

Phone No. ____________________

Which of the following best describes your industry or service? (check one)

- A ☐ Electronics
- B ☐ Computers
- C ☐ Communications
- D ☐ Transportation/Automotive
- E ☐ Aerospace
- F ☐ Defense
- G ☐ Government
- H ☐ Materials/Chemicals
- I ☐ Industrial Equipment
- J ☐ Manufacturing
- K ☐ Power/Energy
- L ☐ Biomedicine
- M ☐ University
- N ☐ Research Lab
- O ☐ Other

specify____________________

Which of these products do you recommend, specify, or authorize the purchase of? (check all that apply)

- A ☐ Electronic Components & Systems
- B ☐ Software
- C ☐ Computers/Peripherals
- D ☐ CAD/CAE/CAM/CASE
- E ☐ Lasers/Optics
- F ☐ Materials
- G ☐ Mechanical Components
- H ☐ Positioning Equip./Motion Control
- I ☐ Test/Measurement Instruments
- J ☐ Sensors/Transducers
- K ☐ Data Acquisition
- L ☐ Video/Imaging Equipment
- M ☐ Industrial Controls/Systems
- N ☐ Communications Equipment
- O ☐ Laboratory Equipment

Your principal job function is: (check one)

- A ☐ General & Corporate Management
- B ☐ Design & Development Engineering
- C ☐ Engineering Services - Tests/Quality
- D ☐ Basic Research
- E ☐ Manufacturing/Production
- F ☐ Purchasing/Procurement
- G ☐ Other

specify:____________________

Please register me for the following:

- A ☐ Complete Registration $250
- B ☐ One-Day Symposia/Exhibits $85
  check day: ☐ 11/8 ☐ 11/9 ☐ 11/10
- C ☐ Awards Dinner Only $50
- D ☐ LaserTech '94 upgrade fee $35
  (Technology 2004 complete registrants ONLY.)
- E ☐ Exhibits Only .... Free

TOTAL: $ ____________________

☐ Check/MO enclosed (payable to Technology Utilization Foundation)
☐ Charge my: ☐ Mastercard ☐ VISA ☐ Am Ex

____
Card No. Expire Date

____
Signature Date

Registrations and Awards Dinner reservations are transferrable and may be cancelled until October 21, 1994. After that date no cancellations will be refunded.

Return with payment to: Technology Utilization Foundation c/o Technology 2004, PO Box 614, Brookfield, IL 60513-0614

For fastest registration fax to: (708) 344-9482

Call For Nominations

FIFTH ANNUAL INDUSTRY AWARDS FOR EXCELLENCE IN TECHNOLOGY TRANSFER

Sponsored by the Technology Utilization Foundation and the Federal Laboratory Consortium for Technology Transfer

Private sector organizations that have commercialized technologies developed by/for/with federal government agencies or laboratories are invited to submit nominations for Awards of Excellence In Technology Transfer. Two winners will be chosen by a blue ribbon panel of judges and the awards presented at the Fifth Annual Technology Transfer Awards Dinner, to be held November 9, 1994 at the Washington, DC Renaissance Hotel. The Awards Dinner is the central event of the Technology 2004 National Technology Transfer Conference and Exposition (Nov. 8-10, 1994, Washington, DC Convention Center).

Letters of nomination must include the organization's name and address, a contact and phone number, and a 200-300 word description of the commercialized product or process, focusing on its importance (such as its economic or societal impact) and novelty in the marketplace. The description also should highlight the federal government's role in the technology's development and transfer. Up to ten pages of supporting materials may be included with the letter of nomination.

DEADLINE FOR NOMINATIONS IS AUGUST 1, 1994.
Nominees will be notified by September 15, 1994.

MAIL NOMINATIONS TO: Technology Utilization Foundation, 1994 Awards, 41 East 42nd St., #921, New York, NY 10017 or fax to: (212) 986-7864.

QUESTIONS? CALL WENDY JANIEL AT (212) 490-3999.

Computational Simulation of Fiber-Pushout Tests

Step-by-step procedures to perform computational simulation, establish bounds of interfacial bond strength, and interpret interfacial bond quality are described.

Lewis Research Center, Cleveland, Ohio

A computational procedure to simulate fiber-pushout tests has been developed. In a fiber-pushout test, faces of a composite-material specimen perpendicular to the fibers are polished; then one of the fibers is pushed out by use of an indenter, and the pushout force is measured. Pushout tests are performed to obtain values of shear bond strength and interfacial friction between matrices and fibers. These values — especially bond strengths — are important because they affect the mechanical properties of the composites and, in particular, because the degradation of bond strengths affects the ultimate strengths, impact resistances, fatigue resistances, and other important properties of these materials.

The need for computational simulations of fiber-pushout tests arises from the difficulty of performing such tests at the high temperatures at which composites are normally used. Computational simulations can be helpful in planning a fiber-pushout test, establishing bounds on interfacial bond strength, and interpreting the results of the test in terms of the quality of the bonds.

The computational simulation involves a three-dimensional finite-element model. It is based on the physics of the fiber-pushout test. The maximum interfacial shear stress occurs just inside the loaded end of the specimen. Debonding starts at that location. As the load on the fiber is increased, interfacial fracture progresses until the full length of the fiber is debonded and the fiber just slides out from the other end. For progressive fracture to occur, the local interfacial shear stress must exceed the corresponding strength. As the shear stress approaches interfacial bond shear strength, the interfacial shear stiffness decreases rapidly.

The process is nonlinear, and the full shear stress/strain behavior for the interface bond would be needed for an accurate simulation. However, the present computational procedure follows an alternate approach in which the interfacial material is replaced with an anisotropic material with a greatly reduced shear modulus and the simulated phenomena are made linear up to the pushout load. This simplification makes the simulation computationally very effective, and it provides a direct means to estimate the interfacial shear strength. The distribution of shear stress at the instant of pushout can also be determined.

The average interface shear strength obtained from the pushthrough load can easily be separated into two components: one that comes from frictional stresses and the other from a combination of (1) chemical adhesion between the fiber and the matrix and (2) mechanical interlocking that develops from shrinkage of the composite because of phase changes during processing. The effect of normal stress distribution at the interface, caused by thermal mismatch, is readily taken into account by modifying the shear modulus of the interface. The fiber-pushout load as a function of temperature can also be predicted.

This work was done by Subodh K. Mital of University of Toledo and Christos C. Chamis of **Lewis Research Center**. *For further information,* ***write in 91*** *on the TSP Request Card.* *LEW-15610*

Multiple Pages Intentionally Left Blank

Cooled-Spool Piston Compressor

The temperature of compressed gas would be limited to a safe value.

Lyndon B. Johnson Space Center, Houston, Texas

The proposed cooled-spool piston compressor would be driven by hydraulic power and would feature internal cooling of the piston by the flowing hydraulic fluid to limit the temperature of the compressed gas. In general, the temperature of a gas rises during compression by an amount that increases with the compression ratio. It is necessary to limit the temperature rise for the sake of safety and/or the purity of the compressed gas: this is especially so when the compressed gas is one that decomposes at high temperature or is reactive (e.g., oxygen) and could react with the compressor materials. Thus, because of the limited capability for cooling the compressed gas in a conventional piston compressor, it is necessary to limit the compression ratio and/or avoid reactive gases.

The cooled-spool piston compressor would provide sufficient cooling for higher compression ratios or reactive gases. Unlike in a conventional piston compressor, all parts of the compressed gas would lie at all times within a relatively short distance of a cooled surface so that the gas would be cooled more effectively. This compressor (see figure) would resemble a shuttle valve with a spoollike piston, which would be driven back and forth by hydraulic fluid that would enter the compressor body alternately at its ends. A narrow passage in the disk at each end of the piston would allow a small flow of hydraulic fluid along the hollow core of the piston; this would serve as the coolant flow. The coolant flow from the down stream end of the piston would be channeled, by external valves, through a coolant passage in the compressor body, then through an external heat sink and returned to the reservoir of hydraulic fluid.

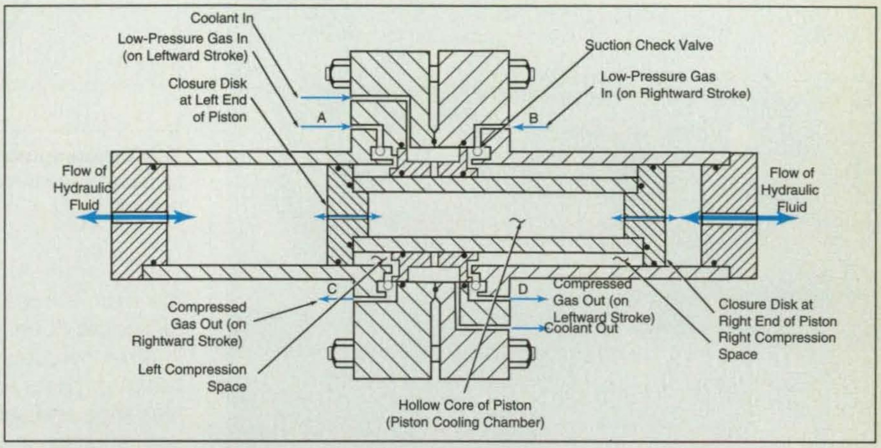

The **Cooled-Spool Piston Compressor** would limit the temperature rise of the compressed gas to a safe level. It would also provide two suction and two compression strokes during each cycle; this makes it possible to obtain one or two stages of compression, depending on the configuration of plumbing connected to ports B and C.

Depending on the instantaneous direction of stroking of the piston, the gas to be compressed would enter the left or right compression space during the suction stroke through a suction check valve in port A or B, respectively. The compressed gas would be expelled from the left or right compression space on the compression stroke through a discharge check valve in port C or D, respectively.

The rightward stroke would produce compression in the left compression space and suction in the right compression space; the leftward stroke would produce suction in the left compression space and compression in the right compression space. Thus, unlike in a conventional piston compressor, each cycle of operation would include two suction and two compression strokes. Because of this, the compressor could be configured as a single- or double-stage configuration unit. In the single-stage configuration, ports A and B would both be connected to the low-pressure gas supply, and ports C and D would both be connected to the high-pressure output gasline. In the two-stage configuration, port A would connected to the low-pressure gas supply, port B to port C, and port D to the high-pressure output gasline.

This work was done by Brian G. Morris of **Johnson Space Center**. *For further information,* ***write in 84*** *on the TSP Request Card.*

This invention has been patented by NASA (U.S. Patent No. 5,238,372). Inquiries concerning nonexclusive or exclusive license for its commercial development should be addressed to the Patent Counsel, Johnson Space Center [see page 20].

Refer to MSC-22020.

Low-Noise Spiral Bevel Gears

Noise was reduced by 12 to 19 dB.

Lewis Research Center, Cleveland, Ohio

Modified spiral bevel gears that generate relatively little noise and vibration have been designed and fabricated for use in the U. S. Army OH-58D helicopter. The unmodified spiral-bevel gears on which they are based are speed-reducing gears in the transmission between the gas-turbine engine and the main rotor of the helicopter, and have been identified as

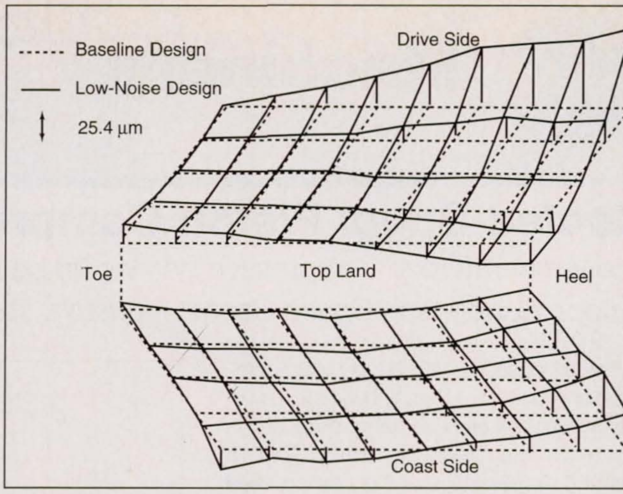

This **Topographical Plot** shows the slight differences between the spiral bevel gear-tooth surfaces in the baseline and low-noise designs.

the main source of noise and vibration in the transmission. Similar low-noise, low-vibration spiral bevel gears could be used in other helicopters, with consequent benefits in comfort and health of pilots and passengers, enhancement of pilots' performance and safety through reduction of audible distraction, and reduction in cost and weight of the helicopters through reduction in the amount of sound-proofing material. Low-noise, low-vibration spiral bevel gears could also be used in drive axles of cars and trucks for smoother, quieter rides.

The low-noise modified gears are made on the same grinding machine as that used to manufacture the unmodified gears, but the machine-tool settings are changed slightly from those of the baseline or unmodified design to reduce the kinematic error. As used here, "kinematic error" denotes the relative motion (deviation from simple rotation at the theoretical speed ratio) of an output gear with respect to an input gear with which it meshes. Kinematic error is the major cause of gear noise, and it is a product of the geometric and manufacturing complexities of the gears.

The methodology for designing the modified gears is embodied in a computer program that incorporates the principles of kinematics and dynamics in fabrication and operation. First, the program determines the geometry of the teeth on the basis of the manufacturing process. Next, it analyzes the gears to determine proper contact and meshing action. Finally, it determines modified machine-tool settings that reduce kinematic error.

In an experiment, a transmission that contained, at different times, the modified and unmodified gears was mounted on a test stand (see figure). The transmission was operated under identical conditions of speed (6,016 rpm) and torque (274 to 686 N•m) with each set of gears. Noise was measured by use of microphones connected to a spectrum analyzer, while vibration was measured by accelerometers mounted on the transmission housing. The measurements showed that the noise generated by the transmission when equipped with the modified gears was 12 to 19 dB below that generated with the unmodified gears. Vibration was reduced by a similar order of magnitude.

This work was done by David G. Lewicki and Robert F. Handschuh of the U.S. Army Research Laboratory, John J. Coy of **Lewis Research Center**, *Zachary Henry of Bell Helicopter Textron, John Thomas of the Gleason Works, and Faydor L. Litvin of the University of Illinois at Chicago. For further information,* ***write in 59*** *on the TSP Request Card.*
LEW-15772

Computerized Inspection of Gear-Tooth Surfaces

Machine-tool settings can be corrected to make the surfaces more precise.

Lewis Research Center, Cleveland, Ohio

A method of manufacturing gears with precisely shaped teeth involves computerized inspection of the gear-tooth surfaces followed by adjustments of machine-tool settings to minimize deviations between the real and theoretical versions of the surfaces. Thus, iterated cycles of cutting gear teeth, inspection, and adjustments can help to increase and/or maintain the precision of subsequently manufactured gears.

Essential to the method is a modern computer-controlled coordinate-measuring machine, which includes a precise rotary table and a spherical-tip probe that can be translated in three dimensions, as required, to make contact with the gear-tooth surface. The coordinates of the center of the probe tip in three dimensions can be measured precisely. The gear to be inspected is mounted on the rotary table so that its back face is flush with the base plane of the coordinate-measuring machine and its axis coincides with the axis of rotation (see Figure 1).

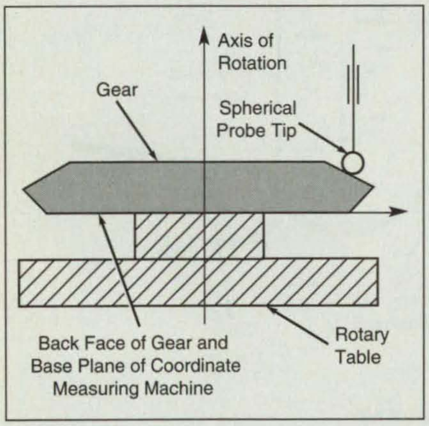

Figure 1. The **Gear Is Placed on the Rotary Table** of the coordinate-measuring machine, and the probe is placed in contact with the gear-tooth surface. The orientation of the probe (vertical as shown here, or else horizontal) is chosen according to the angle of the pitch cone.

The deviations of a real gear-tooth surface from the corresponding theoretical gear-tooth surface are to be characterized in terms of distances between actual surface points and the corresponding theoretical surface points along lines perpendicular to the theoretical surface. For this purpose, a measurement grid is defined by a set of nominal contact points chosen on the theoretical surface (see Figure 2). One of the points serves as a reference point for the initial installation of the probe. The coordinates of the probe tip (measurement coordinates) that correspond to the nominal contact points are then computed from the equations of the theoretical surface, with a correction for the radius vector of the spherical tip at the contact point.

By coordinated, computer-controlled motions of the rotary table and probe, the probe tip and the gear-tooth surface are made to approach contact along the perpendicular to the theoretical surface at each nominal contact point. The coordinates of the probe at actual contact are measured, and from this measurement, the deviation (that is, the distance between the actual and nominal contact points along the local perpendicular) is computed.

The surface deviations measured and the surface deviations produced by changes in machine-tool settings can be represented by an overdetermined system of linear equations. These equations can be solved by use of a least-squares technique to compute changes in machine-tool settings that will minimize the deviations between the real and the theoretical surfaces.

This work was done by R. F. Handschuh of the U.S. Army Aviation Systems Command and F. L. Litvin, Y. Zhang, and C. Kuan of the University of Illinois at Chicago for **Lewis Research Center**. *For further information,* ***write in 60*** *on the TSP Request Card. LEW-15736*

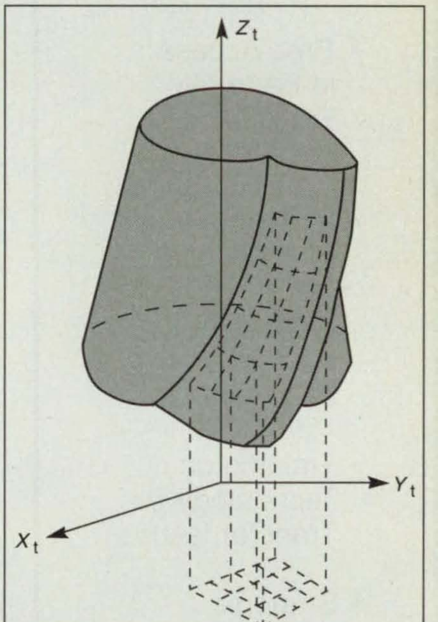

Figure 2. The **Measurement Grid on the Surface** of the gear tooth is defined by nominal contact points on the theoretical tooth surface.

Making Skew-Resistant Fabrics for Composite Layups

Adhesives prevent excessive shifting of warp and fill yarns with respect to each other.

Langley Research Center, Hampton, Virginia

Fabrics used in curved composite-material structures can be prevented from skewing during composite layup by weaving them in a modified process in which the warp and fill yarns are bonded together at their points of contact. (The bonding concept may prove similarly beneficial for braided and knitted fabrics.) Skewing — changes in the spacing and orientation of fill yarns relative to warp yarns — occurs in fabrics that are woven so that the fill and warp are not at the desired angles. Skewing necessitates much extra labor during layup to orient the fabrics correctly, and even then the fibers may no longer be uniformly distributed.

In the modified weaving process, the warp and fill yarns are locally bonded by applying adhesive to them. The amount of adhesive and/or the number of bond points are made large enough to prevent or resist skewing, but not so large as to embrittle the fabric or reduce its drape.

The adhesive can be applied in any of a variety of forms and techniques. For example, it can be applied as a powder or yarn, in which case it can be melted by a heating element in the tip of the clamping bar of the weaving machine (see figure). After the clamping bar is opened, a jet of cool air solidifies the adhesive so that the yarns adhere at their points of contact.

In another version of the process, the adhesive is dissolved in a volatile solvent, and the solution is sprayed on each fill yarn as it is inserted into the warp. The solvent evaporates quickly, leaving a tacky surface. Light pressure can then be applied to the fabric to ensure bonding, and a jet of air can speed the evaporation of the solvent.

In a third version of the process, the adhesive is melted and sprayed on the fill yarn as a hot liquid as it is extracted from its spool, just before it is inserted into the warp. It may be necessary to clamp the fabric briefly to ensure bonding.

In a fourth version, yarn as supplied already contains the adhesive, which can be, for example, a powdered adhesive resin, or a thermoplastic adhesive yarn prewrapped into the fill yarn. After the fill yarn has been inserted into the warp yarn, the heated tip of the clamping bar is pressed against the fabric, locally melting the adhesive contained in the fill. Only a small amount of the adhesive is melted — just enough to lock the fill to the warp. As before, a jet of cool air accelerates solidification.

This work was done by Gary L. Farley of the U.S. Army Vehicle Structures Directorate at the **Langley Research Center**. *No further documentation is available.*

Inquiries concerning rights for the commercial use of this invention should be addressed to the Patent Counsel, Langley Research Center, [see page 20].

Refer to LAR-15007 .

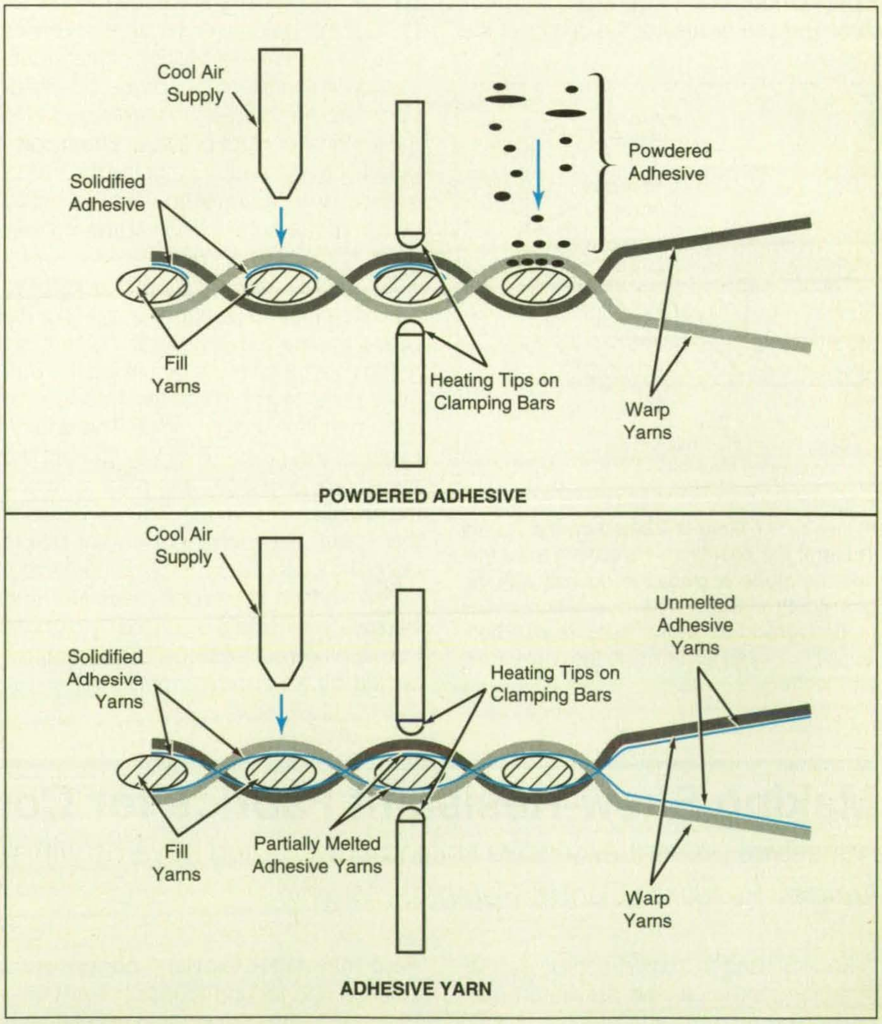

Edge Views of a Fabric show two techniques for bonding the warp and fill yarns to each other. Adhesive powder is applied to the yarns as they are woven, then melted to join them. Alternatively, an adhesive yarn is woven with the warp and fill, then melted briefly.

Improved Locally Adaptive Vector Quantization

Complexity and coding time are less than those of some other data-compression schemes.

NASA's Jet Propulsion Laboratory, Pasadena, California

Several refinements have been introduced to improve the performance of the data-compression scheme described in "Adaptive Vector-Quantization Scheme" (NPO-18186), *NASA Tech Briefs*, Vol. 16, No. 2 (February 1992), page 112. In vector quantization in general, a block of data (e.g., pixel values within a specified rectangular subdivision of an image) is represented exactly or approximately by a code vector that is, in turn, represented by an index number. The specific vector-quantization scheme of the noted prior article effects lossless compression of textual data or slightly lossy compression of image data by use of a simple heuristic "move-to-front" coding protocol that generates the codebook "on the fly" in both the transmitter and the receiver. The codebook is a numerically indexed list of code vectors that is inherently adapted to the local or most recent characteristics of the source data in that the most recent and most frequently used code vectors are closer to the top of the list. Thus, the scheme is called "locally adaptive vector quantization" (LAVQ).

The principal advantages of LAVQ over some other data-compression schemes are that it is less complex and that it does not require a priori knowledge of either the codebook or the statistics of the source data. LAVQ coding can be done rapidly, in a single pass over the source data, thus offering the potential for real-time compression of video data.

One deficiency of basic LAVQ occurs in blocks of pixels in areas of low detail, where pixel values (colors and brightnesses) vary gradually with position: Small errors in quantization can make the boundaries of the blocks visible in the image reconstructed at the receiver (see figure). The improved LAVQ scheme reduces this effect by use of a form of difference coding in which each code vector represents the differences between the pixel values of the present block and the mean code-vector pixel value of the most recent previously coded block: this enables more-accurate reconstruction of regions of gradual variation, without the extensive use of new codewords. Of course, the mean must be updated after each block is processed in both the encoder and the decoder. Those errors that continue to make the boundaries between blocks visible after difference coding are smoothed out by horizontal and vertical interpolations across the boundaries. With careful choice of interpolation techniques, the boundaries can be made invisible without destroying details excessively or causing a blurry appearance.

Although the index numbers in basic LAVQ are compressed representations of the source data, it is possible to effect further compression by applying a lossless compression code to the index numbers themselves. In the improved LAVQ scheme, this is accomplished by an adaptive arithmetic code based on updating of the probability of each code symbol after each use. This code approaches global symbol entropy closely.

The improved LAVQ scheme includes bit stripping of new codeword values, which can be used independently from or in conjunction with difference coding to obtain more compression. The least-significant bits of either a block of pixels or a vector of differences tend to be uniformly random: therefore, stripping these bits before sending data to the decoder and reinserting a mean value at the decoder decreases the number of bits sent when a new codeword is generated for the codebook, with a small increase in distortion. The amount of additional error incurred is not readily noticeable in most images.

When difference coding is used with bit stripping, only a few values typically occur, and these may be represented by a relatively small number of quantization levels. However, an image could contain sharp edges, which could give rise to large differences between pixel values in adjacent blocks. This can cause large errors at edges if linearly quantized difference values are too small to keep up with the sharp changes in pixel values. To minimize this error, nonlinear quantization can be used. Because the image statistics are unknown to the encoder and cannot be easily transmitted to the decoder, the sizes of the quantization steps cannot be made adaptive, and an arbitrary choice must be made in advance.

This work was done by Kar-Ming Cheung and Masahiro Sayano of Caltech for **NASA's Jet Propulsion Laboratory**. *For further information,* ***write in 77*** *on the TSP Request Card.*
NPO-18885

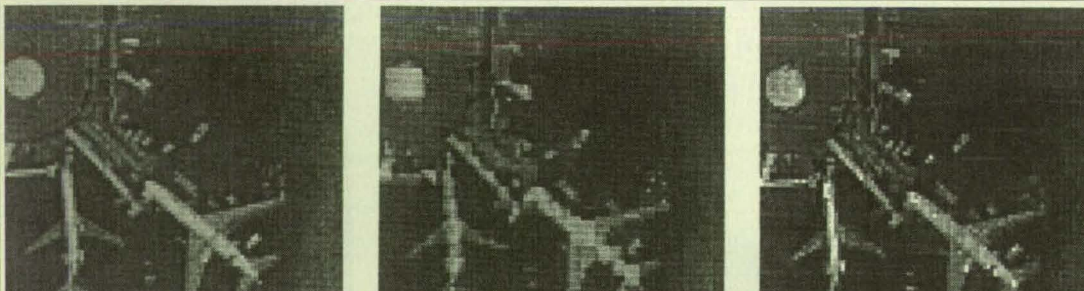

ORIGINAL LBG LAVQ

The **Image as Reconstructed After LAVQ** preserves most of the detail of the original image, but exhibits blockiness in areas of low detail. For comparison, an image reconstructed after Linde–Buzo–Gray (LBG) coding is shown. LBG coding is slower and preserves less detail.

Regenerable Iodine Water-Disinfection System

The service life of an iodination bed is lengthened.

Lyndon B. Johnson Space Center, Houston, Texas

An iodinated resin bed for disinfecting water can be regenerated to extend its useful life. In a demonstration, the resin bed was as biocidally effective after eight regenerations as it was when it was first operated. Presumably, it could have regenerated many more times.

The regeneration system (see figure) includes a bed of crystalline iodine. Normally, the flow of water is diverted around the crystalline iodine and directed through the iodinated resin bed, where it absorbs a small amount of biocidal iodine before entering the potable-water system. When the iodine in the resin bed approaches depletion, the concentration of iodine in the effluent water drops to a low level. At this point, the flow of water is diverted through the crystalline-iodine regeneration bed. The water dissolves iodine in the regeneration bed and carries it to the resin bed, where it is absorbed.

When the iodine in the resin bed is fully restored, as determined by measurement of the concentration of iodine in the effluent, the flow through the regeneration bed is once again diverted around the regeneration bed. When the concentration of iodine in the effluent decreases below the minimum acceptable level, the regeneration cycle is repeated.

The regeneration concept was demonstrated in a small-scale prototype. The system was operated 24 hours a day for 114 days with an average iodine concentration in the effluent of 2.9 mg/L. The test was stopped after eight regenerations, but there were no indicators that it could not have been continued indefinitely.

The first five regenerations, done at a rate of flow of 8.5 mL/min, produced spikes of 6 to 11 mg/L of iodine in the effluent, as shown in the figure. This rate of flow proved unnecessarily large, inasmuch as the high concentration was lost when the iodinated effluent was mixed with a much larger volume of water in a storage tank. Accordingly, the rate of flow during the last three regenerations was reduced to 3 mL/min, corresponding to a residence time of 0.8 min in the regenerator bed. This provided adequate iodine uptake and limited spikes to 4 to 5 mg/L.

The demonstration showed that regeneration increases the life of the resin bed, in terms of the amount of water disinfected, from only 60 L of water per cubic centimeter—and probably much more. At the end of the demonstration, the system was producing 4 mg of residual iodine per liter of water, just as it did at the beginning.

A further benefit of regeneration is that the regeneration bed can provide a highly concentrated biocide source (200 mg/L) when needed. The concentrated biocide can be used to superiodinate the system after contamination from routine maintenance or an unexpected introduction of a large concentration of microbes.

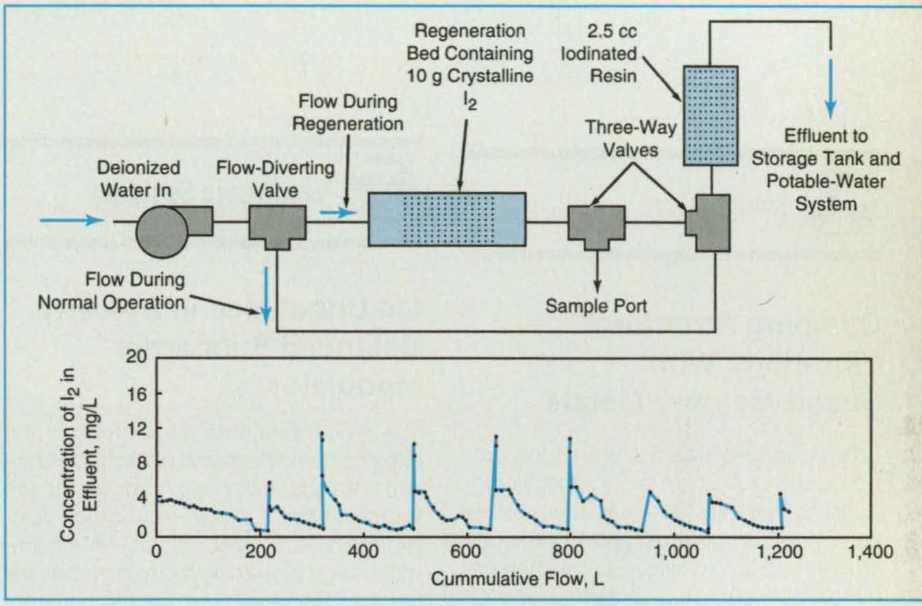

Water Flows Through a Regeneration Bed of crystalline iodine during regeneration. At other times, the flow is diverted around the regeneration bed. Although the regeneration cycle was manually controlled in a demonstration, it could readily be automated to start and stop according to signals and stop according to signals from concentration sensors.

This work was done by Richard L. Sauer of **Johnson Space Center** *and Gerald V. Colombo and Clifford D. Jolly of Umpqua Research Co. For further information,* ***write in 83*** *on the TSP Request Card.*

This invention is owned by NASA, and a patent application has been filed. Inquiries concerning nonexclusive or exclusive license for its commercial development should be addressed to the Patent Counsel, Johnson Space Center [see page 20]. Refer to MSC-21763.

Books & Reports

These reports, studies, and handbooks are available from NASA as Technical Support Packages (TSPs) when a Request Card number is cited; otherwise they are available from the NASA Center for Aerospace Information by calling (410) 859-5300, ext. 394.

Mechanics

Damping Structural Vibrations With Shape-Memory Metals

A report presents a study of the proposed use of shape-memory-metal components to damp vibrations in structures as diverse as buildings, bridges, aircraft, spacecraft, and ships. Shape-memory metals offer enormous potential for such applications because they can dissipate energy in any mode of cyclic motion — shear, torsion, bending, or compression, for example — at high stress without fatigue. The shape-memory properties of these materials also provide means of both assembling and prestressing structures.

*This work was done by Darel Hodgson and Robert Krumme of E*Sorb System for* **Marshall Space Flight Center**. *To obtain a copy of the report, "Structural Damping With Shape-Memory Alloys,"* ***write in 54*** *on the TSP Request Card.*

Inquiries concerning rights for the commercial use of this invention should be addressed to the Patent Counsel, Marshall Space Flight Center [see page 20].

Refer to MFS-27307.

Principles of Linear Elastic Fracture Mechanics

A NASA technical memorandum discusses the principles of linear elastic fracture mechanics. The document follows a straightforward approach with emphasis on practical problems, and is intended especially to help structural engineers understand fracture-mechanics software.

This work was done by Christopher D. Wilson of **Marshall Space Flight Center**. *Further information may be found in NASA TM-103591 [N92-30416/TB], "Linear Elastic Fracture Mechanics Primer."*

Copies may be purchased [prepayment required] from the NASA Center for AeroSpace Information, Linthicum Heights, Maryland, Telephone No. (301) 621-0394. Rush orders may be placed for an extra fee by calling the same number.

MFS-27288.

Electronic Systems

On Unbalance in a Nearly Balanced Subcarrier Modulator

A report presents an analysis of the effects of amplitude and phase imbalance in a nominally balanced modulator in the transmitter of a phase-modulation non-return-to-zero (NRZ) binary-data communication system. In the transmitter, the balanced modulator is used to generate a suppressed-subcarrier signal that carries NRZ-data amplitude modulation in its sidebands. This suppressed-subcarrier signal is then used to phase-modulate the carrier signal. In the presence of unbalance in the nominally balanced modulator, the transmitted signal (the phase-modulated carrier signal) contains undesired spectral components that can degrade the performance of the overall communication system: in particular, these spurious components can interfere with the operation of the carrier-signal-tracking loop in the receiver and can produce bit errors in the received data signal.

This work was done by Tien M. Nguyen of Caltech for **NASA's Jet Propulsion Laboratory**. *To obtain a copy of the report, "On the Effects of a Spacecraft Subcarrier Unbalanced Modulator,"* ***write in 101*** *on the TSP Request Card.*

NPO-18705

Performances of Five Symbol-Lock Detectors

A report discusses the performances of the two older and three newer symbol-lock detectors described in "Three Alternative Symbol-Lock Detectors" (NPO-18521), *NASA Tech Briefs*, Vol. 17, No. 9 (September 1993) page 66. A symbol-lock detector is an analog and/or digital subsystem of a binary-data-communication radio receiver that decides, according to a preset criterion, whether the symbol-detecting operation of the receiver is synchronized ("in lock") with the binary-symbol period *T*, or whether it is slipping cycles. If it is slipping cycles, then one cannot rely on the detected symbols.

The work was done by Mazen M. Shihabi, Sami M. Hinedi, and Biren N. Shah of Caltech for **NASA's Jet Propulsion Laboratory**. *To obtain a copy of the report, "Symbol Lock Detection in the ARX II and Block V Receivers,"* ***write in 47*** *on the TSP Request Card.*

NPO-18623

Life Sciences

Daily GPS-Derived Estimates of Axis of Rotation of Earth

A report describes a study in which data gathered by a worldwide network of 21 Global Positioning System (GPS) receivers during a 3-week experiment in January and February 1991 were used to estimate the location of the axis of rotation of the Earth.

The GPS data were reduced by use of orbit-determining and baseline-estimating software called "GIPSY" and two basic alternative strategies: (1) a standard parameter-estimation strategy with three "fiducial" stations constrained to a priori coordinates, and (2) the free-network strategy, in which there are no fixed sites. The standard strategy for the daily solutions can be summarized as follows: Station locations, satellite-epoch states, and carrier-phase-bias parameters were estimated as constants. Station- and satellite-clock data were assumed to contain white process noise. A 2.2-meter zenith tropospheric delay was removed, and the residual delay was estimated by use of a random-walk stochastic model.

This work was done by Ulf J. Lindqwister, Geoffrey Blewitt, and Adam Freedman of Caltech for **NASA's Jet Propulsion Laboratory**. *To obtain a copy of the report, "Daily Estimates of the Earth's Pole Position With the Global Positioning System,"* ***write in 99*** *on the TSP Request Card. NPO-18799*

New on the Market

Sharp Electronics Corp., Camas, WA, has introduced the first **RAM and ROM combination chip**. By permitting access to both RAM and ROM at the same speed, the LH6P81T simplifies address management and software development while conserving board space. The chip eliminates unused surplus memory space on the ROM side for full use of its 8-Mbit capacity.

For More Information Write In No. 712

BE Designer™ **modeling and simulation software** from BE Software Co., Portland, OR, permits users to create, edit, assemble, and play back visual behavior models of complex objects and systems. These include geometric representations of mechanical devices, mechanical systems such as factories and molecular structures, and invisible systems such as communications, planning, and scheduling.

For More Information Write In No. 704

Summagraphics Corp., Seymour, CT, has introduced a **desktop tablet** with a cordless pressure system for graphic arts, illustration, and animation. The SummaSketch® FX™, available in 12" x 12" and 18" x 12" active-area versions, uses electromagnetic technology with a pen-like, three-button stylus offering 256 levels of pressure sensitivity. It feature 2540-dpi resolution and 0.010" standard accuracy.

For More Information Write In No. 700

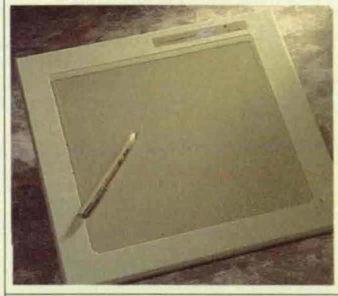

Patent It Yourself, Windows software from Nolo Press, Berkeley, CA, and Electronic Data Systems, enables users to prepare and file a US patent application without a lawyer. The package provides all necessary forms and instructions, flowcharts and checklists for evaluating patentability and commercial potential, and on-line legal assistance.

For More Information Write In No. 709

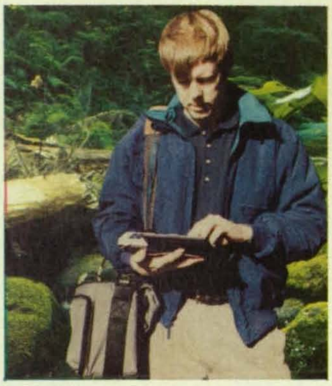

A GPS-based **data logging and management system** from the Collins Avionics & Communications Division of Rockwell International Corp., Cedar Rapids, IA, offers enhanced methods for locating, annotating, and mapping information gathered at all field site types. The GEO-NET™ 2000 Data Logger comprises a base station and a handheld field unit with a Rockwell Trooper™ GPS receiver, portable PC, and software to automatically format information into a tabular or graphic database.

For More Information Write In No. 705

TrueSurf Master **3D surface modeling software** from CADMAX Corp., Baltimore, MD, integrates NURBS surfaces with the company's *Hidden Line Design* feature to improve 3D design productivity. *Hidden Line Design* offers hidden line and shaded views rather than 3D wireframes and permits use of a single database for model and detail drawings to reduce design errors. Coupled with NURBS surfaces, it can be used to create precise geometry to express any 3D shape.

For More Information Write In No. 703

The Software Wedge™ from T.A.L. Enterprises, Philadelphia, PA, adds complete, two-way, **serial I/O capabilities** to any DOS, Windows, OS/2, or NT application. The product converts incoming serial data to keystrokes so that data appears as if being typed in, and helps eliminate manual data entry, expensive hardware additions, and custom programming. Serial data can be logged directly to a disk file in the background while the user works with other programs in the foreground.

For More Information Write In No. 710

New on the Market

Airpot Corp., Norwalk, CT, has released a line of **air cylinders** that virtually eliminate starting and running friction. Designed for applications requiring very smooth motion, low speeds, short strokes, or low pressures, the Airpel cylinders feature a glass liner to prevent corrosion, need no lubrication, and have a pressure rating of 100 psi.
For More Information Write In No. 701

MARECHAL S.A., Paris, France, has introduced **electronic decontactors** designed to improve reliability and safety over electrical plugs and switches in the connection and disconnection of industrial electrical equipment. Silver-tipped spring-assisted butt contacts provide high-quality connection and eliminate oxidation. The decontactors are available with current ratings up to 1000 A, voltages up to 1100 V, and as many as 37 prongs per piece.
For More Information Write In No. 706

Diamond-turned **plastic optics** from Janos Technology Inc., Townshend, VT, are available in aspheric shapes to enhance optical performance and reduce the number of focusing lenses needed. Designed for use in detector systems, solar apparatus, colorimetry, and medical instrumentation, the optics' irregular profiles also resolve some of the mounting restrictions encountered with conventional lenses.
For More Information Write In No. 707

Barry Controls, Brighton, MA, has unveiled an active **electropneumatic control** to regulate the position and damping of any existing vibration isolation system. The modular VIP™ system consists of a controller, three electropneumatic servo valves, three height sensors, a solenoid valve, an air filter, a pressure regulator, and cables. By minimizing rocking and tilting, it offers improved precision, settling times, and repeatability.
For More Information Write In No. 708

Adjustable speed drives from Baldor Electric Co., Fort Smith, AR, combine with high-efficiency motors to improve performance and reduce energy consumption. The AC inverters can result in savings of 25 to 40 percent, according to the manufacturer, and are best suited to fans, pumps, and blowers.
For More Information Write In No. 713

The first commercial **signal and test system** from ESL Inc., a TRW subsidiary in Sunnyvale, CA, provides a single point of control for mixed-signal design and test, execution, and analysis. All measurement hardware and components within the TRW VP8000—including a data acquisition module, playback module, signal generator, and analyzer—communicate via ESL's proprietary bus. The unit captures data in real time, featuring sample rates up to 500 MB/sec. and storage capacity up to 64 MB per snapshot.
For More Information Write In No. 711

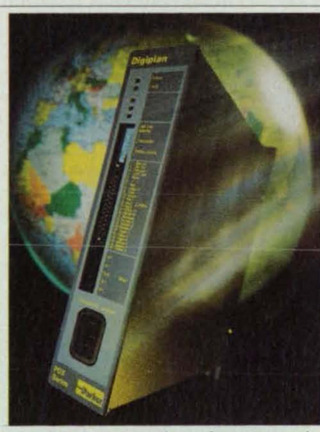

The PDX series of single-axis packaged **motor drives** from the Digiplan Division of Parker Hannifin Corp., Harrison City, PA, features built-in RS-232C indexers and advanced ministepping techniques for output resolutions of up to 4000 steps/rev. The drives have an integral self-adaptive switch-mode power supply, allowing direct on-line operation from any AC supply in the range of 95 V to 265 V.
For More Information Write In No. 702

New Literature

Intelligent Instrumentation, Tucson, AZ, has released the seventh edition of the *Handbook of Personal Computer Instrumentation,* a 228-page guide addressing PC-based **data acquisition, test, measurement, and control**. Topics include fundamentals of signal conditioning, wiring, shielding, and data acquisition.
For More Information Write In No. 717

Electronic gas and liquid flow sensors, flow meters, and flow controllers are highlighted in a 36-page catalog from McMillan Co., Georgetown, TX. Gas flow sensors measure flow rates from 20 ml/min. to 500 l/min., while liquid flow sensors measure flow rates from 13 ml/min. to 10 l/min. Pulse and voltage output are optional.
For More Information Write In No. 715

An engineering guide published by 3M Electronic Products Division, Austin, TX, helps designers select **board-level interconnect products** for I/O, board stacking, IC socketing, and board-to-backplane applications. The booklet includes photos and specifications of 3M's sockets, headers, and high-density stacking connectors. Tables allow users to match the appropriate headers and sockets based on board spacing requirements, pin or lead counts, contact quantities, and pitch.
For More Information Write In No. 718

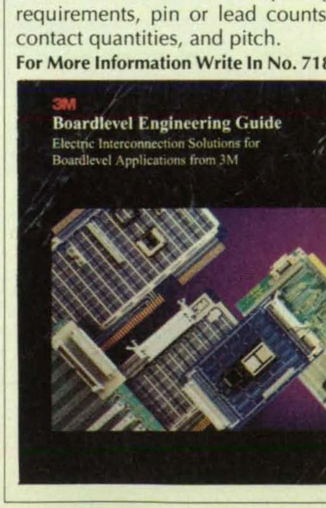

The MacNeal-Schwendler Corp., Los Angeles, CA, has published the first in a series of white papers entitiled *What Managers Need To Know About Finite Element Analysis.* The series is designed to help managers obtain a better understanding of FEA technology and aid their decision making. Future issues will address geometry, software quality assurance, and optimization.
For More Information Write In No. 720

American Variseal, Broomfield, CO, has released a 220-page technical manual for its Variseal™ line of **spring-energized seals** made from high-performance polymers. The guide serves as a training manual and technical support book, offering sections on design concept, preliminary design considerations, seal materials, spring loads, rod and piston seals, face seals, rotary shaft seals, installation, and hardware.
For More Information Write In No. 719

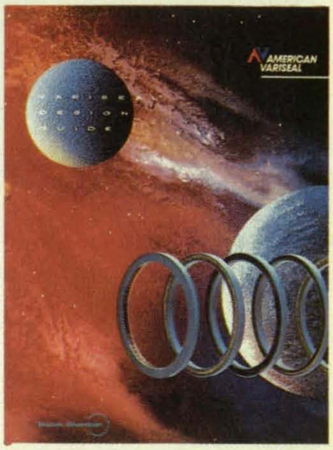

The 59-page PowerAc™ design guide from Nook Industries Inc., Cleveland, OH, features **screw assemblies** with centralized thread forms milled or precision-ground to customer specifications. Twin-lead Acme screws offer cost-efficient dual-opposing linear motion on one drive system. The guide highlights stainless steel screws and precision preloaded nut assemblies that can be adjusted to the preload level required.
For More Information Write In No. 714

DC permanent magnet and gear motors are showcased in a catalog from Barber-Coleman Co. Motor Division, Rockford, IL. Ranging in diameter from .97" to 2.12", the motors provide maximum output from 7.5 to 81 W. Gear motor torque ratings range from 1.3 lb-in. to 300 lb-in. The 60-page book also describes motor weights, component materials, applications, and performance characteristics.
For More Information Write In No. 716

HIGH-TECH PRODUCT NEWS

Highest Performance in VME 6U Form Factor

The SPARC® CPU-5CE™ from FORCE COMPUTERS delivers SPARCstation 10 class performance in a low cost, single-slot VME board. Memory capacity is 8, 16, 32, or 64 MBytes of DRAM. The processor includes a full range of I/O which can be expanded to support a wide array of off-the-shelf solutions. Fully compatible with previous SPARC products. **Write In No. 693**

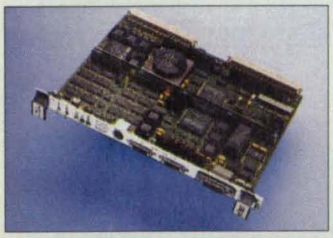

Don't miss the September issue of High-Tech Product News

Call Wayne Pierce at 800-944-NASA

SKYsytem: 20 GFLOPS Right Out of the Box

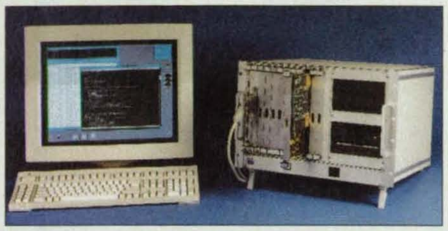

SKY Computers breaks the 20 GFLOP barrier with advanced SKYsystem—configured, tested and guaranteed ready-to-run right out of the box. SKYsystem includes: 1-16 SKYbolt 6U or 9U processors, the SKYvec® Software Development Environment and a SPARC-based slot #1 controller. The SKYsystem 6U delivers 5 GFLOPS. The 9U screams at 20 GFLOPS. To have SKY evaluate your application, call Seth Bardash today at 1-800-486-3400. **Write In No. 694**

RUSSIA'S TOP TECHNOLOGIES UNVEILED FOR THE FIRST TIME

...in Russian Tech Briefs, the official technology transfer publication of the Russian Space Agency. This new bimonthly newsletter features exclusive reports of licensable inventions and novel engineering solutions in electronics, computing, biotech, materials, manufacturing, and much more. A treasure-trove of previously classified technologies now available to U.S. companies.

Write in no. 659 for information on subscribing to Russian Tech Briefs.

HEADHUNTER™

HEAD & EYE SLAVED POINTING SYSTEM

COMPLETE, NON-INVASIVE, REAL-TIME HARDWARE AND SOFTWARE INSTRUMENTATION TO COMPUTE AND ANALYZE COMBINED HEAD AND EYE VECTORS FOR ADVANCED WEAPONS POINTING, SIMULATION /TRAINING & HUMAN FACTORS ASSESSMENT.

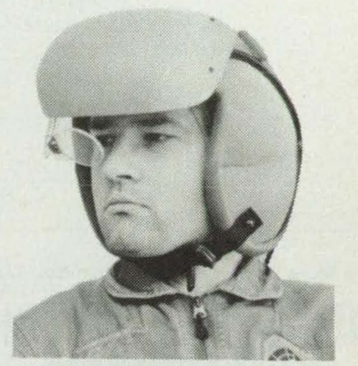

ISCAN®

125 CAMBRIDGEPARK DR.
CAMBRIDGE, MA 02140
TEL: 617-868-5353 FAX: 617-868-9231

For More Information Write In No. 424

NONLINEAR SIMULATION AND CONTROL WITH VisSim™

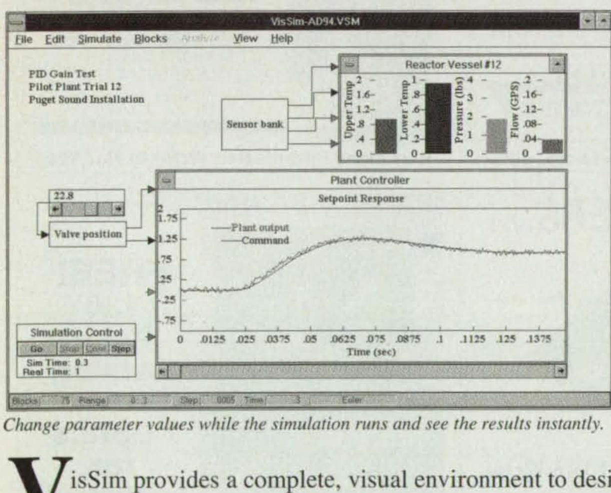

Change parameter values while the simulation runs and see the results instantly.

"VisSim is the best software for the design and simulation of nonlinearities in control systems today."

Art Wroble
Senior Control Engineer
Cadillac Gage Textron

Features

- Visually programmed diagram language
- Hierarchical design
- 80+ built-in block functions
- Integrate custom blocks in C or Fortran
- Extensible toolbox libraries
- Nonlinear and linear
- Parameter optimization NEW
- Hybrid, continuous, and discrete multi-rate
- 7 integration methods for fixed step, adaptive step, and stiff systems
- Multi-input/multi-output state-space NEW
- Multi-channel 20mA/10V real-time (opt.)
- DDE and ASCII file import/export
- Linearization, zero & pole finder, and root locus & Bode plots (opt.)
- Implicit system solver
- Dynamic meters and bar graphs NEW
- Time history, FFT, XY plots, strip charts NEW

VisSim provides a complete, visual environment to design, simulate, and perform real-time verification of complex, dynamic systems. VisSim is used worldwide for modeling the behavior of servo systems, drive systems, digital communication systems, power systems, and biomedical processes.

Companion software

- VisSim/Analyze
- VisSim/C-Code NEW
- VisSim/Neural-Net
- VisSim/RT

VisSim runs on MS/Windows, MS/Windows-NT, and Unix/X operating systems.

Call 508/392-0100
for a free working demo

Visual Solutions INCORPORATED
487 Groton Road
Westford, MA 01886
508/392-0100
508/692-3102 FAX

For More Information Write In No. 408

MARKETPLACE To Advertise—Call (212) 490-3999

REGISTER NOW FOR NORTHEAST PHOTONICS COMMERCIALIZATION CONFERENCE AND WORKSHOP

Creating New Business Opportunities In Optoelectronics

SEPTEMBER 15-16, 1994

Sturbridge Host Hotel/Conference Center, Sturbridge, Massachusetts

Sponsored by:

- NASA Goddard Space Flight Center Office of Commercial Programs.
- *Laser Tech Briefs*
- NASA Northeast Regional Technology Transfer Center — Center for Technology Commercialization.

In cooperation with CONNECT: the New England Alliance for Photonics Technology Deployment.

Photonics industry attendees at this one and-a-half-day conference/workshop, the first in a planned series, will come face to face with advanced laser, optoelectronic, and imaging technologies developed initially for the space program that hold promise for commercial exploitation.

The program will feature:

- Inventors and technical program managers from Goddard Space Flight Center in individual and roundtable sessions;
- Researchers, patent counsel, and technology transfer experts available for one-on-one discussions of commercialization opportunities;
- A "networking reception" for all participants on September 15.

BRINGING TOGETHER

From NASA Goddard Space Flight Center:

- Researchers and scientists from the Photonics Branch (Laser Ranging and Altimetry, Remote Sensing), Optics Research and Design Branch, Solid State Device Development Branch, Electronic Systems Branch (Data Processing, Signal Processing), Environmental Sensors Lab, and more.

From the Regional Photonics Industry:

- Designers, engineers, and technology managers whose companies are searching for innovative ways to develop and test new products, improve manufacturing/production processes, initiate new business lines.

For more information on attending, write in 692 on the Reader Information Request Form.

ADVERTISERS INDEX

*RAC stands for Reader Action Card. For further information on these advertisers, please write in the RAC number on the Reader Action Card in this issue. This index is compiled as a service to our readers and advertisers. Every precaution is taken to insure its accuracy, but the publisher assumes no liability for errors or omissions.

NASA Tech Briefs, ISSN 0145-319X, USPS 750-070, copyright© 1994 in U.S., is published monthly by Associated Business Publications Co., Ltd., 41 E. 42nd St., New York, NY 10017-5391. The copywrited information does not include the (U.S. rights to)individual tech briefs which are supplied by NASA. Editorial, sales, production and circulation offices at 41 East 42nd Street, New York, NY 10017-5391. Subscription for non-qualified subscribers in the U.S., Panama Canal Zone, and Puerto Rico, $75.00 for 1 year $125.00 for 2 years; $200.00 for 3 years. Single copies $10.00. Foreign subscriptions one-year U.S. Funds $150.00. Remit by check, draft, postal, express orders or VISA, MasterCard, or American Express. Other remittances at sender's risk. Address all communications for subscriptions or circulation to NASA Tech Briefs, 41 East 42nd Street, New York, NY 10017-5391. Second Class postage paid at New York, NY and additional mailing offices.

POSTMASTER: please send changes to NASA Tech Briefs, 41 E. 42nd Street, Suite 921, New York, NY 10017-5391.

The screen on our new recorder is so big, this may be all that's missing.

Ready for some real wide-screen excitement? The real-time monitor on the Gould TA6000 thermal array recorder is a full 50% larger than competitive monitors! That means you get a clearer view of details as they occur — from 8 to 64 channels of waveforms. Scrolling speeds range from 0.01 to 200 mm/s, either synchronized or non-synchronized with the chart paper. And an optional high resolution color monitor is available to view waveforms up to 100 feet away.

But the show doesn't stop there. With the TA6000 recorder, setup is vastly improved: It's simpler since you don't have to run the chart, while basic recorder control is accomplished with easy-to-use pushbuttons and touchscreen menus. This allows faster and more reliable test setups, and can generate greater productivity.

There are more reasons why the TA6000 is getting "thumbs up" reviews from everyone who sees it: The modular design is expandable, with an optional internal hard drive for signal capture that can range from 210 megabytes to 1 gigabyte. RS-422 and IEEE-488 communication ports are standard, and four dedicated slots are available for signal conditioning modules so you can expand without sacrificing functions.

The TA6000 is one feature presentation you don't want to miss. Call us today for more details at (216) 328-7000, or mail or fax this coupon to (216) 328-7400.

GOULD
Instrument Systems

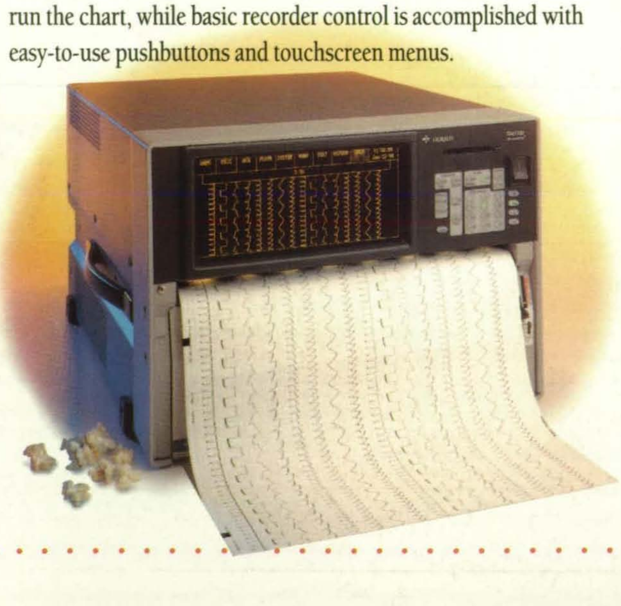

Send this coupon and we'll bring the TA6000 *and* the popcorn!

- ❑ Yes, I'd like a Gould sales representative to visit with a product demonstration of the TA6000!
- ❑ My needs are more short term at this time. Please send me information on the advantages of renting from GE Rental/Leasing (1-800-GE-RENTS).

Name: ____________________

Title: ____________________

Company: ____________________

Address: ____________________

City: __________ State: __________ Zip: __________

Telephone: __________ Fax: __________

Mail this coupon to the address below or fax it to (216) 328-7400.
Gould Instrument Systems, Inc., 8333 Rockside Road, Valley View, OH 44125.
Phone: (216) 328-7000.

NTB 7/94